



„Theoretical issues and experimental opportunities in searches for time reversal invariance violation using neutrons”, Dec. 6-8, 2018, Amherst MA

T-violating observables in neutron decay - experimental opportunities

Kazimierz Bodek

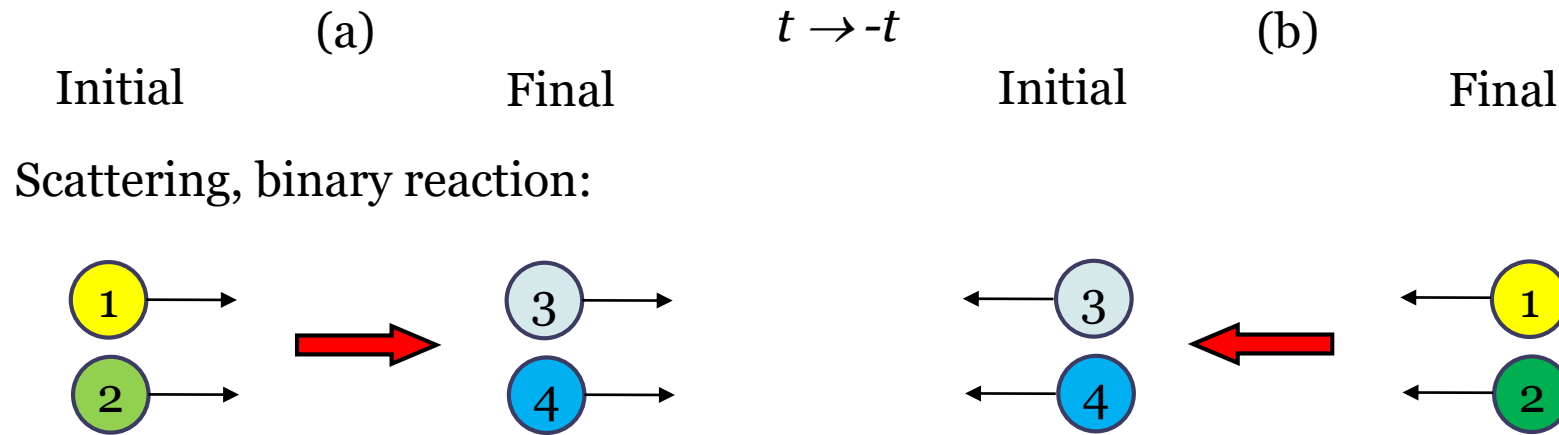
Marian Smoluchowski Institute of Physics, Jagiellonian University, Krakow, Poland

Outline

- ❑ T-odd correlations in neutron β -decay
- ❑ D- and R-correlations
- ❑ Experiments in the past: emit, Trine and nTRV
- ❑ emit+Trine+nTRV together (?) → BRAND
- ❑ Potential benefits of BRAND
- ❑ T-odd correlation in radiative neutron decay
- ❑ Challenges and strategy
- ❑ Conclusions

TRV tests

- ☐ True TRV tests require (i) reversal of motion and (ii) exchange of initial and final states



- ☐ In particle decay exchange of initial and final states is impossible

Particle decay:



- ☐ If interaction violates TR symmetry:

$$\Gamma(a) \neq \Gamma(b)$$

D - and R -correlations

- In ordinary neutron decay, two observables are particularly interesting

$$\mathbf{D} \sim \langle \mathbf{J} \rangle / J \cdot (\mathbf{p}_e \times \mathbf{p}_\nu)$$

$$\mathbf{R} \sim \langle \mathbf{J} \rangle / J \cdot (\mathbf{p}_e \times \boldsymbol{\sigma})$$

- \mathbf{D} -correlation (C-odd, P-even, T-odd)

$$\frac{d\Gamma}{dE_e d\Omega_e d\Omega_{\bar{\nu}}} = S(E_e) \left[1 + a \frac{\mathbf{p}_e \cdot \mathbf{p}_{\bar{\nu}}}{E_e E_{\bar{\nu}}} + b \frac{m_e}{E_e} + \boxed{\frac{\langle \mathbf{J} \rangle}{J}} \cdot \left(A \frac{\mathbf{p}_e}{E_e} + B \frac{\mathbf{p}_{\bar{\nu}}}{E_{\bar{\nu}}} + \mathbf{D} \frac{\mathbf{p}_e \times \mathbf{p}_{\bar{\nu}}}{E_e E_{\bar{\nu}}} \right) \right]$$

- \mathbf{R} -correlation (C-even, P-odd, T-odd)

$$\frac{d\Gamma}{dE_e d\Omega_e} = S(E_e) \left[1 + b \frac{m_e}{E_e} + A \frac{\langle \mathbf{J} \rangle}{J} \cdot \frac{\mathbf{p}_e}{E_e} + G \frac{\mathbf{p}_e \cdot \boldsymbol{\sigma}}{E_e} + \boxed{\frac{\langle \mathbf{J} \rangle}{J}} \cdot \left(Q \frac{\mathbf{p}_e}{E_e} \frac{\mathbf{p}_e \cdot \boldsymbol{\sigma}}{E_e + m_e} + N \boldsymbol{\sigma} + \mathbf{R} \frac{\mathbf{p}_e \times \boldsymbol{\sigma}}{E_e} \right) \right]$$

$$\frac{d\Gamma}{dE_e d\Omega_e} = S(E_e) \left[1 + b \frac{m_e}{E_e} + \boxed{\frac{\langle \mathbf{J} \rangle}{J}} \cdot \left(A \frac{\mathbf{p}_e}{E_e} + N \boldsymbol{\sigma}_\perp + \mathbf{R} \frac{\mathbf{p}_e \times \boldsymbol{\sigma}_\perp}{E_e} \right) \right]; \quad \boldsymbol{\sigma}_\perp \perp \mathbf{p}_e$$

D-correlation

J.D. Jackson et al., Phys. Rev. 106, 517 (1957); J.D. Jackson et al., Nucl. Phys. 4, 206 (1957); M.E. Ebel et al., Nucl. Phys. 4, 213 (1957)

- For left-handed V-A interactions ($C_V = C'_V$, $C_A = C'_V$), defining $\lambda = C_A/C_V$, neglecting terms quadratic in C_S and C_T , point charge, no recoil:

$$D = D_{\chi} + D_{FSI} \approx D_{\chi} + 1.2 \times 10^{-5}$$

$$\begin{aligned} D_{\chi} &\approx \frac{1}{1+3|\lambda|^2} \left\{ -2 \frac{\text{Im}(C_V C_A^*)}{|C_V|^2} + \frac{\text{Im}(C_S C_T^* + C'_S C'^*_T)}{|C_V|^2} \right\} \\ &+ \frac{\alpha m}{p_e} \frac{1}{1+3|\lambda|^2} \text{Re} \left(\lambda^* \frac{C_T^* + C'^*_T}{C_A^*} - \lambda^* \frac{C_S + C'^*_S}{C_V} \right) \end{aligned}$$

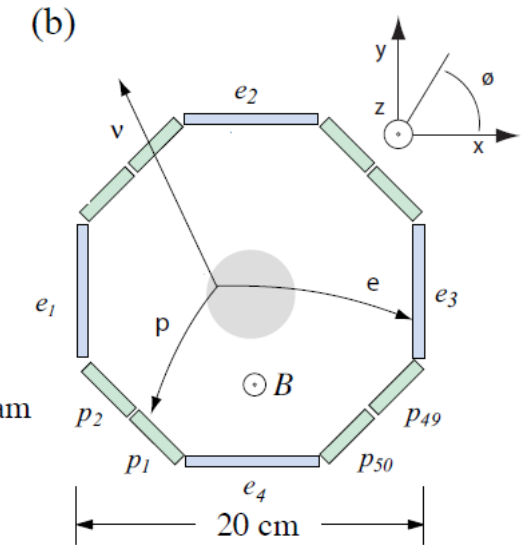
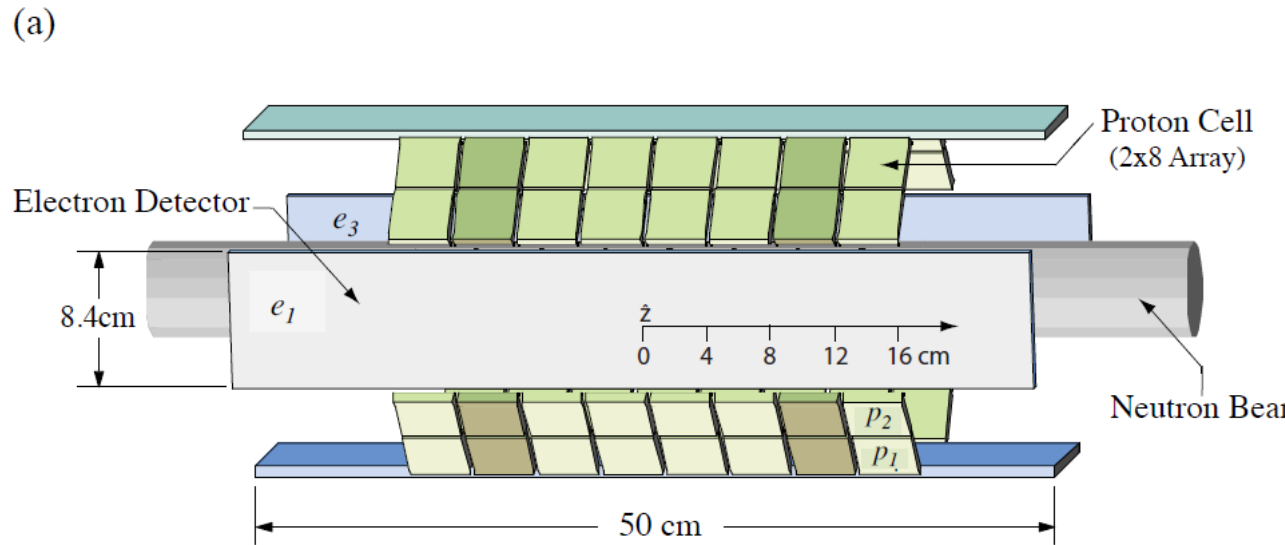
$$D_{\chi} \approx \frac{1}{1+3|\lambda|^2} \left\{ 2 \sin \phi_{AV} + \text{Im}(S^+ T^{+*} + S^- T^{-*}) \right\}; \quad S^\pm = \frac{C_S \pm C'_S}{C_V}, \quad T^\pm = \frac{C_T \pm C'_T}{C_A}$$

$$D_{\chi}^{VA} \approx 0.435 \sin \phi_{AV}$$

D-correlation, emit-II

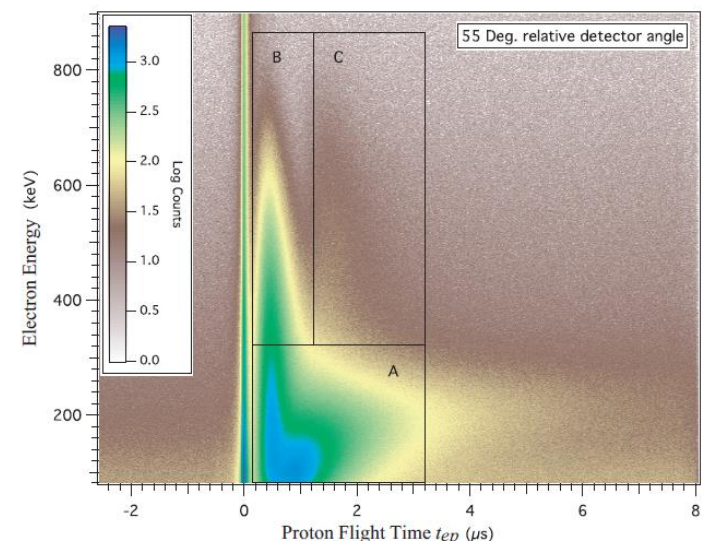
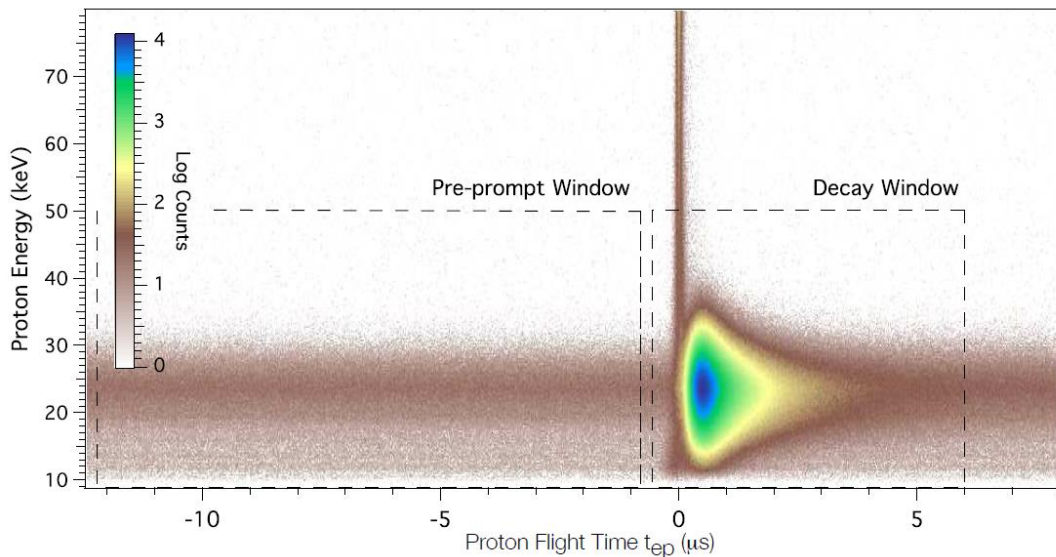
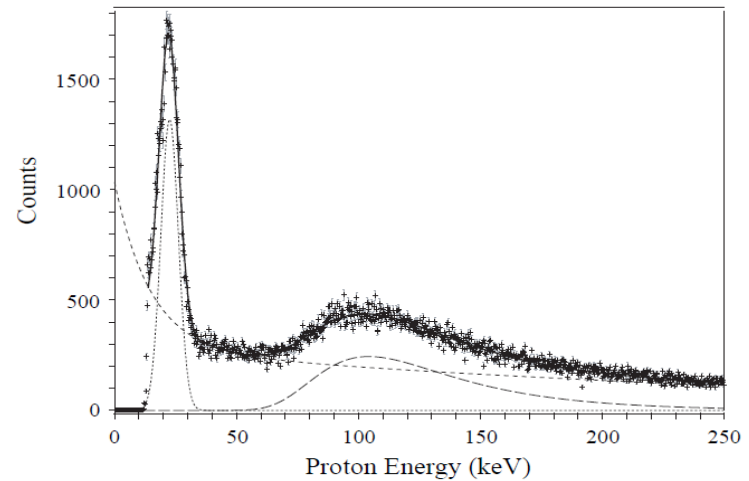
emiT-II (NIST):

- NG6 cold neutron beam
- Longitudinally polarized (~ 0.95) in the fiducial volume
- Compact, symmetric setup with azimuthally alternating electron- and proton-detectors
- Proton detectors segmented ($4 \times 4 \text{ cm}^2$) SBD, accelerating potential $\sim 25 \text{ kV}$

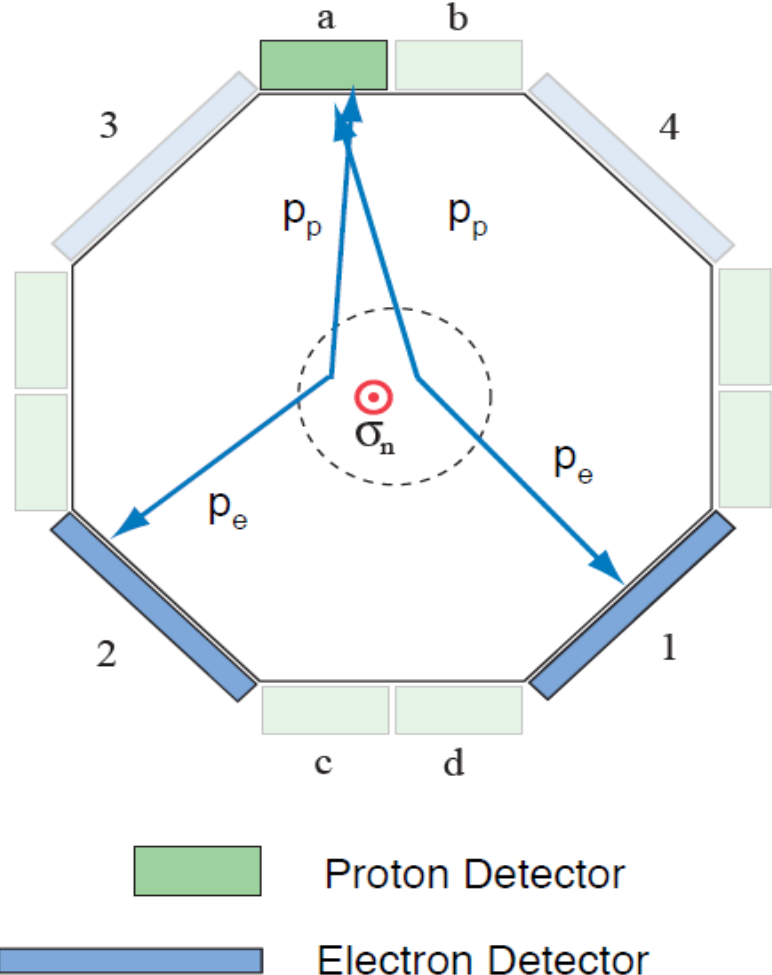


D-correlation, emit-II

- Acquired information
 - e-p coincidences, ToF
 - Electron energy
 - (Accelerated) proton energy
- Isolation of *D* using:
 - Symmetry of detectors
 - Periodic neutron spin flip



emiT blind analysis



Efficiency independent ratio,

$$w^{p_i e_j} = \frac{N_+^{p_i e_j} - N_-^{p_i e_j}}{N_+^{p_i e_j} + N_-^{p_i e_j}} + \mathcal{B}\hat{z} \cdot \tilde{\mathbf{K}}_D^{p_i e_j}$$

↑
hidden blind offset

w is sensitive to D , but also to A , B
Define a parameter,

$$v^{p_i} = \frac{1}{2}(w^{p_i R} - w^{p_i L})$$

For a symmetric uniform detector,

$$v^{p_i} = PD\hat{z} \cdot \left(\tilde{\mathbf{K}}_D^{p_i e_R} - \tilde{\mathbf{K}}_D^{p_i e_L} \right)$$

Instrumental constant

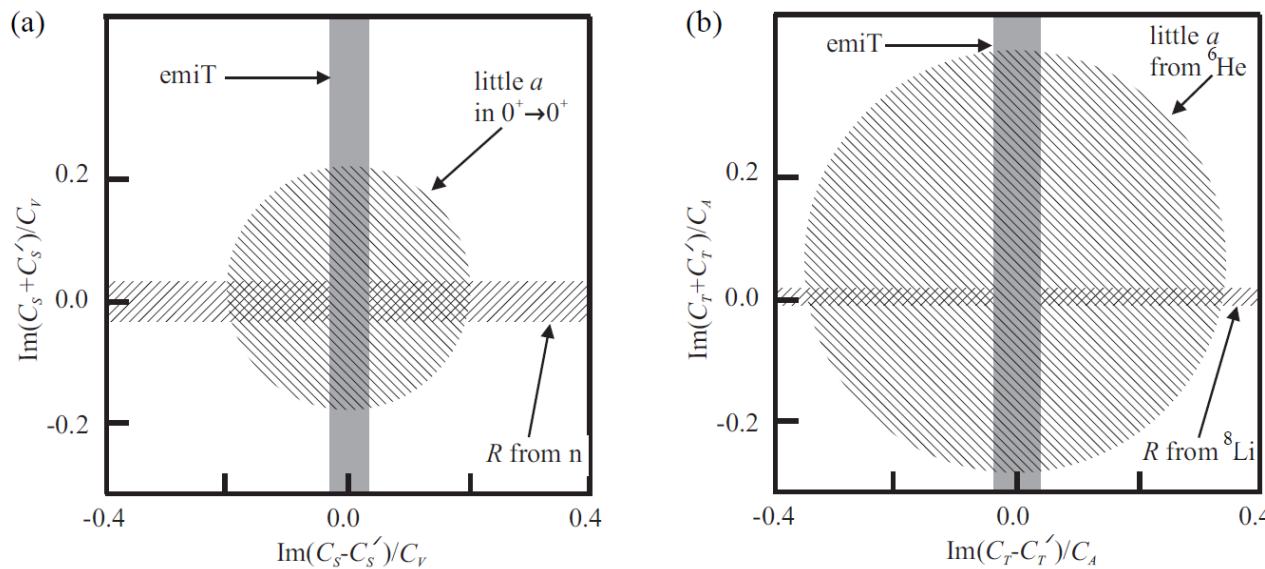
$$\propto \int \frac{p_e \times p_p}{E_e E_p} d\Omega_a d\Omega_2 dV_{beam}$$

D-correlation, emit-II

Result

$$D = [-0.94 \pm 1.89(\text{stat}) \pm 0.97(\text{sys})] \times 10^{-4}$$

$$\phi_{AV} = 180.012^\circ \pm 0.028^\circ \text{ (68% C.L.)}$$



courtesy of H.P. Mumm

emiT II : Systematics & Corrections

Source	Correction	Uncertainty	$(\times 10^{-4})$
Background asymmetry	0 ^a	0.30	
Background subtraction	0.03	0.003	
Electron backscattering	0.11	0.03	
Proton backscattering	0 ^a	0.03	
Beta threshold	0.04	0.10	
Proton threshold	-0.29	0.41	
Beam expansion, magnetic field	-1.50	0.40	
Polarization non-uniformity	0 ^a	0.10	
ATP - misalignment	-0.07	0.72	
ATP - Twist	0 ^a	0.24	
Spin-correlated flux ^b	0 ^a	3×10^{-6}	
Spin-correlated pol.	0 ^a	5×10^{-4}	
Polarization ^c		0.04 ^d	
\bar{K}_D ^c		0.03	
Total systematic corrections	-1.68	1.01	

Most of systematic effects were MC modelled

^a Zero indicates no correction applied.

^b Includes spin-flip time, cycle asymmetry, and flux variation.

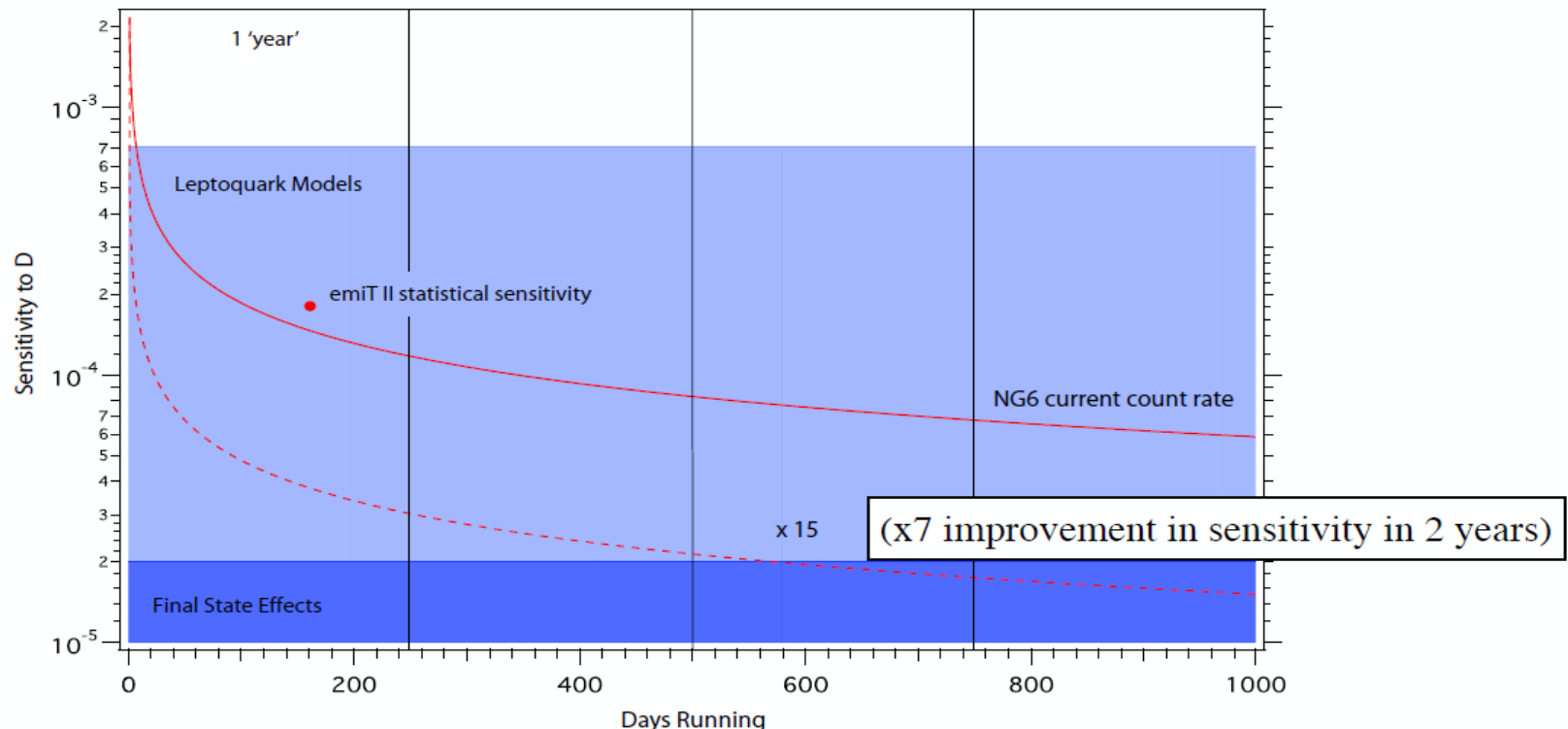
^c Included in the definition of D.

^d Assumed polarization uncertainty of 5%

Future Measurement

emiT-II+NGC

- The new NGC beam line could provide over a factor of 10 increase in neutron flux
- Current emiT apparatus might be capable of reaching $2\text{--}3 \times 10^{-5}$ with modest upgrades and improvements.
- At this level one should see the effect of final state effects.
- No definite plan at this time – starting to think about it.



Future Measurement, sensitivity

- The ‘full’ NGC beam line would provide x 4.3
- Current emiT apparatus ~50 cm, 2 m feasible; x 4.
- Possible beta and proton detection with same detector x 2 .

Statistically a dataset ~1500x larger is imaginable (not crazy)

Ultimate sensitivity ~ 40 x better

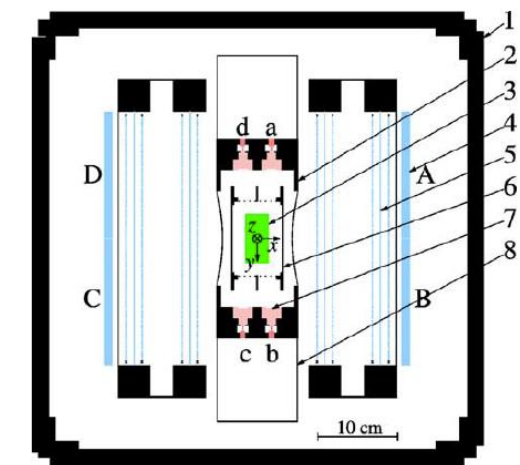
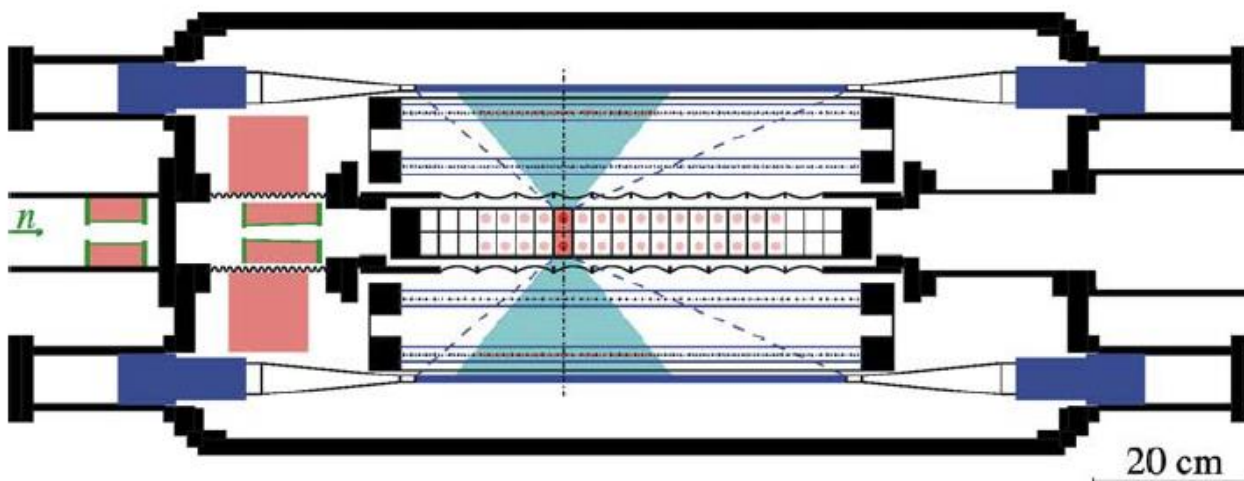
- Hope to detect protons and electrons with one detector (or a layered detector)
- Reduce required proton acceleration voltage (improve energy resolution)
- Exploring detector ideas (bolometer, thin foils, hybrids)
- Test cryostat, dil fridge, beamline available, proof-of-principle?
- Feasible?
- How to proceed?

D-correlation, Trine

T. Soldner, L. Beck, C. Plonka,
K. Schreckenbach, O. Zimmer,
Phys. Lett. B 581 (2004) 49

□ Trine (ILL):

- PF1 cold neutron beam
- Longitudinally polarized (~0.97) in the fiducial volume
- Compact setup with planar geometry
- Electron- and proton-detectors in perpendicular planes
- Proton detectors PIN diodes on ground potential
- Accelerating potential: 25 kV
- MWPC for gamma suppression and selection of angular ranges



D-correlation, Trine

T. Soldner, L. Beck, C. Plonka,
K. Schreckenbach, O. Zimmer,
Phys. Lett. B 581 (2004) 49

- ❑ Excellent S/B ratio of 23
- ❑ Systematic effects and corrections

$$D = [-2.8 \pm 6.4(\text{stat}) \pm 3.0(\text{syst})] \times 10^{-4}$$

$$= (-2.8 \pm 7.1) \times 10^{-4}.$$

$$\phi_{\text{AV}} = 180.04^\circ \pm 0.09^\circ$$

Table 1

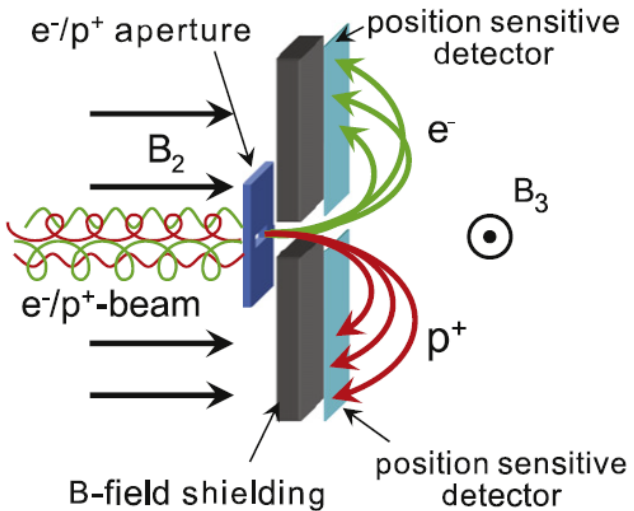
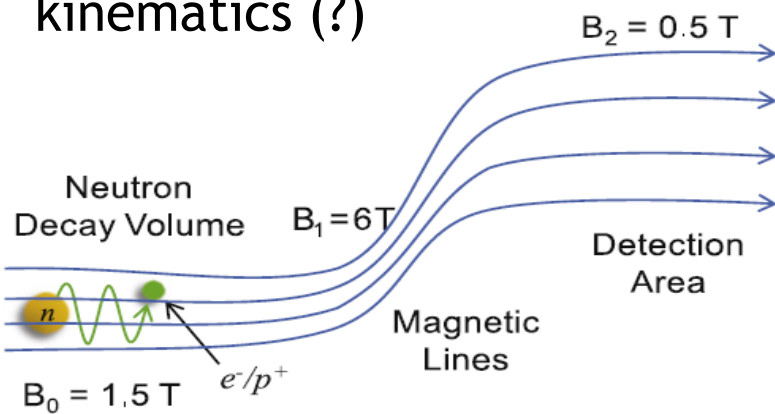
Corrections and uncertainties of the experimental values. All values are given in units of 10^{-4}

	98°		130°	
	Correction	Systematic error	Correction	Systematic error
Asymmetry of beam profile (a)	+0.9	2.0	+0.3	1.5
Scintillator calibration (b)		1.3		0.8
Different spatial dependences (c)		0.3		0.1
Different energy resolutions (d)		0.2		0.1
Asymmetry of scintillator (e)		3.0		1.1
Inhomogeneity of MWPC (f)		2.3		1.6
Size of symmetrisation range (g)		1.0		1.0
Polarisation		0.2		0.07
Detector solid angles		0.3		0.1
Combined systematic error		4.6		2.8

D-correlation with ep/n + MagSpec ?

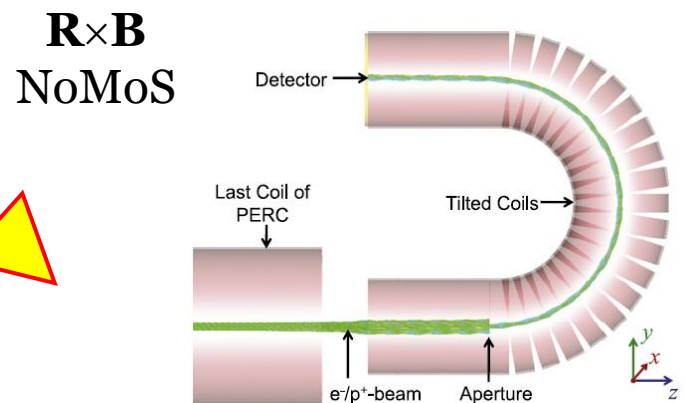
e.g. G. Konrad et al., J. Phys.: Conf. Series **340** (2012) 012048

- ep/n-spectrometers adiabatically coupled to n-decay channel (PERC, ANNI)
- Conserve particle energy and angular (polar) distributions
- Reconstruct $\mathbf{p}_e \times \mathbf{p}_p$ using decay kinematics (?)



- No definite plans yet (B. Maerkisch, TUM)

X. Wang, G. Konrad, H. Abele, NIMA (2012) 254



R-correlation

- For left-handed V-A interactions ($C_V = C'_V$, $C_A = C'_V$), defining $\lambda = C_A/C_V$, neglecting terms quadratic in C_S and C_T , point charge, no recoil:

$$R = R_{\chi} + R_{FSI} \approx R_{\chi} - \frac{\alpha m}{p_e} A_{SM} = R_{\chi} + 9 \times 10^{-4}$$

$$R_{\chi} \approx \frac{1}{1+3|\lambda|^2} \left\{ 4 \frac{\text{Im}(C_T C_A^* + C'_T C'^*_A)}{|C_V|^2} + 2 \frac{\text{Im}(C_S C_A^* + C'_S C_A^* - C_V C'^*_T - C_V C_T^*)}{|C_V|^2} \right\}$$

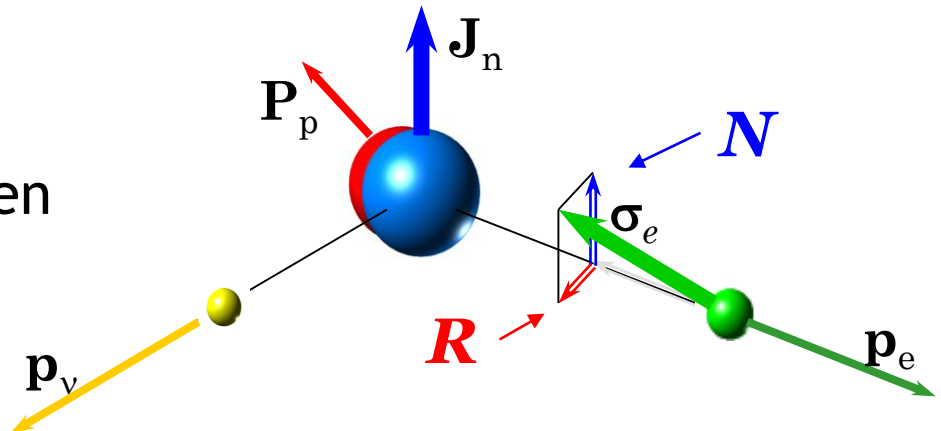
$$R_{FSI} \approx -\frac{\alpha m}{p_e} \frac{1}{1+3|\lambda|^2} \text{Re}[2\lambda(\lambda+1)]$$

$$R_{\chi} \approx \frac{-|\lambda|}{1+3|\lambda|^2} \text{Im}(S^+) + \frac{|\lambda|(1-2|\lambda|)}{1+3|\lambda|^2} \text{Im}(T^+); \quad S^\pm = \frac{C_S \pm C'_S}{C_V}, \quad T^\pm = \frac{C_T \pm C'_T}{C_A}$$

$$R_{\chi} \approx -0.218 \text{ Im}(S^+) + 0.335 \text{ Im}(T^+)$$

N -correlation

- ☐ N is C-even, P-even and T-even



$$N = N_T + N_{SM} \approx N_T - A_{SM} \frac{m}{E_e} = N_T + 7.9 \times 10^{-2}$$

$$N_{SM} \approx -\frac{m}{E_e} \frac{1}{1+3|\lambda|^2} \text{Re} [2\lambda(\lambda+1)]$$

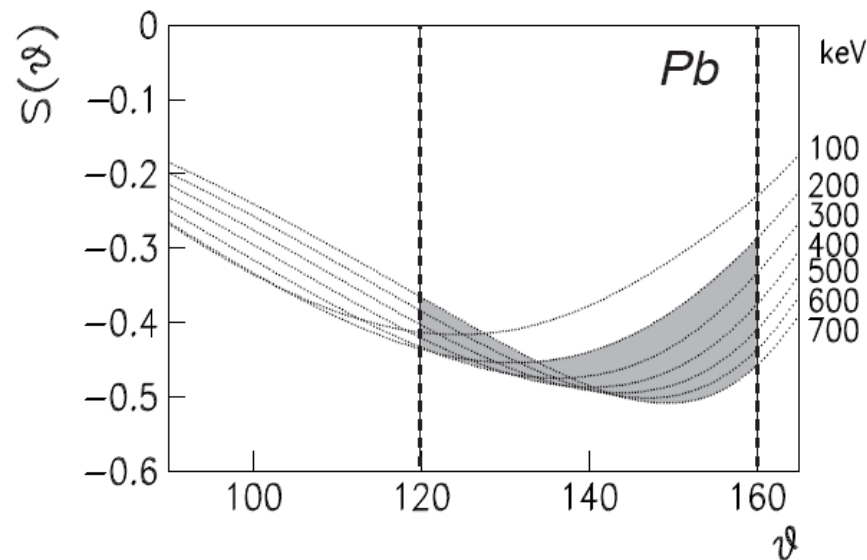
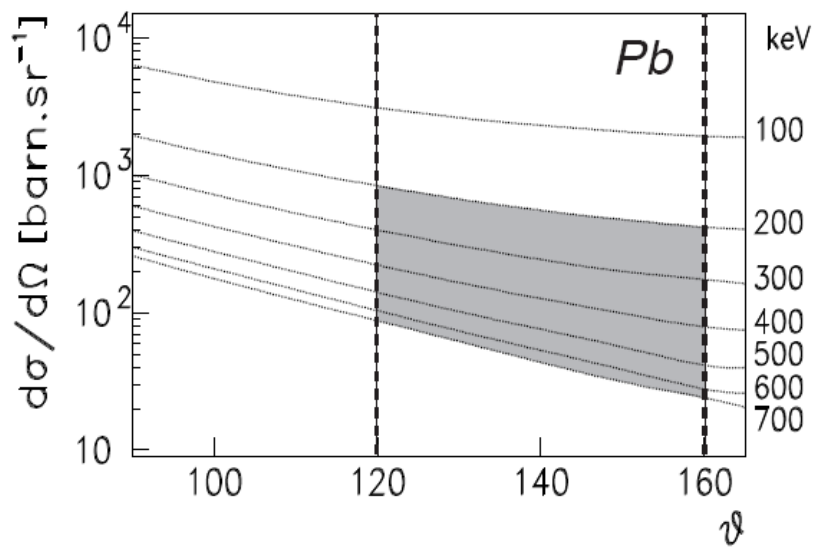
$$N_T \approx \frac{-|\lambda|}{1+3|\lambda|^2} \text{Re}(S^+) + \frac{|\lambda|(1-2|\lambda|)}{1+3|\lambda|^2} \text{Re}(T^+); \quad S^\pm = \frac{C_s \pm C'_s}{C_V}, \quad T^\pm = \frac{C_T \pm C'_T}{C_A}$$

$$N_T \approx -0.218 \text{Re}(S^+) + 0.335 \text{Re}(T^+)$$

Electron spin analysis

❑ Mott scattering:

- Analyzing power caused by spin-orbit force
- Parity and time reversal conserving (electromagnetic process)
- Sensitive exclusively to the transverse polarization



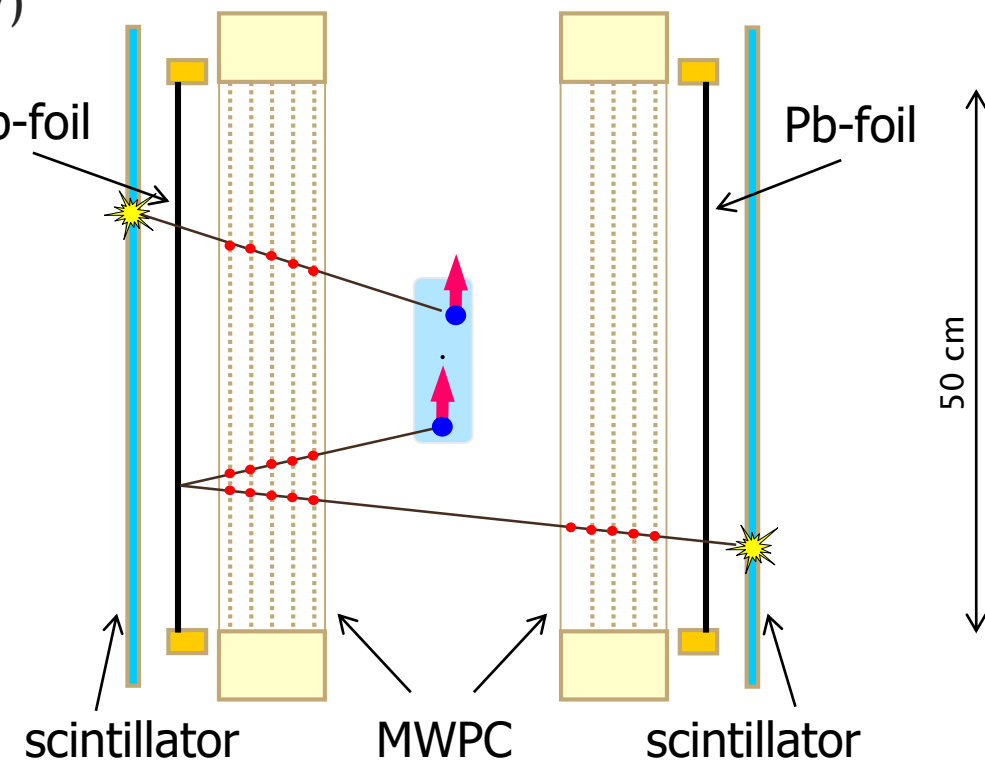
nTRV@PSI - Mott polarimeter

□ Challenges:

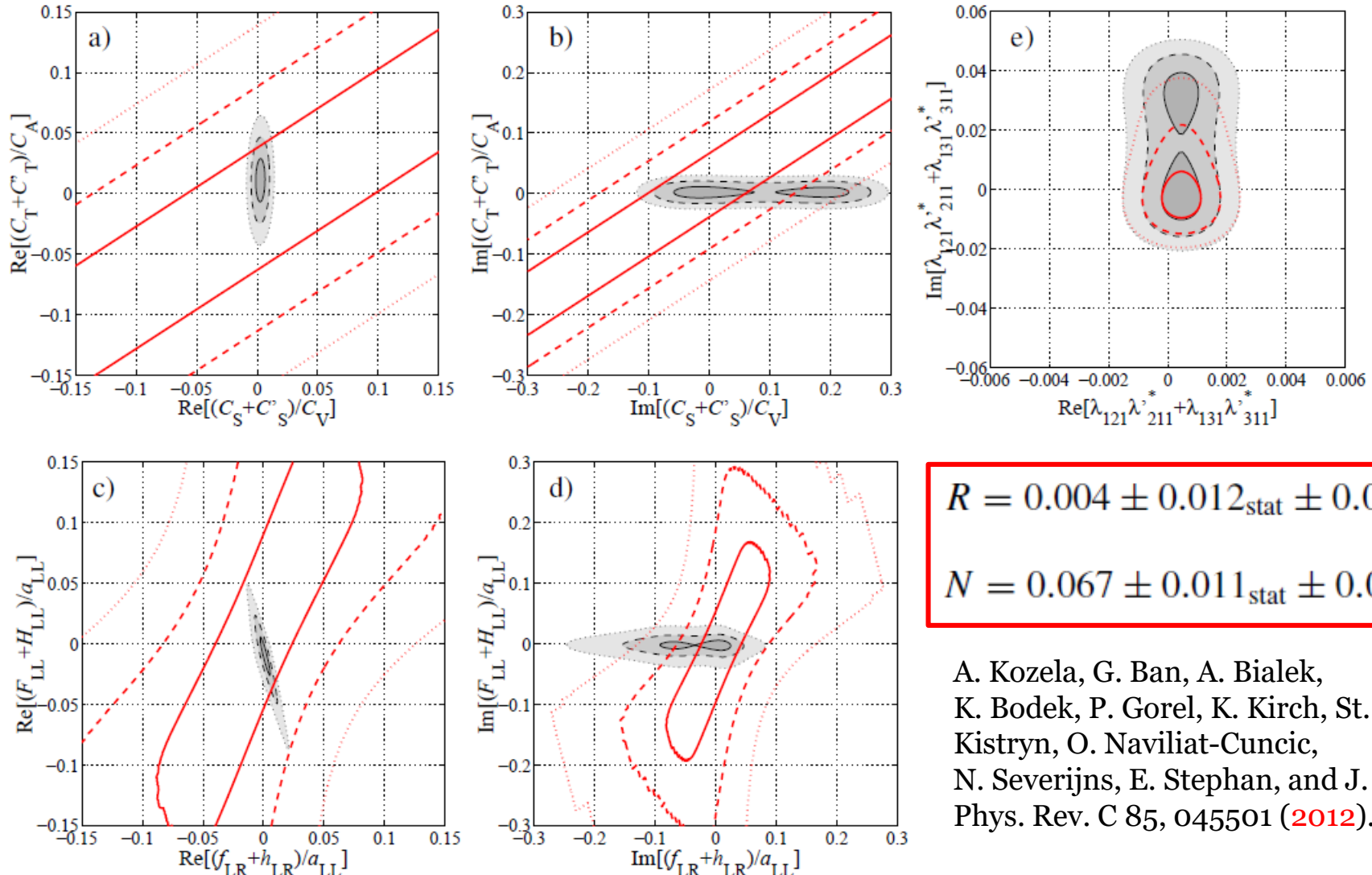
- Weak and diffuse decay source
- Electron depolarization in multiple Coulomb scattering
- Low energy electrons (<783 keV)
- High background (n-capture)

□ Solutions:

- Tracking of electrons in low-mass, low-Z MWPCs
- Identification of Mott-scattering vertex (“V-track”)
- Frequent neutron spin flipping
- “foil-in” and “foil-out” measurements



Limits on S and T contributions



A. Kozela, G. Ban, A. Bialek,
 K. Bodek, P. Gorel, K. Kirch, St.
 Kistryn, O. Naviliat-Cuncic,
 N. Severijns, E. Stephan, and J. Zejma,
 Phys. Rev. C 85, 045501 (2012).

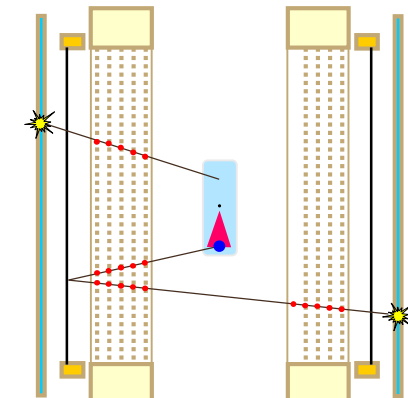
Systematic uncertainties in nTRV@PSI

Dominating systematic uncertainties

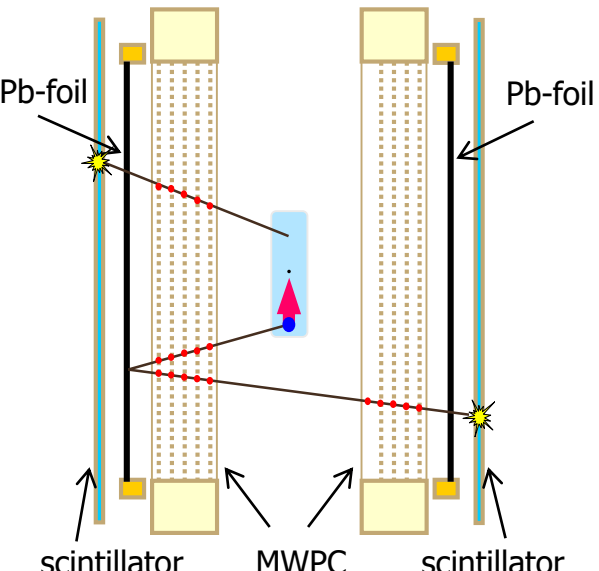
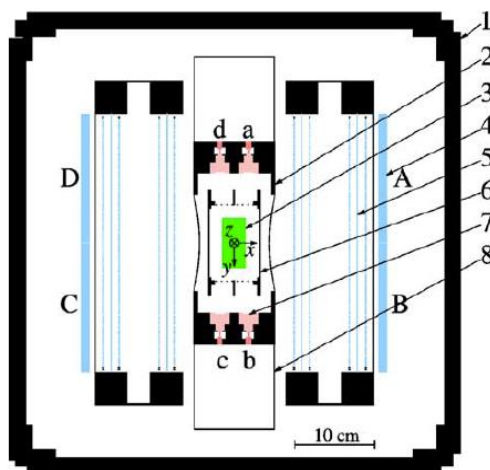
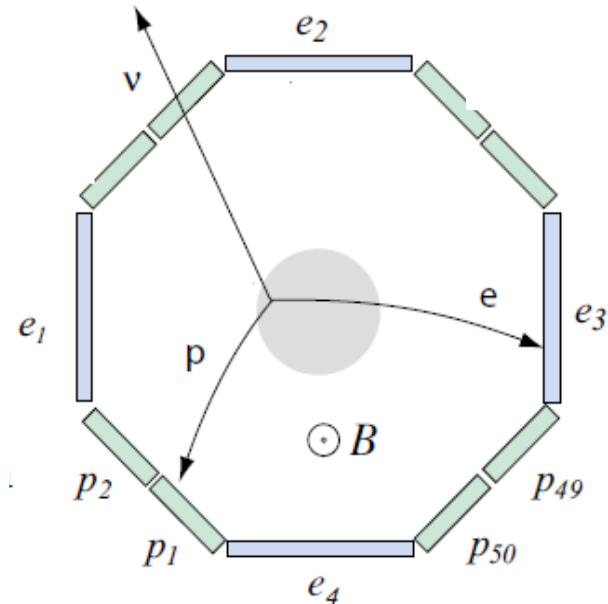
Source	$\delta N \times 10^4$	$\delta R \times 10^4$
1. term $P\beta A\mathcal{F}$	5	23
2. effective Sherman function \bar{S}	29	8
3. guiding field misalignment	3	6
4. background subtraction	46	53
5. dead time variations	8	0.3
Total	55	59

Sample of
analyzed data

1. Combined error from uncertainties of:
 - a) Neutron polarization
 - b) Low energy cut
 - c) Decay asymmetry A measurement (R, N were measured relatively to A)
 - d) Statistical precision of geometry factors
2. Mott target thickness nonuniformity
3. Guiding field map
4. High background (to be subtracted) due to guiding neutron beam in He atmosphere
5. Properties of Front End electronics and DAQ



R- and *D*-correlation in one setup ?



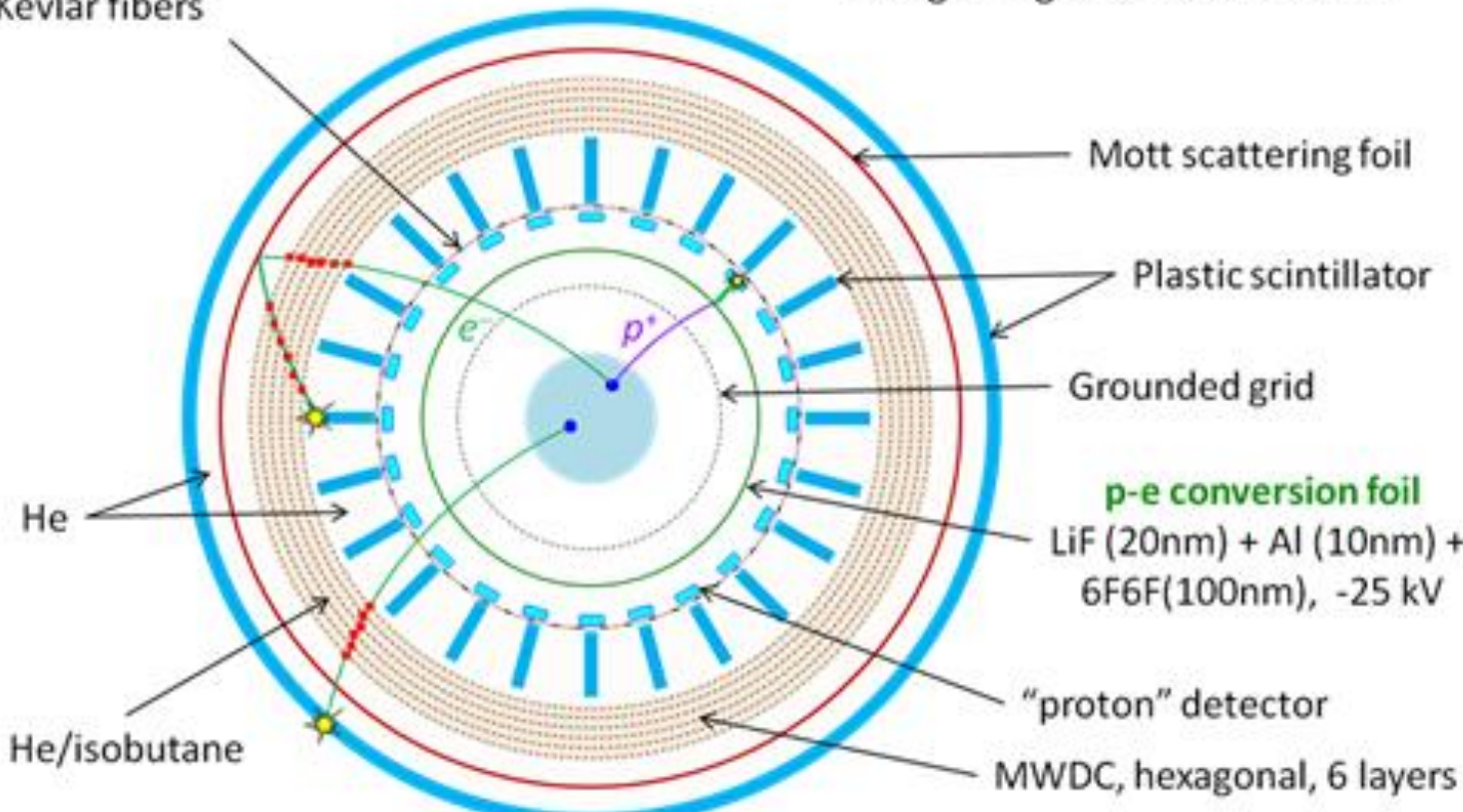
- Neutron beam in vacuum
- Axial geometry
- Alternating position sensitive e- and p-detectors
- Electron tracking
- Proton ToF
- Electron spin analysis with Mott scattering

BRAND
concept

BRAND concept

Grounded vacuum window:
6 μm Mylar, reinforced with
Kevlar fibers

Longitudinal neutron polarization,
Axial guiding field $B=0.1\div0.5\text{ mT}$



Transverse electron polarization

- Measuring electron- and proton-momentum and transverse electron polarization:

$$\begin{aligned}
 d\Gamma \sim & 1 + \textcolor{blue}{a} \frac{\mathbf{p}_e}{E_e} \cdot \frac{\mathbf{p}_{\bar{\nu}}}{E_{\bar{\nu}}} + \textcolor{blue}{b} \frac{m_e}{E_e} + \frac{\langle \mathbf{J} \rangle}{J} \cdot \left[\textcolor{blue}{A} \frac{\mathbf{p}_e}{E_e} + \textcolor{blue}{B} \frac{\mathbf{p}_{\bar{\nu}}}{E_{\bar{\nu}}} + \textcolor{blue}{D} \frac{\mathbf{p}_e}{E_e} \times \frac{\mathbf{p}_{\bar{\nu}}}{E_{\bar{\nu}}} \right] \\
 & + \sigma_{\perp} \cdot \left[\textcolor{red}{H} \frac{\mathbf{p}_{\bar{\nu}}}{E_{\bar{\nu}}} + \textcolor{red}{L} \frac{\mathbf{p}_e}{E_e} \times \frac{\mathbf{p}_{\bar{\nu}}}{E_{\bar{\nu}}} + \textcolor{red}{N} \frac{\langle \mathbf{J} \rangle}{J} + \textcolor{red}{R} \frac{\langle \mathbf{J} \rangle}{J} \times \frac{\mathbf{p}_e}{E_e} \right] \\
 & + \sigma_{\perp} \cdot \left[\textcolor{red}{S} \frac{\langle \mathbf{J} \rangle}{J} \frac{\mathbf{p}_e}{E_e} \cdot \frac{\mathbf{p}_{\bar{\nu}}}{E_{\bar{\nu}}} + \textcolor{red}{U} \frac{\mathbf{p}_{\bar{\nu}}}{E_{\bar{\nu}}} \frac{\langle \mathbf{J} \rangle}{J} \cdot \frac{\mathbf{p}_e}{E_e} + \textcolor{red}{V} \frac{\mathbf{p}_{\bar{\nu}}}{E_{\bar{\nu}}} \times \frac{\langle \mathbf{J} \rangle}{J} \right]
 \end{aligned}$$

\mathbf{p}_e - electron momentum $\mathbf{p}_{\bar{\nu}}$ - neutrino momentum

σ_{\perp} - electron spin projection direction

- All correlation coefficients can be expressed as combinations of real and imaginary parts of exotic (**scalar** and **tensor**) couplings:

$$X = X_{V-A} + X_{FSI} + c_{ReS} \operatorname{Re} \textcolor{red}{S} + c_{ReT} \operatorname{Re} \textcolor{purple}{T} + c_{ImS} \operatorname{Im} \textcolor{red}{S} + c_{ImT} \operatorname{Im} \textcolor{purple}{T}$$

$$\textcolor{red}{S} = \frac{C_s + C_s'}{C_V}, \quad \textcolor{purple}{T} = \frac{C_T + C_T'}{C_A}, \quad c_{ReS}, c_{ReT}, c_{ImS}, c_{ImT} - \text{functions of } \lambda = C_A/C_V \text{ and kinematical quantities}$$

Sensitivity factors for scalar and tensor couplings (leading order, no recoil, point charge)

	SM (λ)	FSI (λ)	$c(\text{Re}S)$	$c(\text{Re}T)$	$c(\text{Im}S)$	$c(\text{Im}T)$
a	-0.1048	0	-0.1714 [†]	0.1714 [†]	-0.0007	+0.0012
b	0	0	+0.1714	+0.8286	0	0
A	-0.1172	0	0	0	-0.0009	+0.0014
B	+0.9876	0	-0.1264	+0.1945	0	0
D	0	0	+0.0009	-0.0009	0	0
H	+0.0609	0	-0.1714	+0.2762	0	0
L	0	-0.0004	0	0	+0.1714	-0.2762
N	+0.0681	0	-0.2176	+0.3348	0	0
R	0	+0.0005	0	0	-0.2176	+0.3348
S	0	-0.0018	+0.2176	-0.2176	0	0
U	0	0	-0.2176	+0.2176	0	0
V	0	0	0	0	-0.2176	+0.2172

* Kinematical factor averaged over electron kinetic energy $E_k = (200,783)$ keV

† $(|C_S|^2 + |C'_S|^2)/2$ instead of $\text{Re}S$ and $(|C_T|^2 + |C'_T|^2)/2$ instead of $\text{Re}T$, respectively

- Cancellation effects are insignificant for transverse electron polarization related correlation coefficients !!!

BRAND – kinematical sensitivity maps

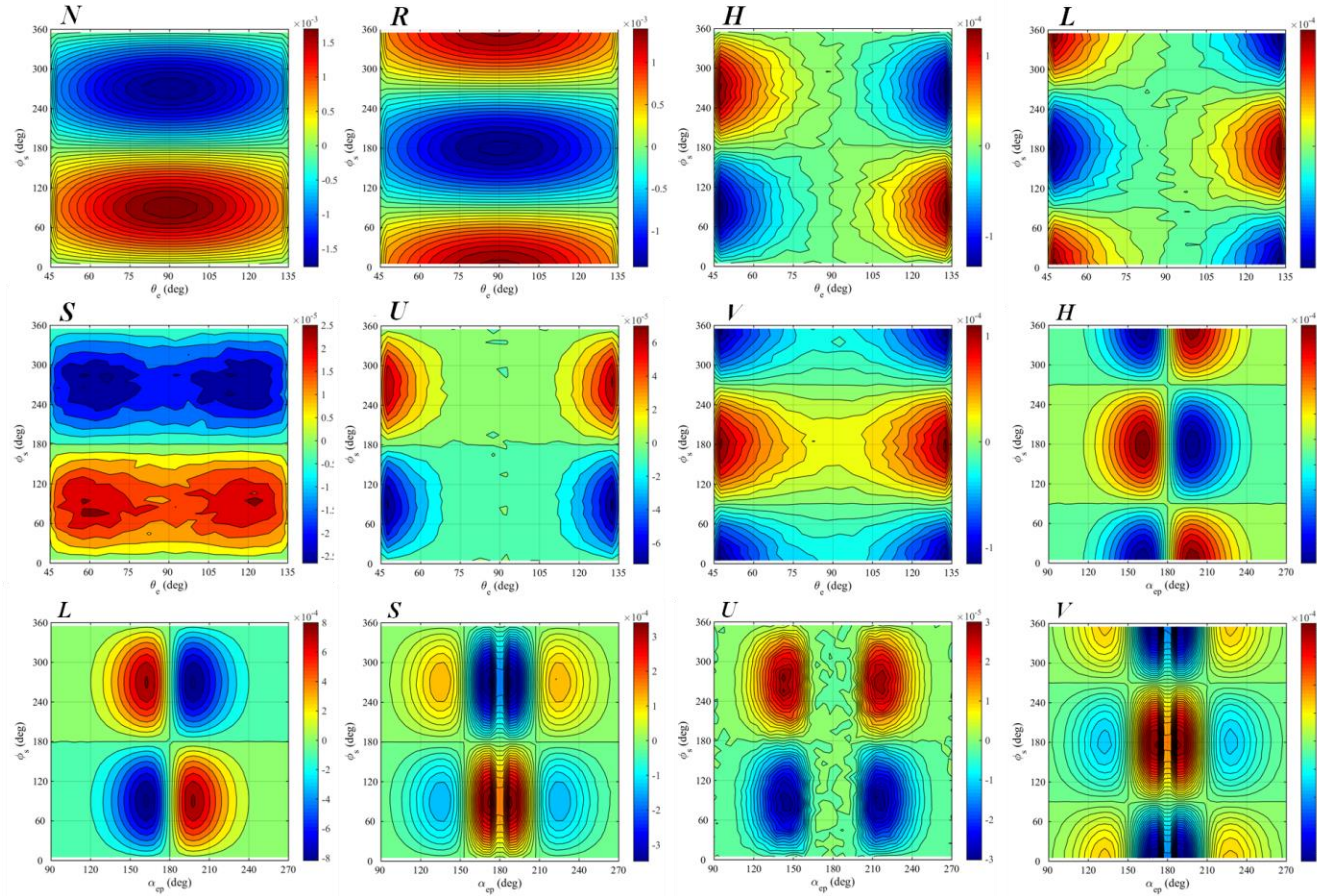
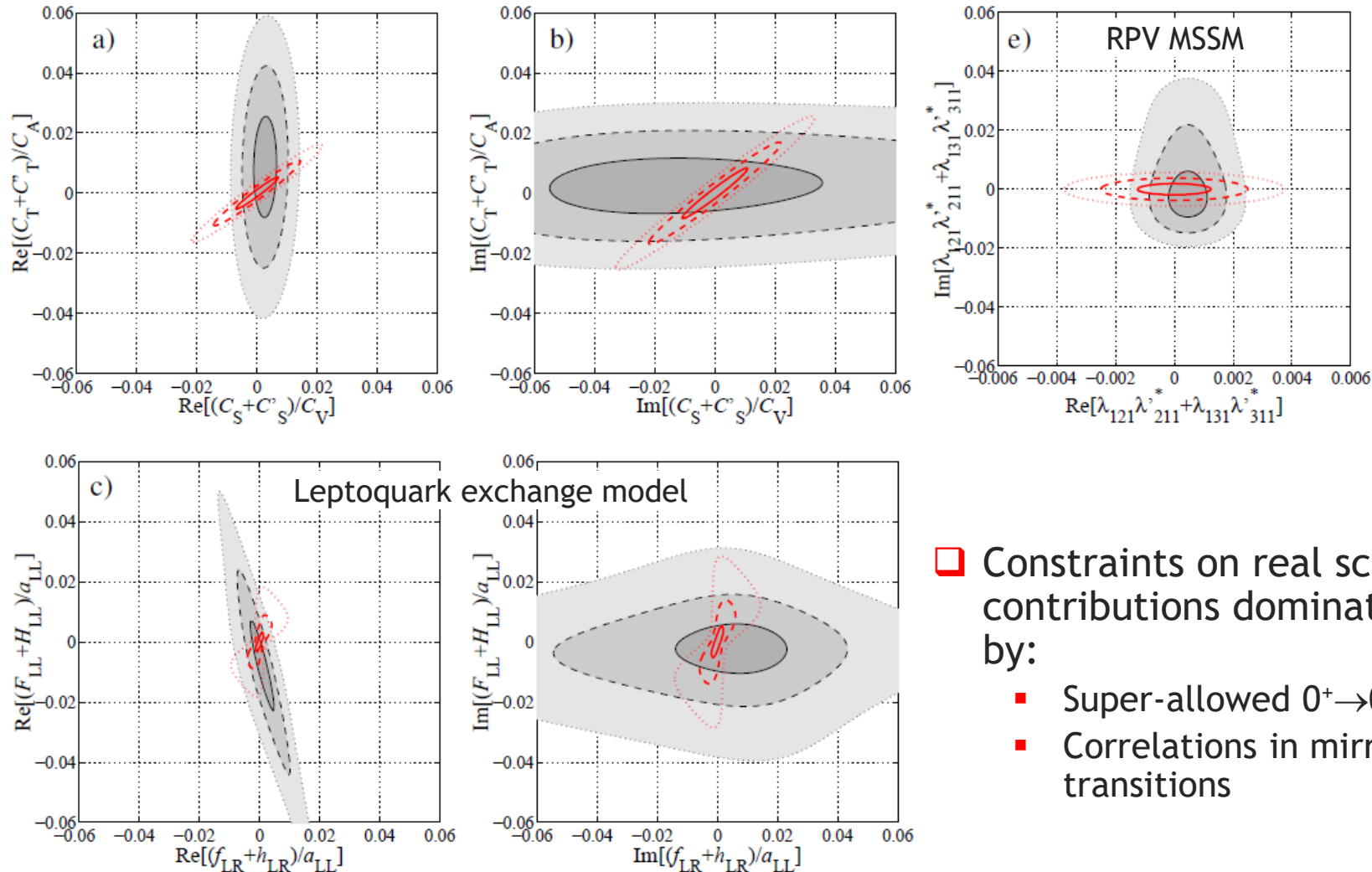


Figure 4: Sensitivity maps for the N , R , H , L , S , U and V coefficient as a function of the polar electron angle θ_e or the relative electron-proton angle and the azimuthal spin projection angle ϕ_s (arbitrary units). Irregularities in contours are due to limited statistics in simulations. The kinematical acceptance is defined by $E_e^{\text{kin}} \in (200, 782)\text{keV}$, $E_p^{\text{kin}} \in (50, 760)\text{eV}$, $\theta_e \in (45^\circ, 135^\circ)$, $\theta_p \in (30^\circ, 150^\circ)$.

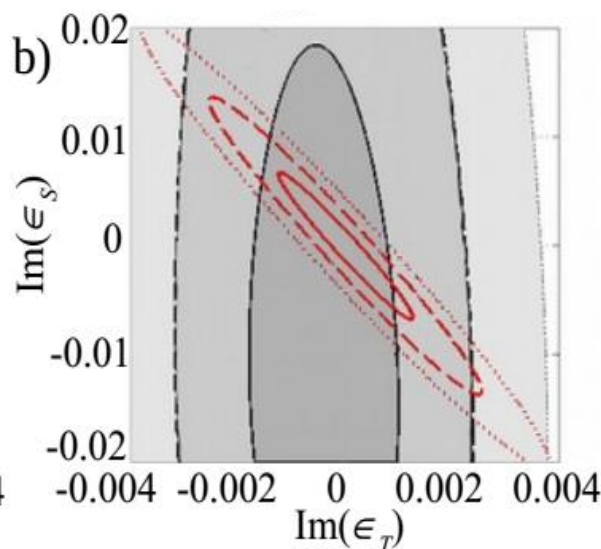
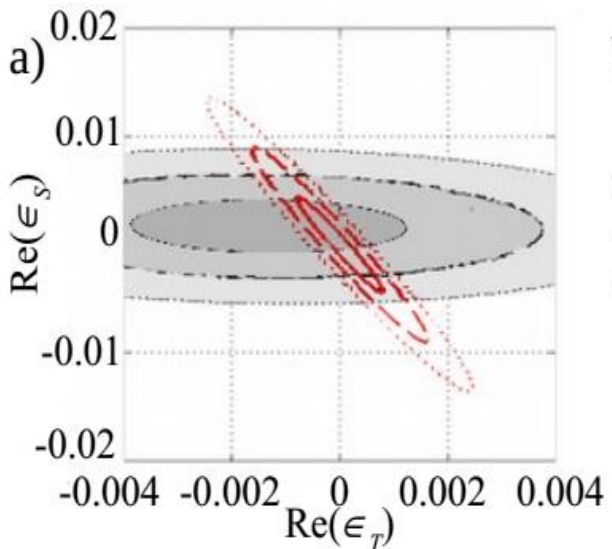
Impact of H, L, N, R, S, U and V measurement with anticipated accuracy of 5×10^{-4}



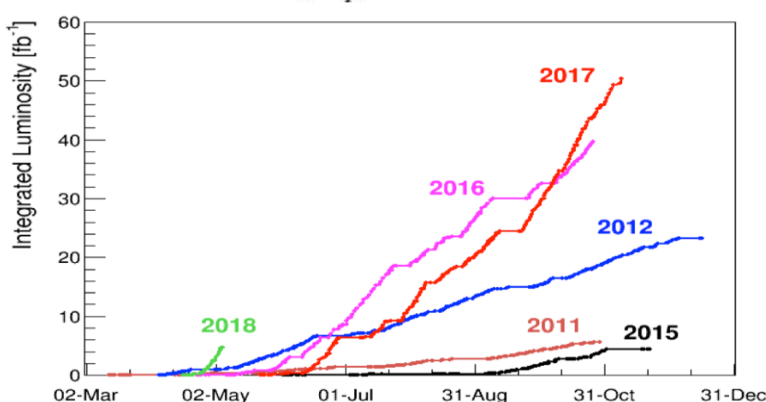
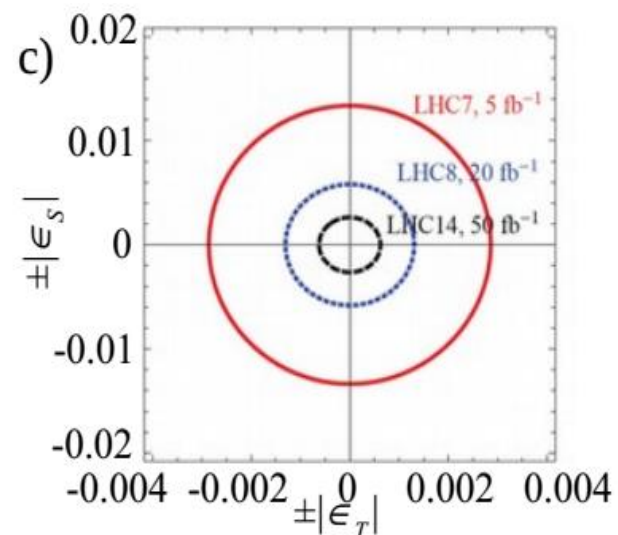
- ❑ Constraints on real scalar contributions dominated by:
 - Super-allowed $0^+ \rightarrow 0^+$
 - Correlations in mirror transitions

Impact of H, L, N, R, S, U and V measurement with anticipated accuracy of 5×10^{-4}

- Translated into EFT parameters



M. Gonzalez-Alonso et al., Ann. Phys. 525 (2013)



- Electrons and missing transverse energy (MET) channel

$$\sigma(pp \rightarrow e + \text{MET} + X)$$

V-correlation

$$\frac{d\Gamma}{dE_{\bar{\nu}} d\Omega_{\bar{\nu}}} \sim 1 + \dots + \color{green}\sigma_{\perp} \cdot \left[\color{red}V \frac{\mathbf{p}_{\bar{\nu}}}{E_{\bar{\nu}}} \times \frac{\langle \mathbf{J} \rangle}{J} \right]$$

$$V = V_{\chi} + V_{FSI} \approx V_{\chi} + 10^{-5} (?)$$

$$V_{\chi} \approx \frac{1}{1+3|\lambda|^2} \frac{\color{green}m}{\color{green}E_e} \left\{ 2 \frac{\text{Im}(C_V C_A^*)}{|C_V|^2} + \frac{\text{Im}(C_S C_T^* + C'_S C'^*_T)}{|C_V|^2} \right\}$$

$$+ \frac{1}{1+3|\lambda|^2} \text{Im} \left(\lambda^* \frac{C_S + C'_S}{C_V} - \lambda^* \frac{C_T + C'_T}{C_A} \right)$$

$$V_{\chi} \approx \frac{1}{1+3|\lambda|^2} \left\{ \frac{\color{green}m}{\color{green}E_e} \left[2 \sin \phi_{AV} + \text{Im}(S^+ T^{+*} - S^- T^{-*}) \right] - |\lambda| \left[\text{Im} S^+ - \text{Im} T^+ \right] \right\}$$

$$V_{\chi}^{VA} \approx 0.261 \sin \phi_{AV}$$

$$(T_e \geq 200 \text{ keV})$$

BRAND – methods, expected performance, strategy

□ Experimental methods:

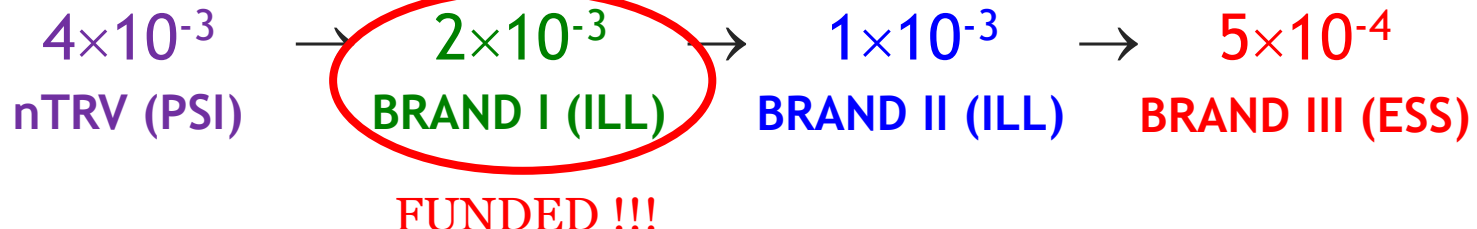
- Measure decay electrons and e - p coincidences
- Electron tracking in hexagonal, low Z , low pressure MWDC
- p - e conversion followed by e detection in scintillator (ToF, position)
- Decay vertex reconstruction
- Electron spin analysis by Mott scattering (vertex reconstruction)

□ BRAND is based on experimentally proven methods (nTRV@PSI)

□ Overall systematic uncertainty floor achieved in nTRV@PSI:

- N correlation: 4×10^{-3}
- R correlation: 5×10^{-3}

□ Gradual improvement of exp. accuracy (systematic uncertainty):



Theoretical corrections (SM)

❑ Final State Interaction (FSI)

- Exist calculations sufficient for a , b , A , B , D , R and N coefficients measurements with accuracy of 10^{-4}
- For H , L , S , U and V coefficients FSI correction exist only in lowest order (point charge) approximation

❑ Recoil order corrections (ROC)

- Main contribution from Weak Magnetism
- No ROC exist for H , L , S , U and V

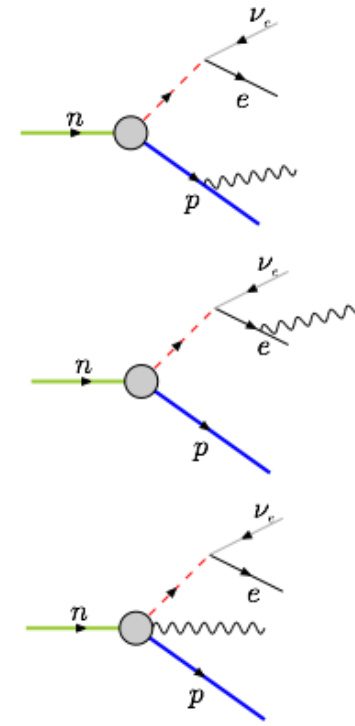
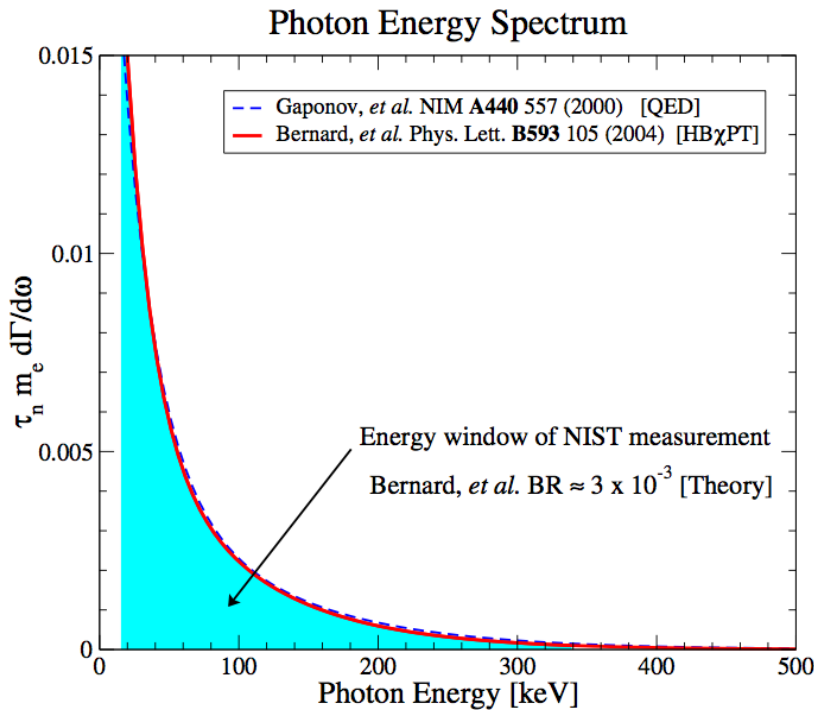
V. Gudkov, et al., 77, 045502 (2008).

A.N. Ivanov et al., Phys. Rev. C 95, 055502 (2017).

A.N. Ivanov et al., Phys. Rev. C 98, 035503 (2018).

courtesy of J. Nico

Radiative Neutron Decay:

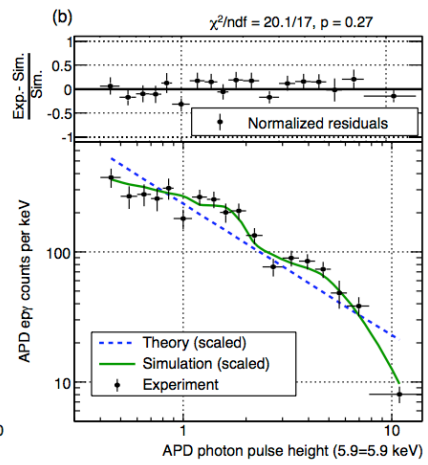
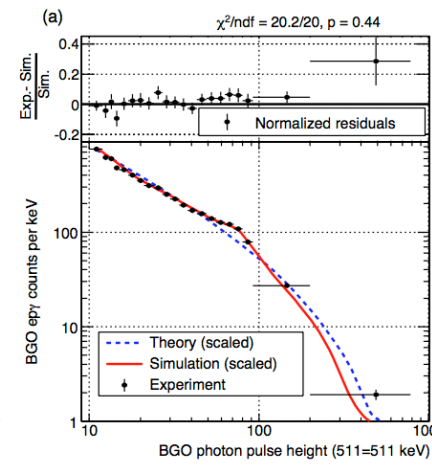
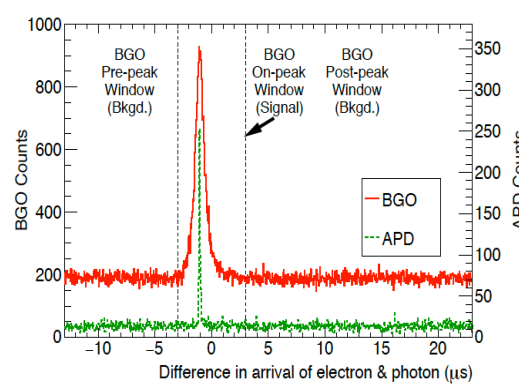
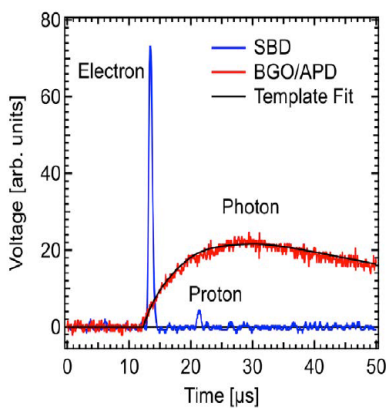
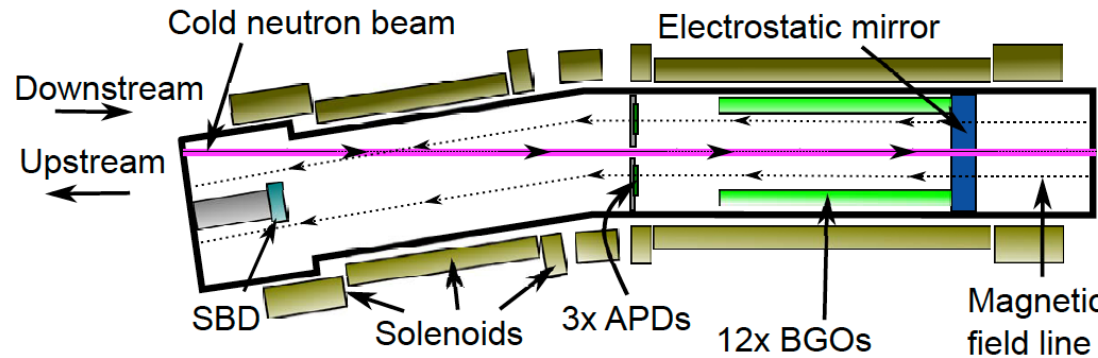


Motivation:

- Improve measurement of branching ratio and measure energy spectrum.
- Investigate a basic process in the fundamental semileptonic decay.
- Test QED in a weak process at 1% level.

courtesy of J. Nico

RDK II Experiment: Precision BR and Spectrum



RDK II Results:

- Measured radiative spectrum over 3 decades of energy using two detectors (400 eV to endpoint of 782 keV).
- Improved measurement of the branching ratio. Results consistent with theory.
- First measurement of the shape of the photon energy spectrum ($\approx 1\%$ level)

curtesy of J. Nico

Prospects with Radiative Decay

Future Possibilities:

- Improve precision to test chiral perturbation theory calculation and recoil order corrections.
- Determination of other correlations using photon as a tag.
- Novel ideas in radiative neutron decay:
 - photon polarization, *i.e.*, non V-A currents (Bernard *et al.*, PLB 2004)
 - examine new class of angular correlations

T-odd Momentum Correlation:

- Measure triple-product correlation of decay-product momenta $\mathbf{k}_e \cdot (\mathbf{k}_p \times \mathbf{K}_\gamma)$
- Correlation is P and T odd but spin independent; sensitive to sources of CP violation not constrained by EDMs (Gardner and He, *PRD* **86** (2012) and *PRD* **87** (2013))
- Possible experiments in neutron and nuclear (Ne-19, Ar-35) decay systems
- Experimentally, design **annular detector** (emiT-style) to detect neutron decay products with high efficiency and good solid angle coverage
- Mount experiment at **high-flux beam line** (e.g., NG-C gives x10 increase over NG-6)
- Avoid incremental improvements: investigate **new detector technologies** (e.g., bolometers)

T-odd landscape in n-decay

- In neutron decay correlation experiments, three major projects are expected to deliver T-odd observables:

emiT-III+T-oddRDK @NGC(NIST)

- Observable: **D** (ϕ_{AV} , ImS, ImT)
- Anticipated improvement x40 (compared to emiT-II) - entering sensitivity of $<10^{-5}$ (FSI will be visible)
- Basic techniques as in emit-II
- Possible development of detectors: cryogenic particle detection - join efforts with **T-oddRDK**
- Observable: **k_e·(k_p×K)** (CPV not constrained by EDMs)

BRAND @PF1B(ILL)/ESS

- Observables: **V** (ϕ_{AV} , ImS, ImT), **R** (ImS, ImT), **L** (ImS, ImT), **D** (ϕ_{AV} , ImS, ImT)
- Gradual improvement up to x30 (compared to nTRV) - (FSI will be visible)
- Basic techniques: combination of **emiT-II**, **Trine** and **nTRV**
- Systematic effects assessment via mapping, calibration and direct measurement (MC confirmed)
- Development of proton detectors
- T-even obs.: **a**, **A**, **B**, **H**, **N**, **S**, **U** (ReS, ReT),

Conclusions

- ❑ **emiT-III@NGC(NIST)** is oriented mainly towards better constraining ϕ_{AV}
- ❑ Relatively low-risk project; if funded, would improve current limit by factor of 5-10 in 4-5 years; further improvement depends on cryogenic particle detection
- ❑ **T-oddRDK@NGC(NIST)** is a pioneering experiment to search for CPV that cannot be constrained by EDM
- ❑ Largely depends on development of cryogenic particle detection - join efforts with emiT-III would be natural
- ❑ **BRAND@PF1B(ILL)/ESS** is devoted mainly to search for scalar and tensor currents
- ❑ “younger” than **emiT** - can be classified as **nTRV-II**
- ❑ Statistical sensitivity for **H, L, N, R, S, U** and **V** is 30 times lower than for **D**
- ❑ Statistical sensitivity for **D**-correlation in full size BRAND will be comparable to emiT-III
- ❑ **Complementarities and synergies:**
 - BRAND has main competition from: (i) HE $pp \rightarrow e + \text{MET}$ and (ii) spectrum shape (Fierz term) in n-decay
 - **emiT-III** and **BRAND** apply different strategies for assessment of systematic errors
 - Some of systematic effects in **emiT-III** and **BRAND** can be compared for e.g. **D**-coefficient
 - Planned R&D for proton detection towards reduction of the accelerating field is important for both projects

Backup slides

Neutron β -decay correlations

- For β transition with vector polarization of parent $\langle \mathbf{J} \rangle / J$
(e.g. neutron decay):

$$\begin{aligned}
 \partial\Gamma \sim & 1 + \mathbf{a} \frac{\mathbf{p}_e}{E_e} \cdot \frac{\mathbf{p}_{\bar{\nu}}}{E_{\bar{\nu}}} + \mathbf{b} \frac{m_e}{E_e} + \frac{\langle \mathbf{J} \rangle}{J} \cdot \left[\mathbf{A} \frac{\mathbf{p}_e}{E_e} + \mathbf{B} \frac{\mathbf{p}_{\bar{\nu}}}{E_{\bar{\nu}}} + \mathbf{D} \frac{\mathbf{p}_e}{E_e} \times \frac{\mathbf{p}_{\bar{\nu}}}{E_{\bar{\nu}}} \right] + \textcircled{...} \\
 & + \boldsymbol{\sigma} \cdot \left[\mathbf{G} \frac{\mathbf{p}_e}{E_e} + \mathbf{H} \frac{\mathbf{p}_{\bar{\nu}}}{E_{\bar{\nu}}} + \mathbf{K} \frac{\mathbf{p}_e}{E_e + m_e} \frac{\mathbf{p}_e}{E_e} \cdot \frac{\mathbf{p}_{\bar{\nu}}}{E_{\bar{\nu}}} + \mathbf{L} \frac{\mathbf{p}_e}{E_e} \times \frac{\mathbf{p}_{\bar{\nu}}}{E_{\bar{\nu}}} + \mathbf{N} \frac{\langle \mathbf{J} \rangle}{J} \right] \\
 & + \boldsymbol{\sigma} \cdot \left[\mathbf{Q} \frac{\mathbf{p}_e}{E_e + m_e} \frac{\langle \mathbf{J} \rangle}{J} \cdot \frac{\mathbf{p}_e}{E_e} + \mathbf{R} \frac{\langle \mathbf{J} \rangle}{J} \times \frac{\mathbf{p}_e}{E_e} + \mathbf{S} \frac{\langle \mathbf{J} \rangle}{J} \frac{\mathbf{p}_e}{E_e} \cdot \frac{\mathbf{p}_{\bar{\nu}}}{E_{\bar{\nu}}} + \mathbf{T} \frac{\mathbf{p}_e}{E_e} \frac{\langle \mathbf{J} \rangle}{J} \cdot \frac{\mathbf{p}_{\bar{\nu}}}{E_{\bar{\nu}}} \right] \\
 & + \boldsymbol{\sigma} \cdot \left[\mathbf{U} \frac{\mathbf{p}_{\bar{\nu}}}{E_{\bar{\nu}}} \frac{\langle \mathbf{J} \rangle}{J} \cdot \frac{\mathbf{p}_e}{E_e} + \mathbf{V} \frac{\mathbf{p}_{\bar{\nu}}}{E_{\bar{\nu}}} \times \frac{\langle \mathbf{J} \rangle}{J} + \mathbf{W} \frac{\mathbf{p}_e}{E_e + m_e} \frac{\langle \mathbf{J} \rangle}{J} \frac{\mathbf{p}_e}{E_e} \times \frac{\mathbf{p}_{\bar{\nu}}}{E_{\bar{\nu}}} \right]
 \end{aligned}$$


\mathbf{p}_e - electron momentum $\mathbf{p}_{\bar{\nu}}$ - neutrino momentum
 $\boldsymbol{\sigma}$ - electron spin sensing direction

J.D. Jackson et al., Phys. Rev. 106, 517 (1957); J.D. Jackson et al., Nucl. Phys. 4, 206 (1957);
M.E. Ebel et al., Nucl. Phys. 4, 213 (1957)

Suppression of sensitivity to $\text{Re}\mathbf{S}$ and $\text{Re}\mathbf{T}$

- Experimental correlation coefficients related to \mathbf{p} , \mathbf{q} , \mathbf{J} and $\boldsymbol{\sigma}$ are deduced from rate asymmetries:

$$ASY = \frac{\Gamma_1 - \Gamma_2}{\Gamma_1 + \Gamma_2}; \quad \mathbf{p} \rightarrow -\mathbf{p}, \quad \mathbf{q} \rightarrow -\mathbf{q}, \quad \mathbf{J} \rightarrow -\mathbf{J}, \quad \boldsymbol{\sigma}_\perp \rightarrow -\boldsymbol{\sigma}_\perp$$

- Instead of X experiments deliver

$$\begin{aligned} \tilde{X} = \frac{X}{\left(1 + \frac{\mathbf{b} m_e}{E_e}\right)} &\simeq X_{\text{SM}} + X_{\text{FSI}} + \boxed{c_{\text{Re}\mathbf{S}}^X - c_{\text{Re}\mathbf{S}}^b} \frac{X_{\text{SM}} + X_{\text{FSI}}}{X_{\text{SM}} + X_{\text{FSI}}} \text{Re}\mathbf{S} \\ &+ \boxed{c_{\text{Re}\mathbf{T}}^X - c_{\text{Re}\mathbf{T}}^b} \frac{X_{\text{SM}} + X_{\text{FSI}}}{X_{\text{SM}} + X_{\text{FSI}}} \text{Re}\mathbf{T} + c_{\text{Im}\mathbf{S}}^X \text{Im}\mathbf{S} + c_{\text{Im}\mathbf{T}}^X \text{Im}\mathbf{T} \end{aligned}$$

- May significantly decrease sensitivity to $\text{Re}\mathbf{S}$, $\text{Re}\mathbf{T}$
(e.g. coefficient \mathbf{B} - complete cancellation in pure transitions)
- If $X_{V-A} + X_{\text{FSI}} \approx 0$, cancellation effects are insignificant !!!

Systematic effects

□ Depolarization by multiple Coulomb scattering

- From deviations between experimental data (120 keV, 14 MeV) and theory (ELSEPA+Geant4) - presently on 1-2% level
- Can be improved by dedicated measurements with polarized electron beam
in the energy range 100-800 keV be neglected

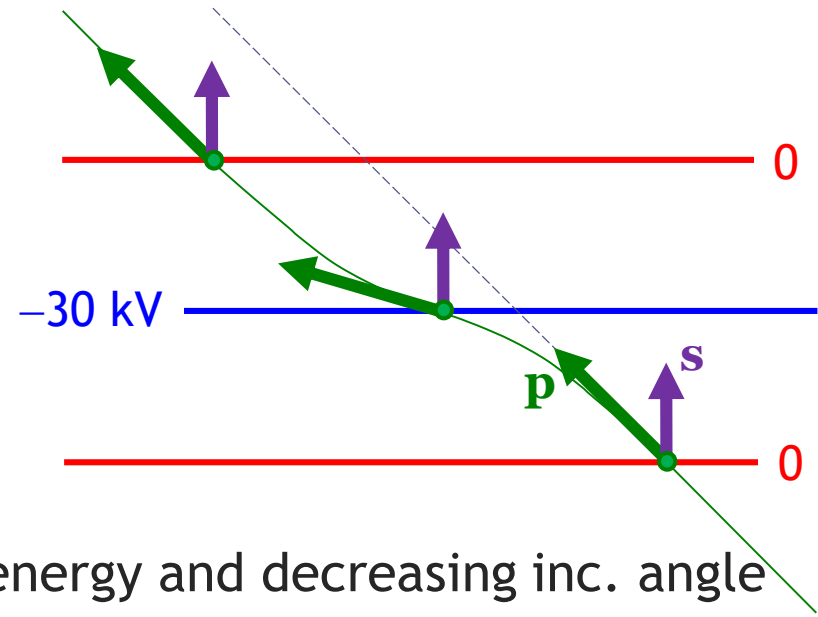
□ „g-2 effect”

- 7 mrad per revolution de-synchronization between spin and momentum
- For 1 mT magnetic field strength – can be neglected
- **Transverse electron polarization related observables cannot be measured in strong magnetic field !**

Systematic effects (cont.)

□ Momentum rotation in external electric field of *pe*-converter

- In uniform field step of 30 kV, incident energy of 100 keV and angle of 45° , momentum vector rotates by about 12°
- Effect decreases with increasing energy and decreasing inc. angle
- In symmetric barrier (e.g. 0–30–0 kV) of uniform field the effect cancels exactly
- It cancels also in asymmetric field barrier, if symmetrically sampled by incidence angles of electrons
- Symmetric barrier appears, if recoil protons are detected using *pe* conversion technique



BRAND summary

- ❑ BRAND project offers systematic exploration of the transverse electron polarization correlation coefficients R, N, H, L, S, U, V in neutron β decay (H, L, S, U, V were never measured before)
- ❑ Combined impact of R, N, H, L, S, U, V on BSM physics is comparable (or better) to Fierz term b and reveals completely different systematics
- ❑ “HE approach” (tracking, vertex reconstruction) allows to measure in low magnetic field which is necessary for transverse electron polarization)
- ❑ Simultaneous measurement of “classical” coefficients a, A, B and D will provide consistency check and comparison of systematic effects specific to high– and low–magnetic field techniques
- ❑ Experiment is challenging and not free of risks, however, most of critical techniques were experimentaly verified in pioneering project nTRV@PSI
- ❑ Conservative planning and proposed step-by-step approach (3 subsequent phases) mitigate risk of failure

Planning

	BRAND I	BRAND II	BRAND III
Site	ILL Grenoble	ILL Grenoble	ESS Lund
Time	3 - 4 years	3 - 4 years	5-6 years
Pressure	Ambient	Ambient	300 mbar
Mott target	Pb (Au)	Pb (Au)	Depleted U
Coverage of azimuthal angle	1/6	Full	Full
Statistical precision (goal)			
<i>A</i>	0.0008	0.00008	0.000016
<i>a, B, D</i>	0.005	0.0005	0.0001
<i>R, N</i>	0.01	0.001	0.0002
<i>H, L, S, U, V</i>	0.02	0.002	0.0004
Systematic errors			
<i>R, N, H, L, S, U, V</i>	0.002	0.001	0.0005

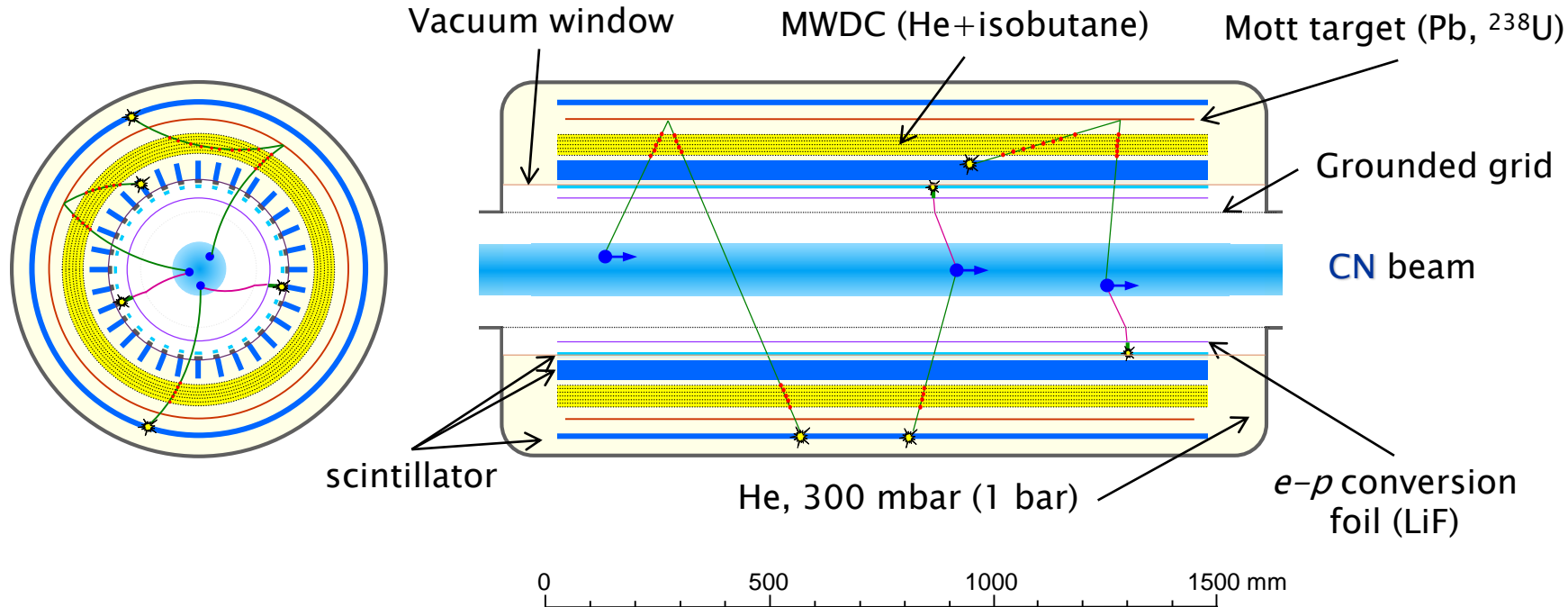
Collaboration and commitments

❑ Presently BRAND collaboration consists of:

- JU Krakow: K. Bodek¹⁾, D. Rozpedzik, J. Zejma¹⁾, K. Lojek:
e- and p-detectors, front end electronics and DAQ, simulations
- INP PAS Krakow: A. Kozela¹⁾, K. Pysz & Co.:
mechanical structure, vacuum window, MWDC tracker, Mott target, Slow Control
- ILL Grenoble: T. Soldner:
polarized CN beam and infrastructure, vacuum
- KU Leuven: N. Severijns¹⁾ & Co.:
guiding magnetic field
- NCSU Raleigh: A.R. Young (?):
pe-converter film
- ...

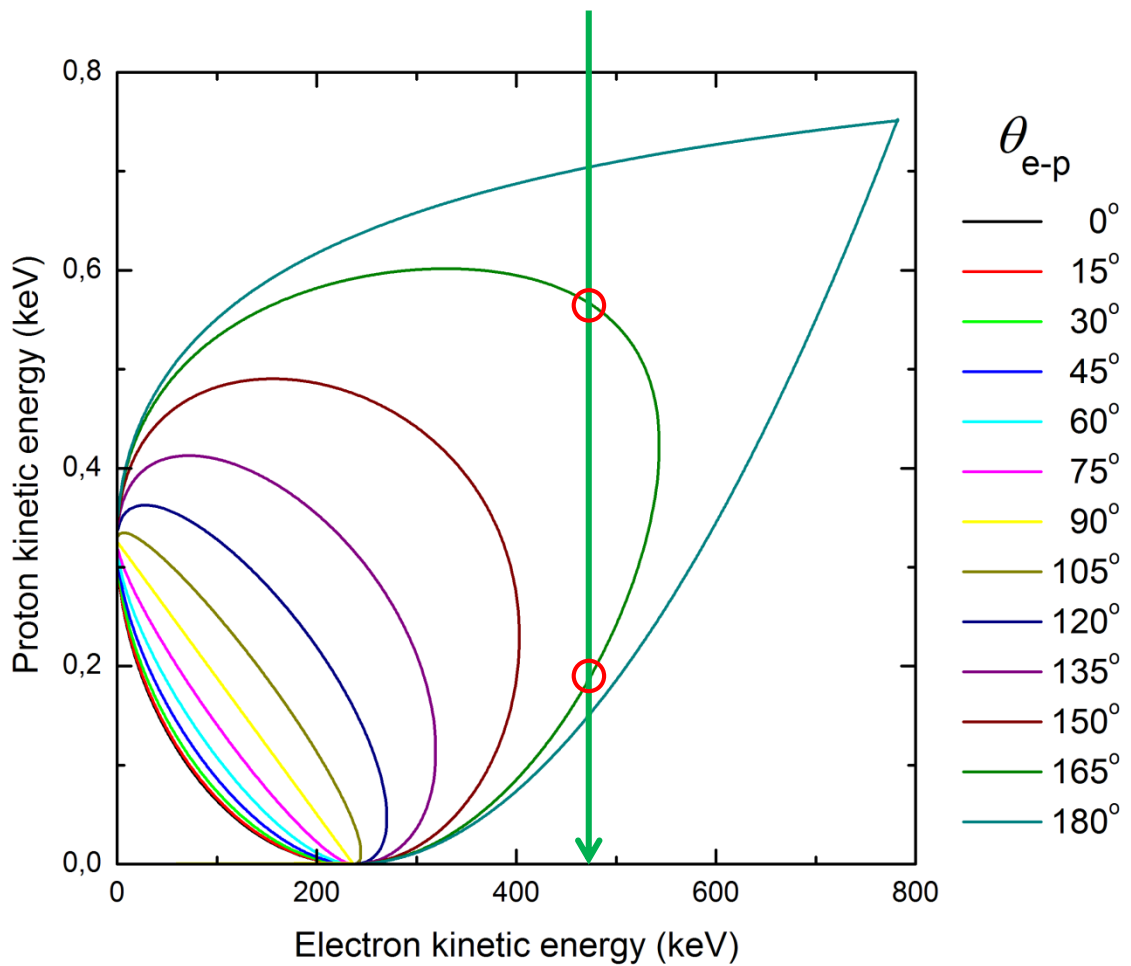
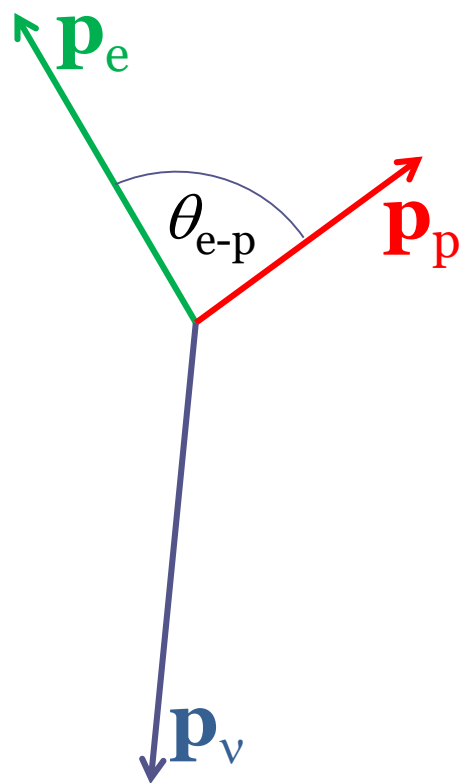
¹⁾ Members of nTRV@PSI

BRAND - layout



- BRAND I, II:
 - ILL, DC beam, pressure 1 bar, Pb target
- BRAND III:
 - ESS, pulsed beam, pressure 300 mbar, depleted U target

n-decay kinematics



Reconstruction of momenta

Actual position of the decay vertex
is not known

But:

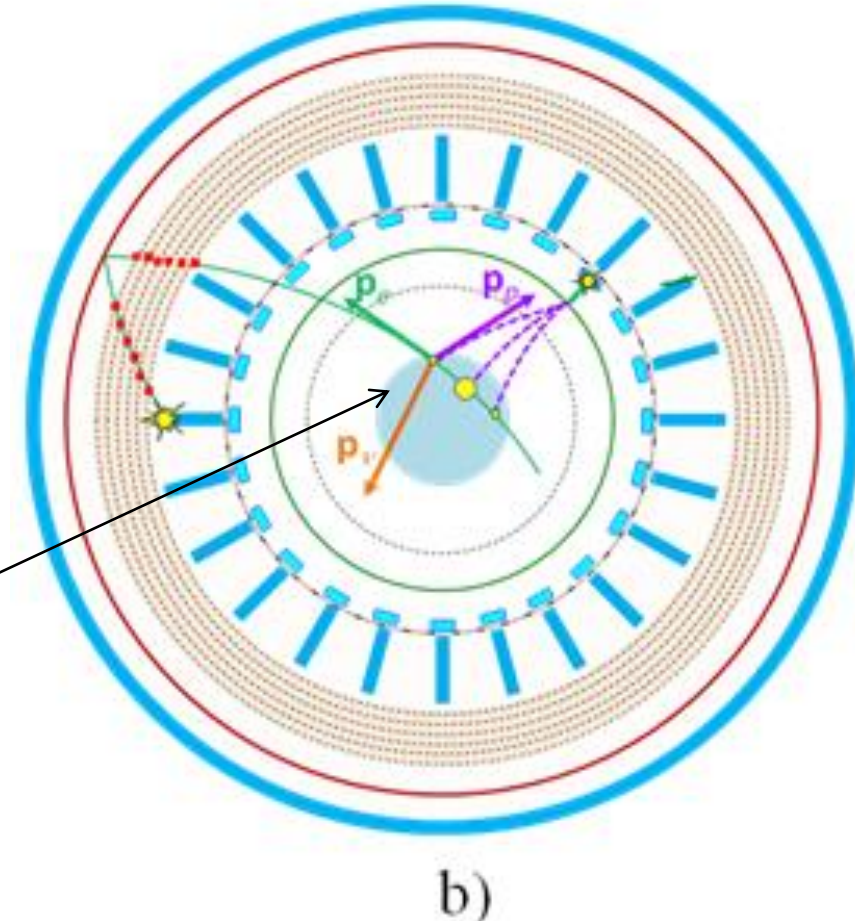
It **must be located** on the electron
trajectory segment coincident with
the beam

Neutron decay density
distribution in the
beam **is known**

Finally:

In extraction of correlation
coefficients we sum over momenta
ambiguity in vertex position is not
essential

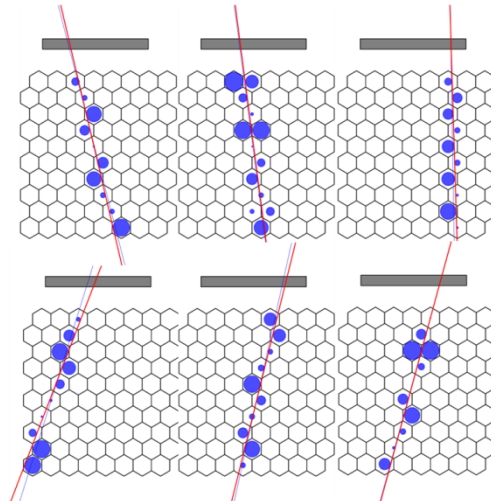
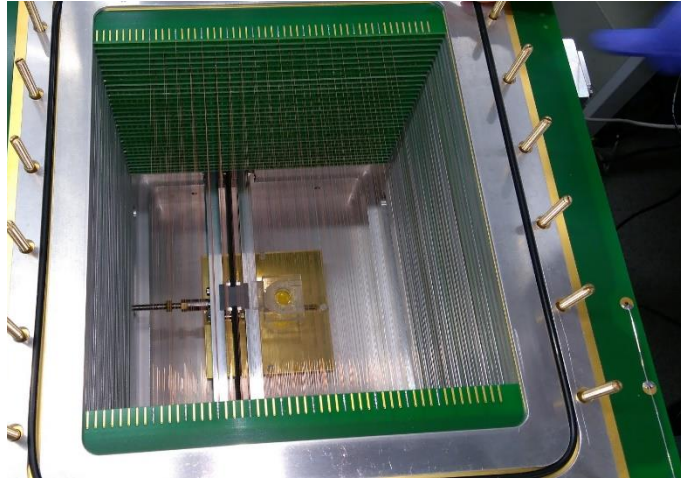
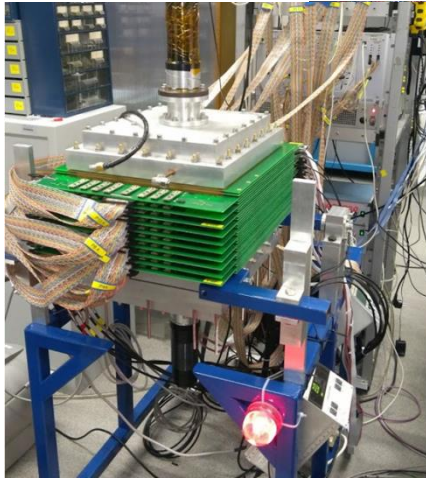
Principle of vertex reconstruction with
3-body kinematics



Assigned weight is proportional
to the decay rate density

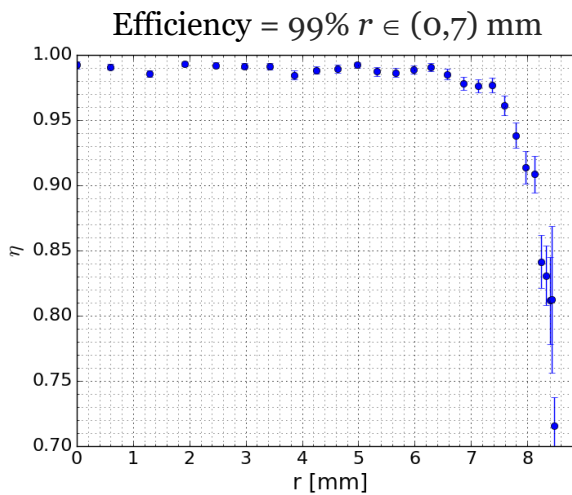
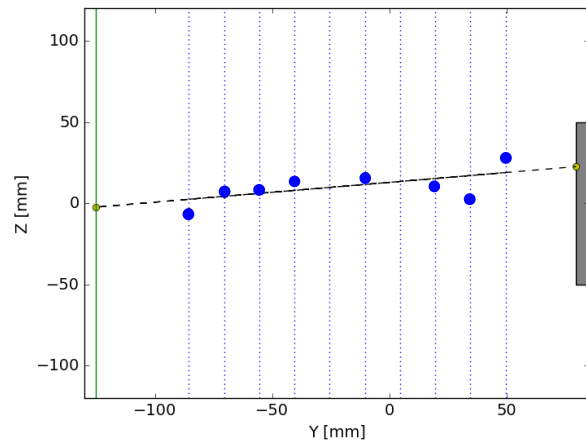
R&D: MWDC

hexagonal, low pressure, low Z, charge division



From drift time: $\Delta r = 0.5 \text{ mm}$

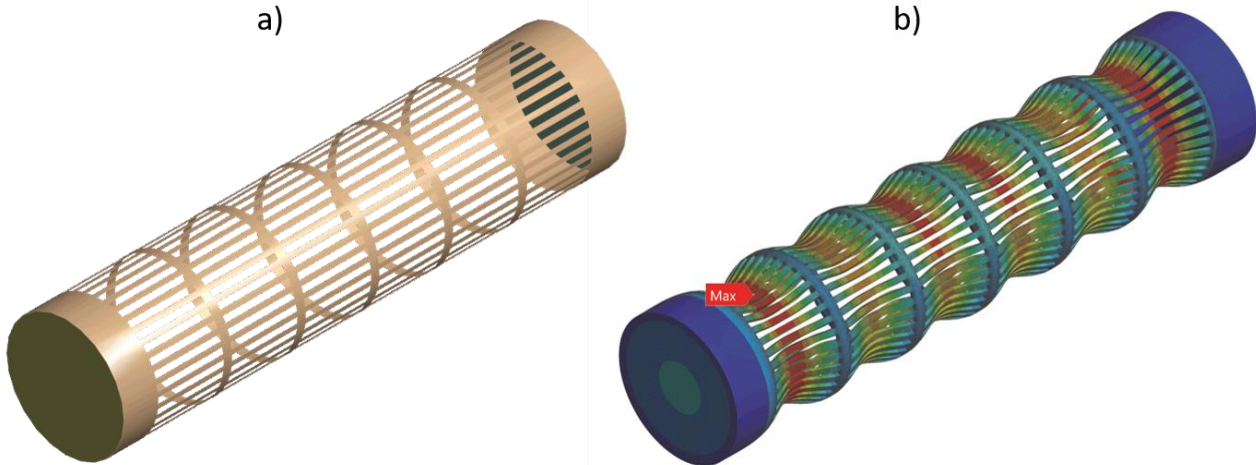
From charge division: $\Delta z/z = 0.02$



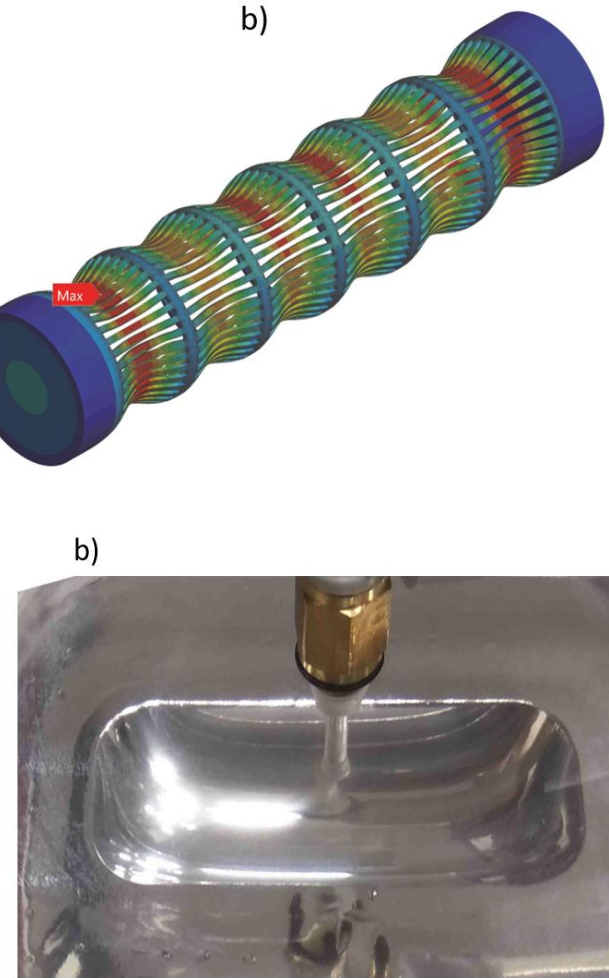
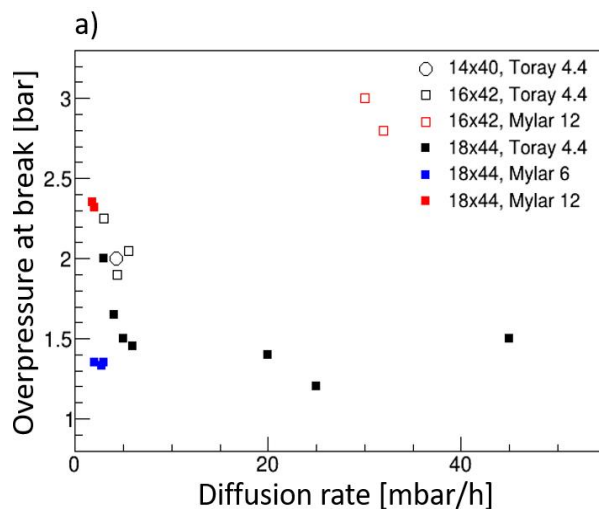
- Expected Mott vertex position uncertainty:
 $\Delta r = 2 \text{ mm}$, $\Delta z = 2 \text{ cm}$;
 $\theta_{\text{Mott}} \in (100^\circ - 150^\circ)$
- Expected significant reduction of uncertainty due to background subtraction (> 10)

R&D: Vacuum window prototype tests

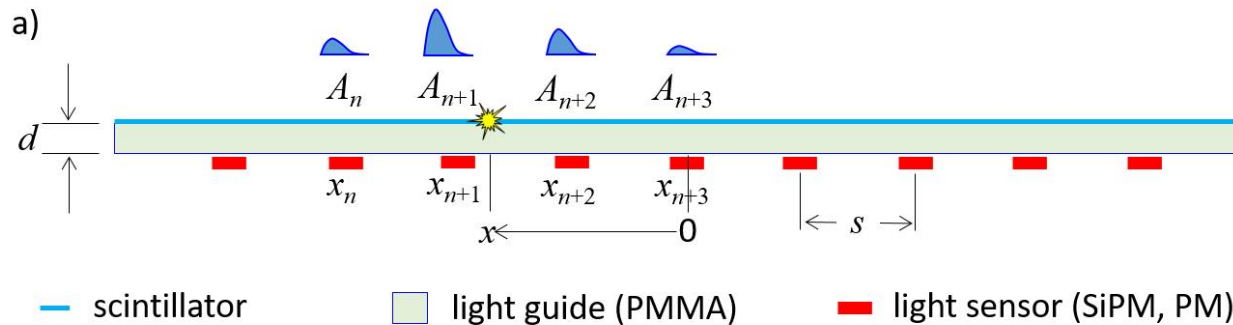
- ❑ AMSYS simulations of mechanical stability



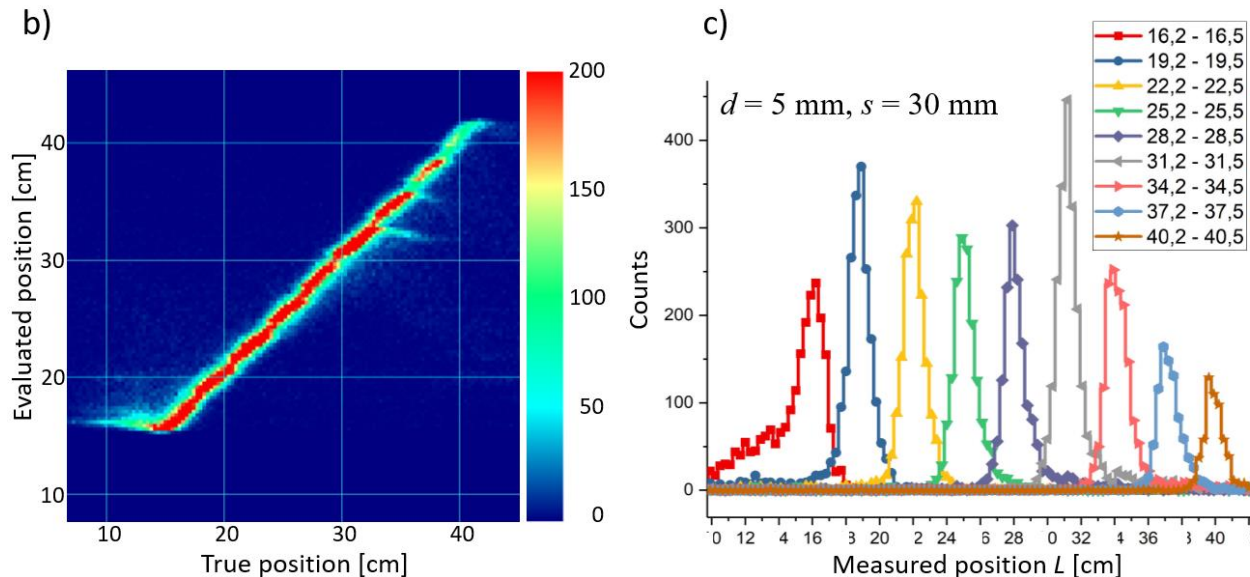
- ❑ Windows sustain overpressure of 1.5 - 2.5 b before rapture
- ❑ Long term stability and leakage rate tests ongoing



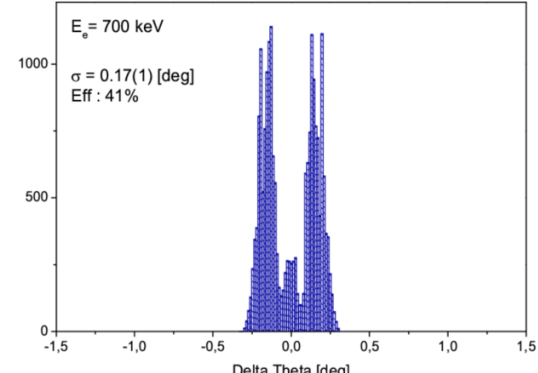
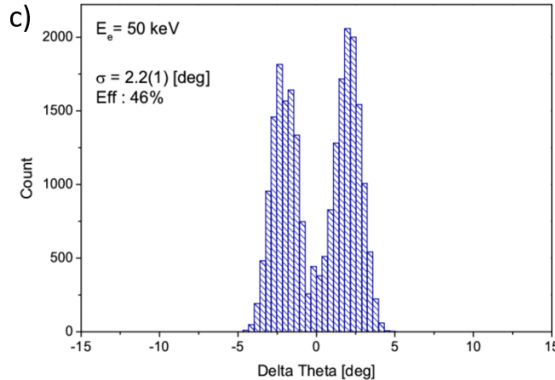
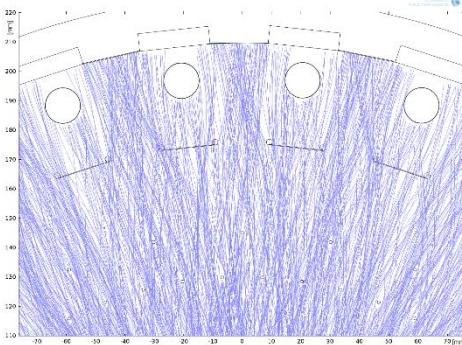
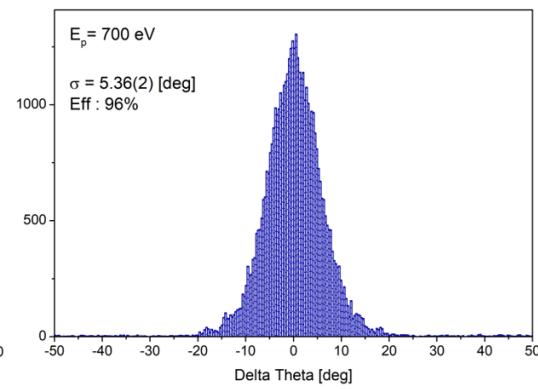
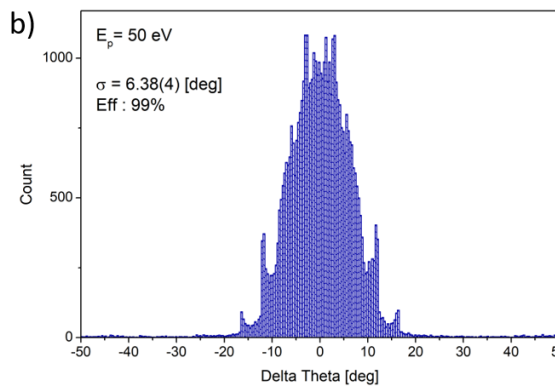
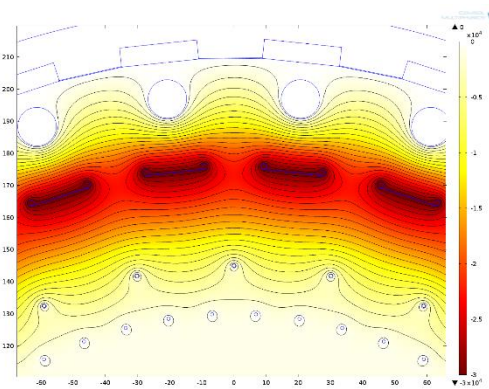
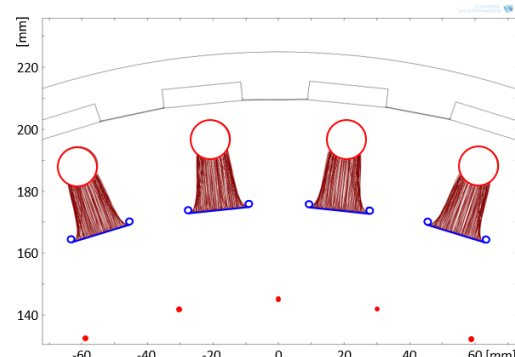
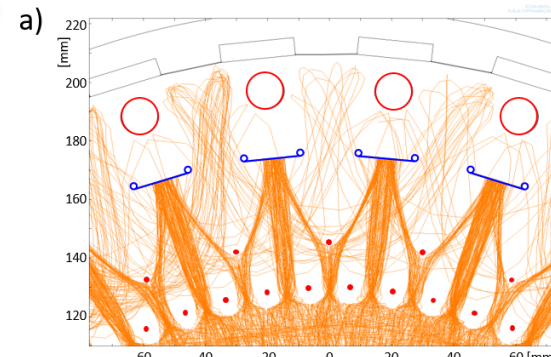
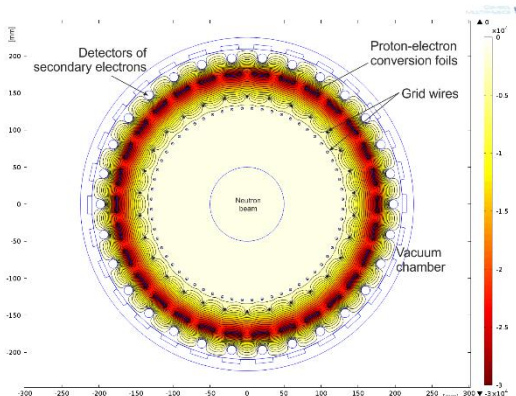
R&D: „Proton” detector



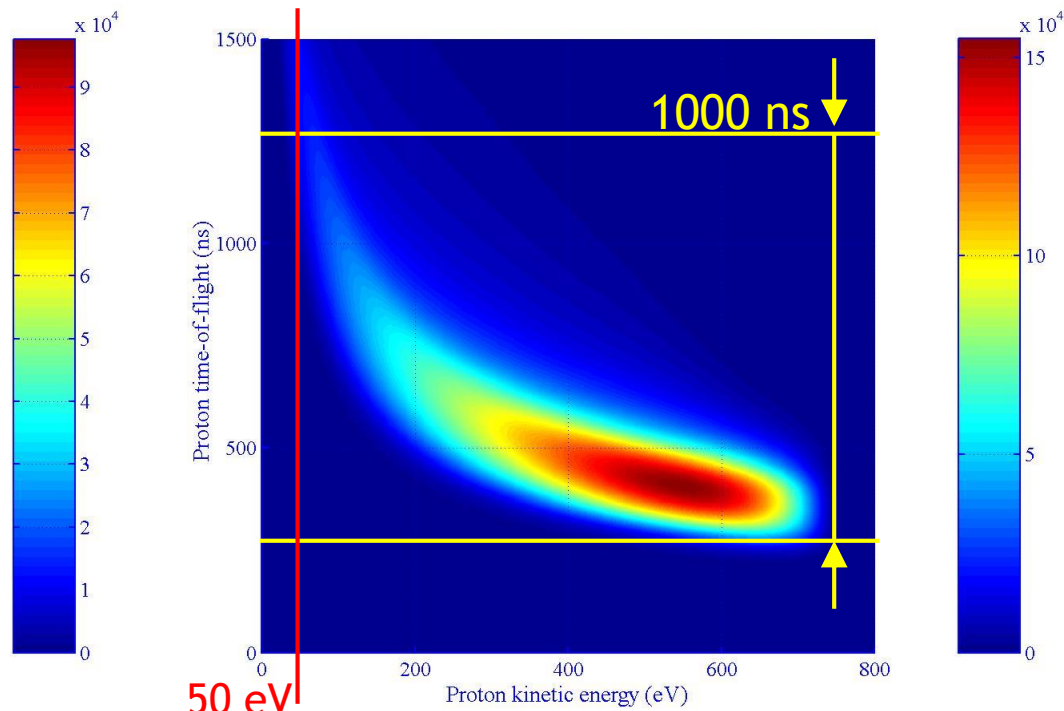
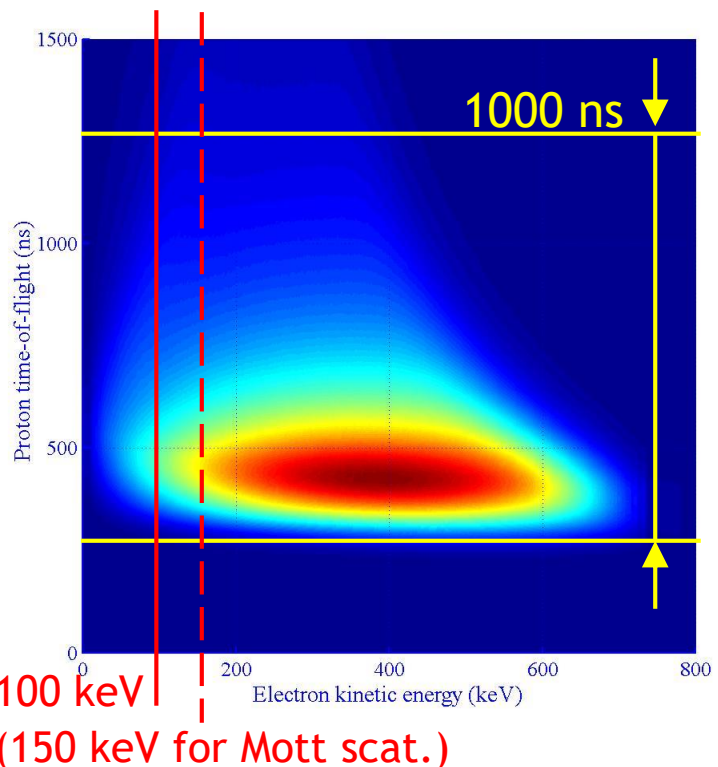
$$x = \sum A_i x_i / \sum A_i$$



COMSOL simulations



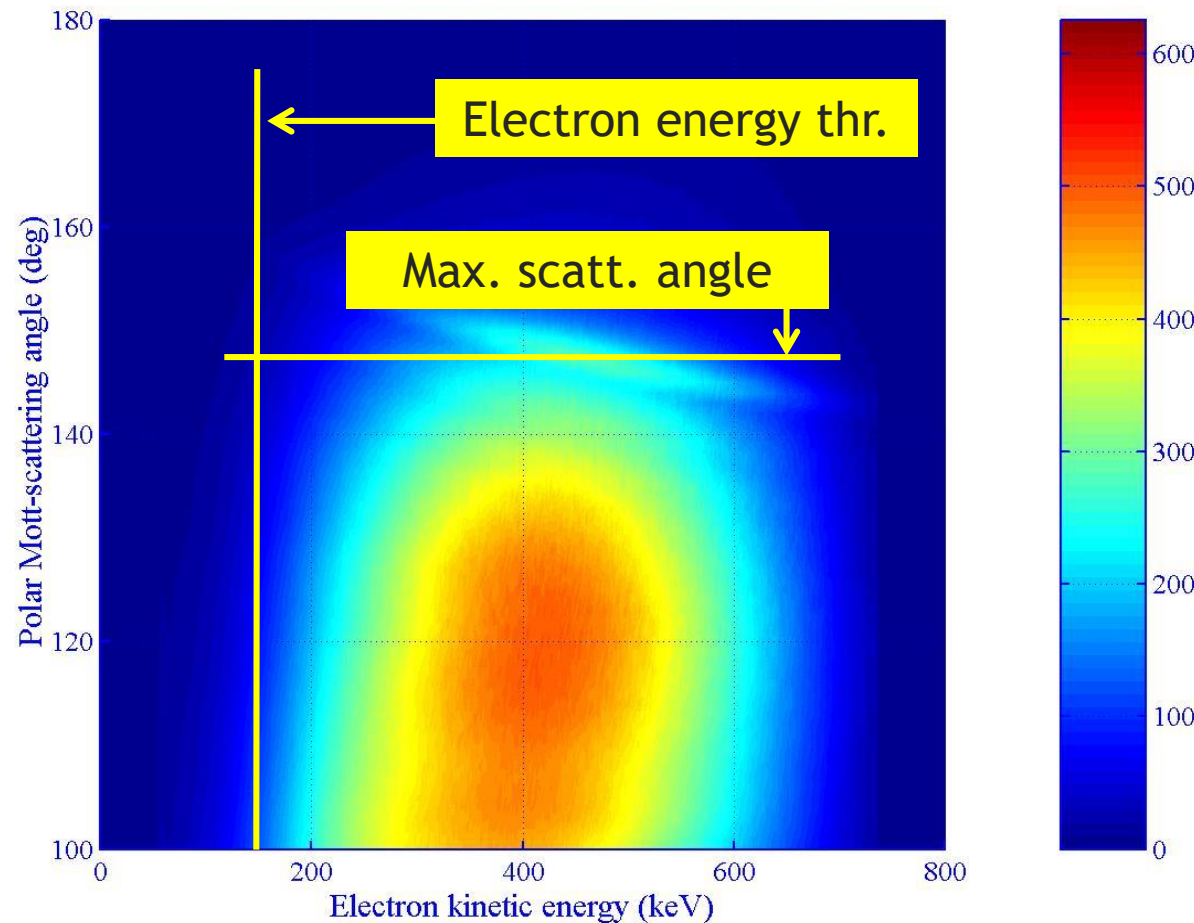
n-decay kinematics



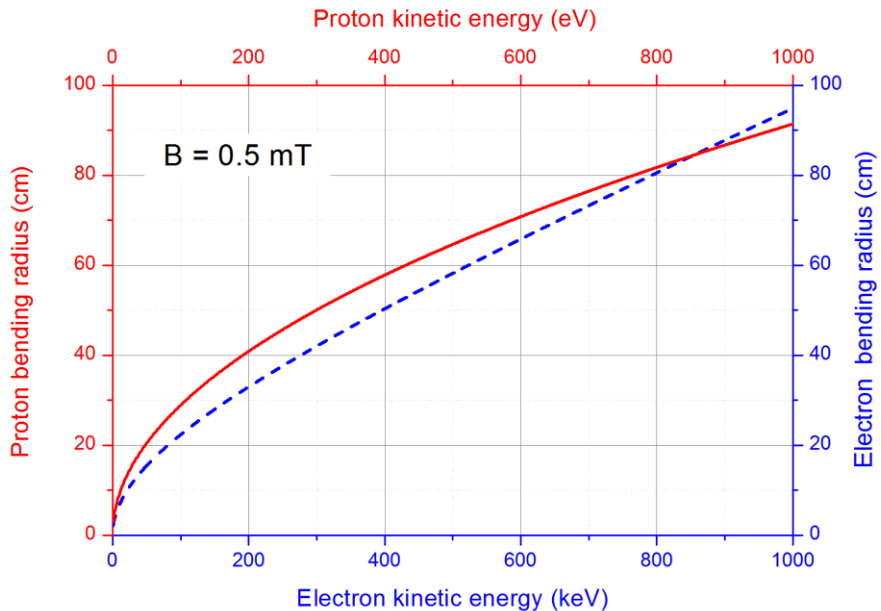
- ❑ Measured electron energy, reconstructed proton flight path and measured proton time-of-flight **must match !**
- ❑ Constraints from 3-body kinematics will considerably **reduce coincidence time**
- ❑ With **10⁵** decays per second: single rate (per wire) < 1 kHz

Figure-of-Merit for Mott scattering

$$FoM = \sqrt{\sigma_{\text{Mott}} \cdot (S_{\text{Mott}}^{\text{eff}})^2}$$

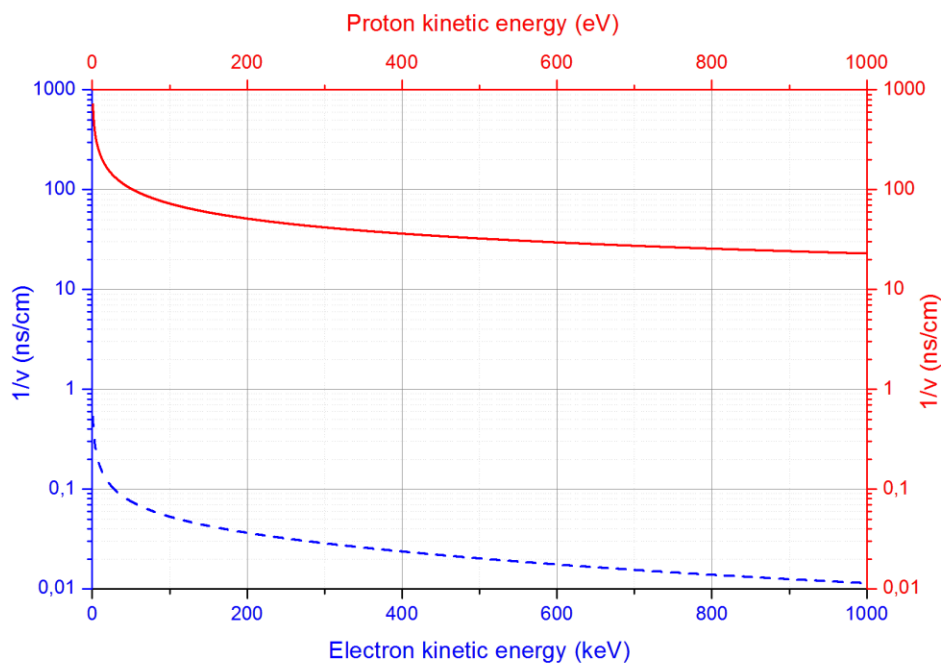


Electron and proton trajectories and ToF

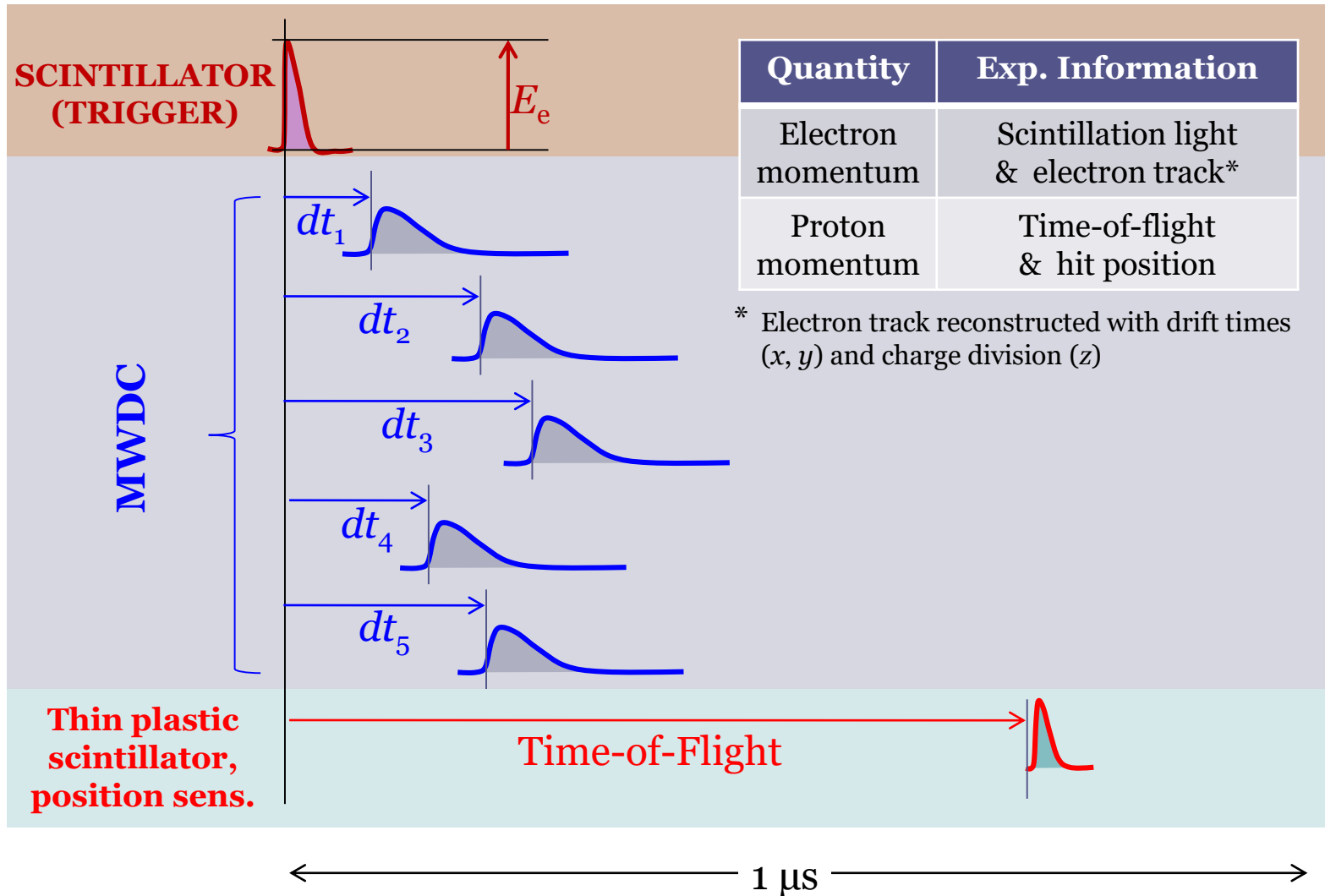


$p-e$ Time-of-Flight difference ranges from 20 to 100 ns (per 1 cm drift path) for interesting proton energy range 50÷800 eV

Bending radii of protons and electrons are similar in the interesting energy ranges:
50÷800 eV for protons and
50÷800 keV for electrons



DAQ



BRAND 0 - test setup

- ❑ Devoted for extensive on-line tests of critical components and beam optimization
- ❑ Should be operational by late Summer 2018

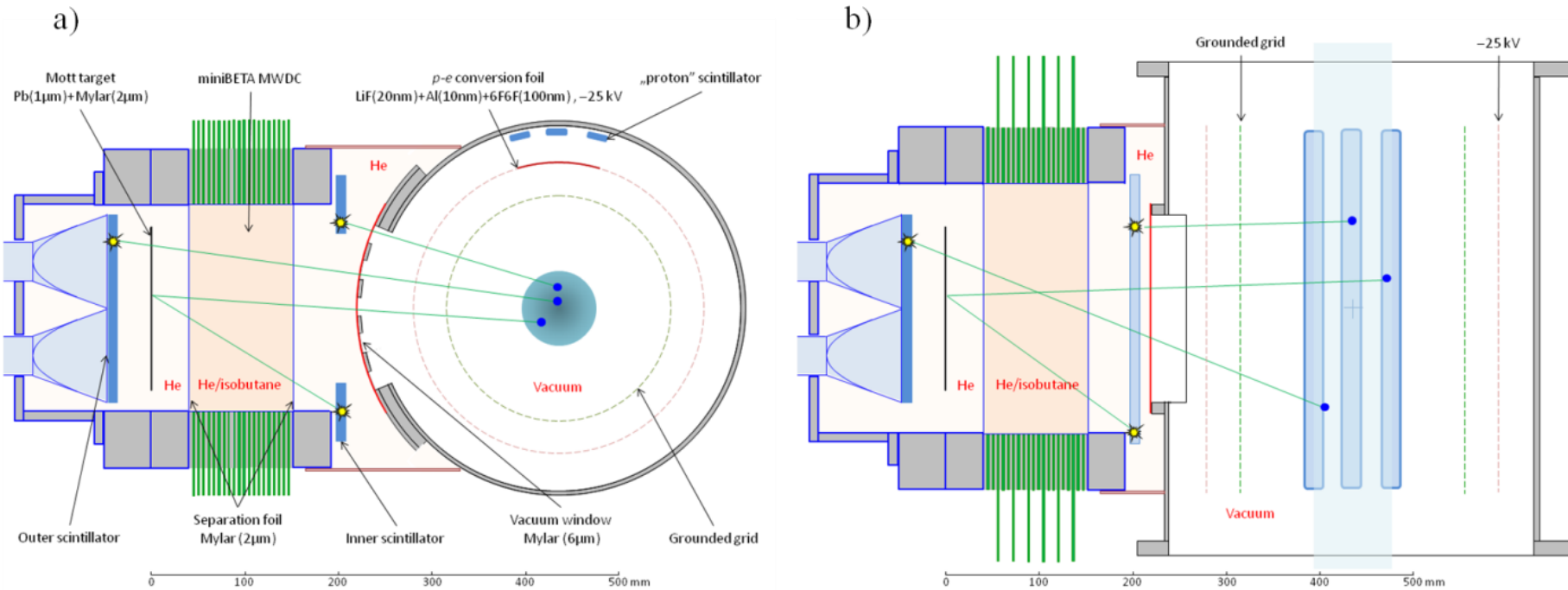


Figure 8: Layout of the test experiment “BRAND 0”. a) Cross section in the plane perpendicular to the beam axis. b) Cross section in the plane containing the beam axis.

FUNSPIN - Polarized Cold Neutron Facility at PSI

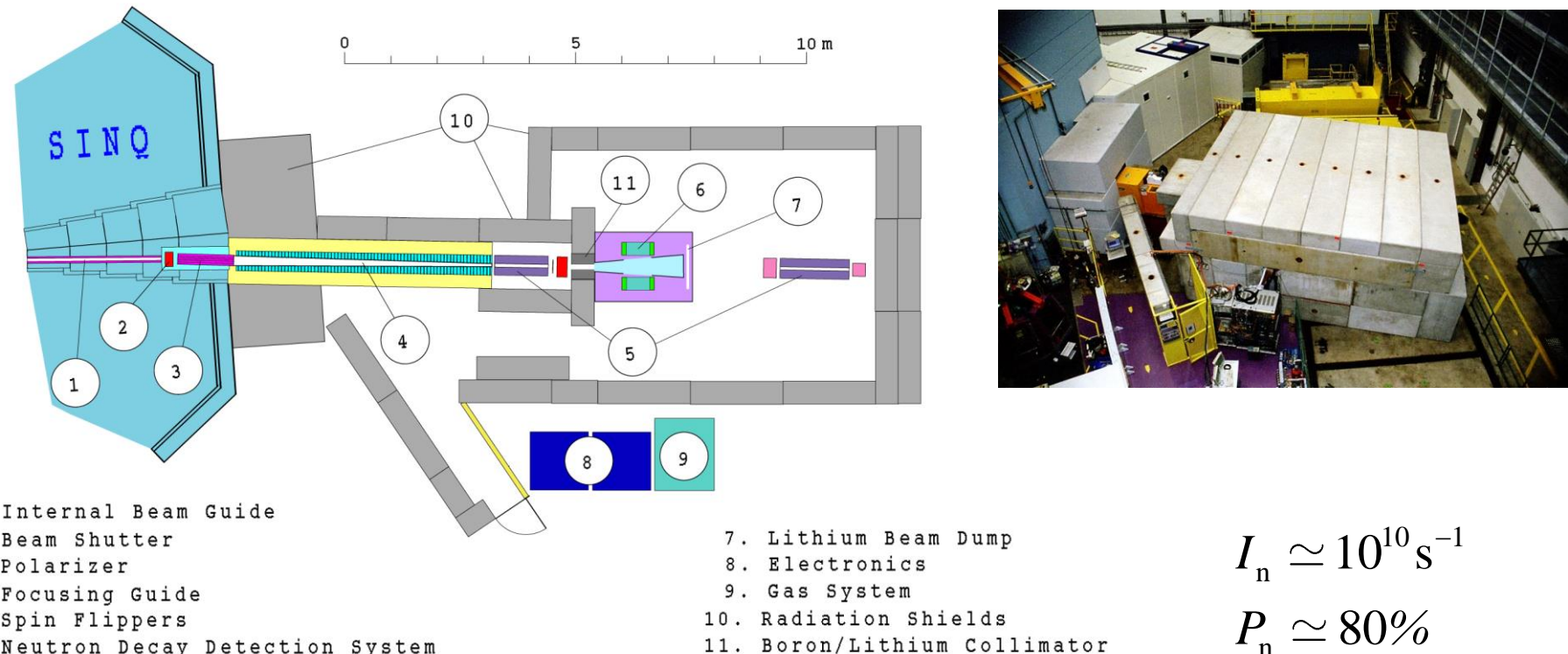
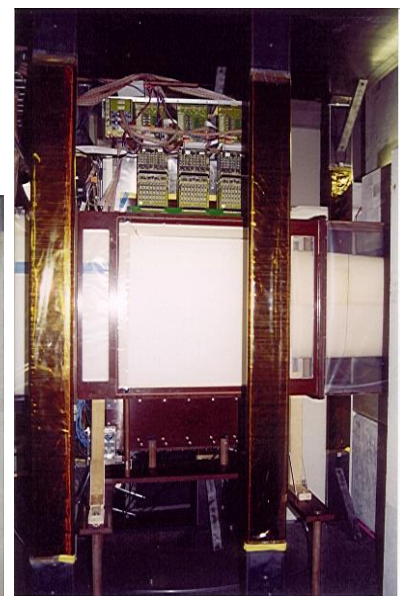
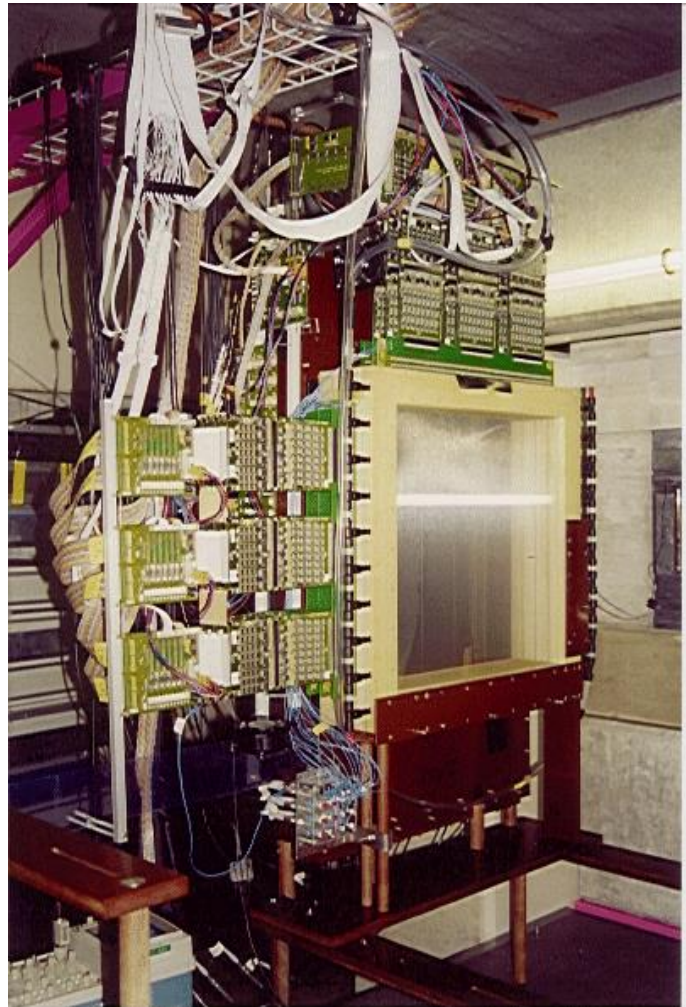
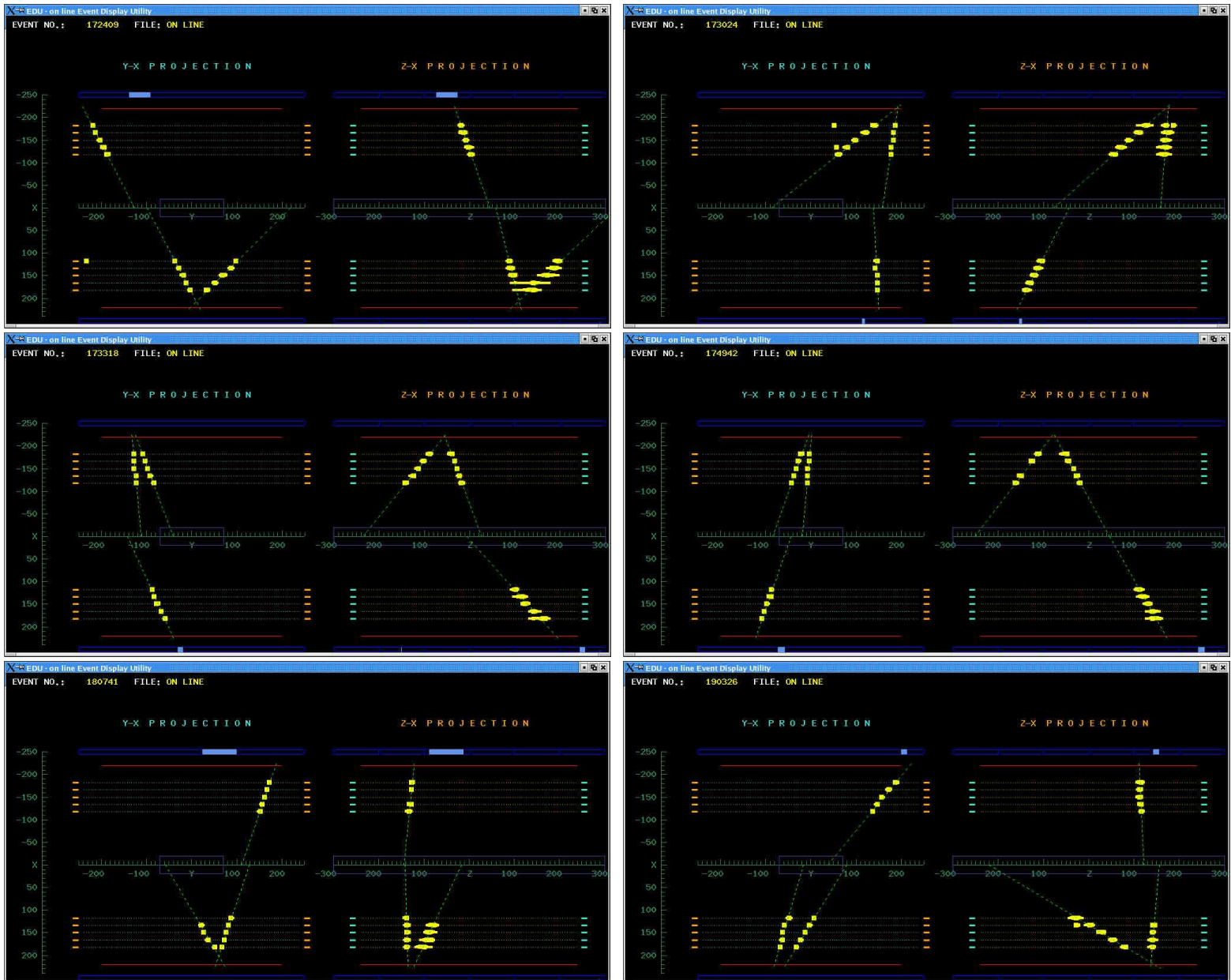


Figure 4: Layout of the Polarized Cold Neutron Facility at PSI.

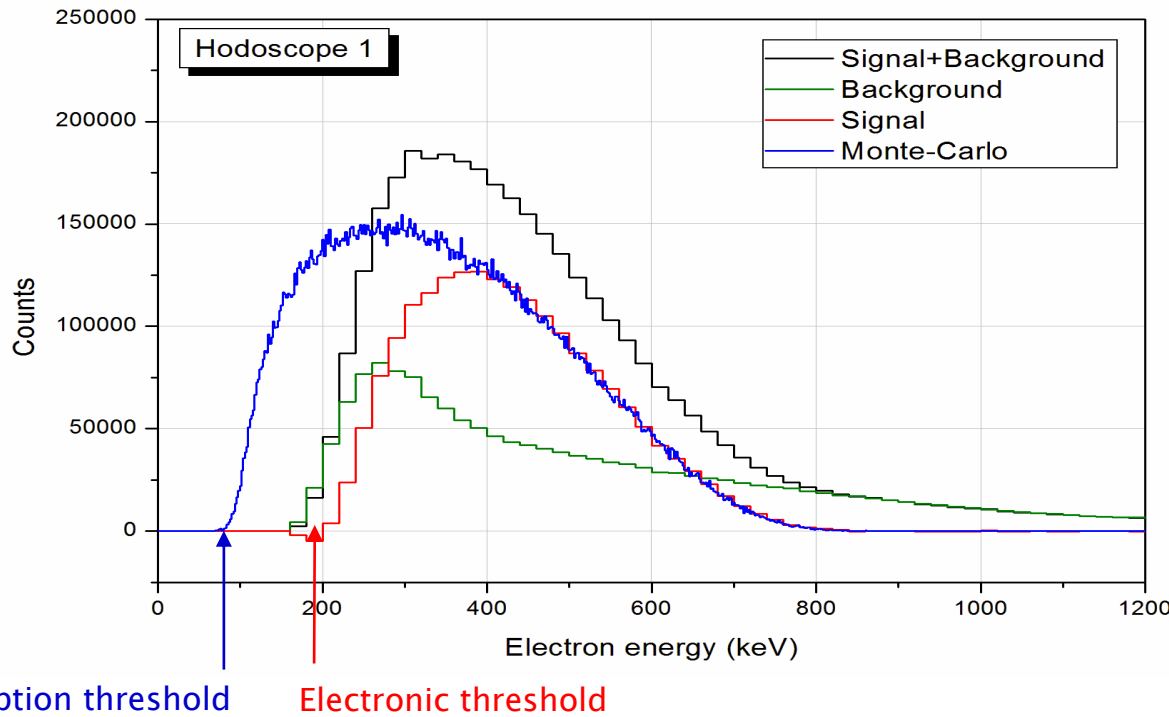
nTRV@PSI - MWPCs, scintillators and electronics



“ ν -track” events - on-line display



nTRV@PSI: Background subtraction



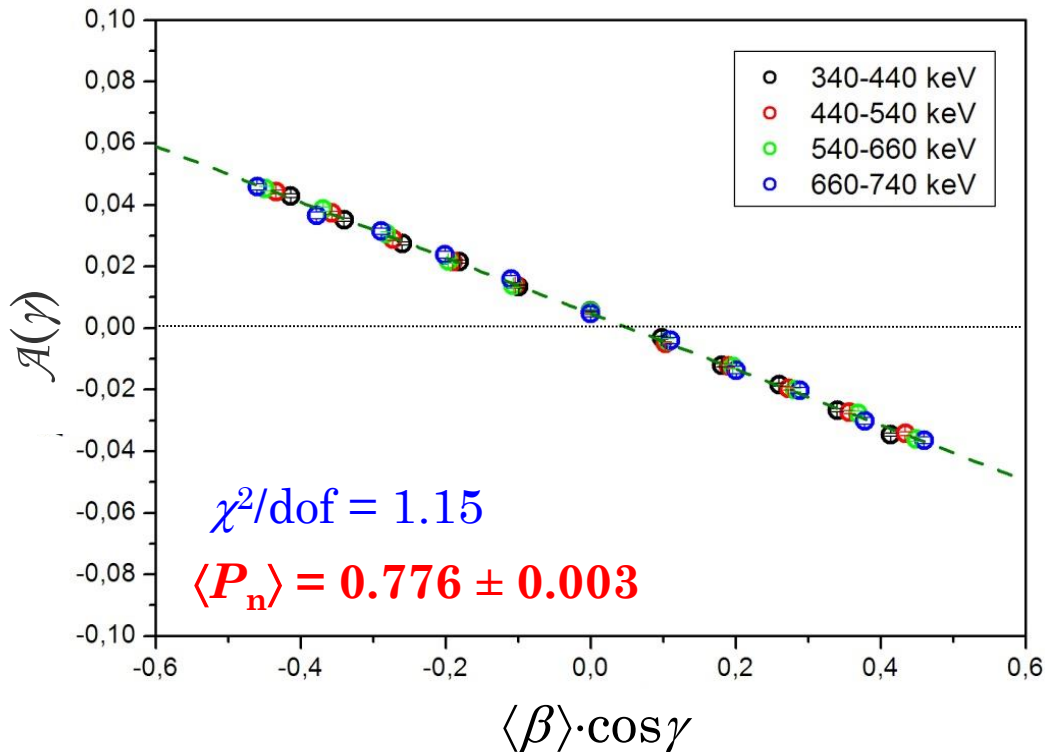
□ Observations:

- Spectral distribution of background depends weakly on the electron origin
- Substantial contribution from prompt electrons

nTRV@PSI: Neutron polarization from decay asymmetry

$$\mathcal{A}(\gamma) \equiv \frac{N(\gamma, +P_n) - N(\gamma, -P_n)}{N(\gamma, +P_n) + N(\gamma, -P_n)} = \langle P_n \rangle \ A_n \langle \beta \rangle \cos \gamma$$

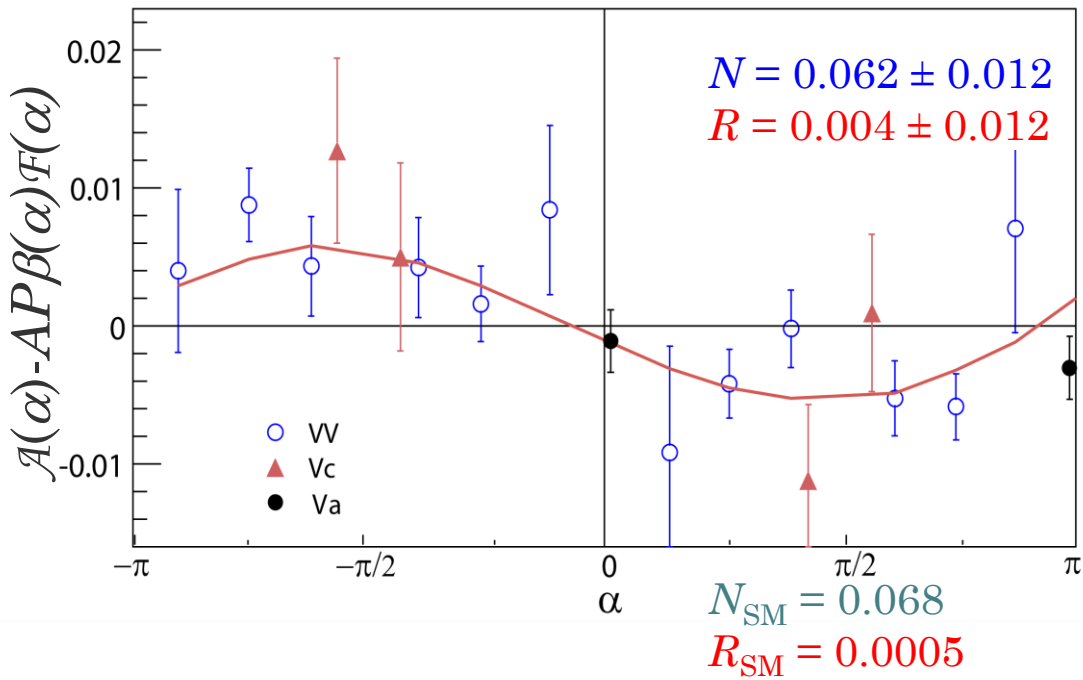
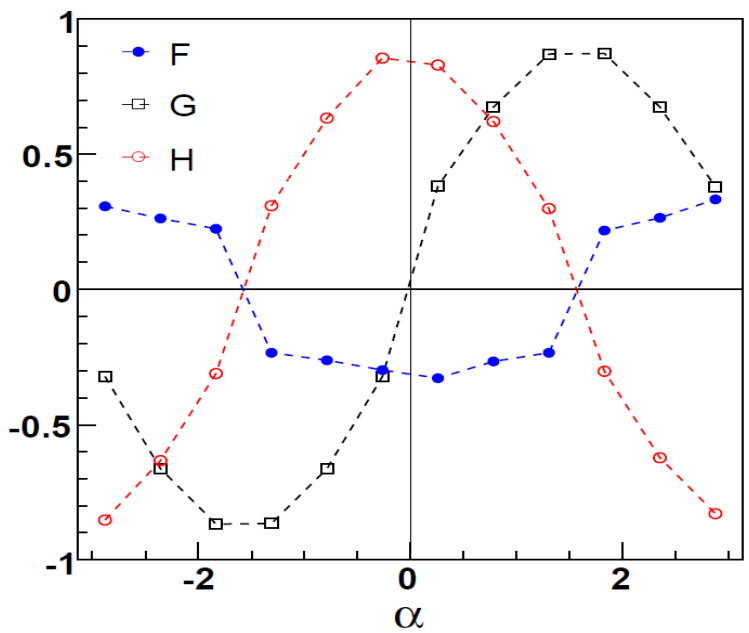
$$A_n = -0.1173$$



- o Average neutron polarization from decay rate asymmetry (“single-track” events)

Effective kinematical factors

$$\begin{aligned}\mathcal{A}(\alpha) &= \frac{n(+P, \alpha) - n(-P, \alpha)}{n(+P, \alpha) + n(-P, \alpha)} \\ &= \textcolor{green}{A} P \beta(\alpha) F(\alpha) + P S(\alpha) [\textcolor{blue}{N} G(\alpha) + \textcolor{red}{R} \beta(\alpha) \mathcal{H}(\alpha)]\end{aligned}$$



nTRV@PSI: Observables

$$\begin{aligned}\mathcal{A}(\alpha) &= \frac{n(+P, \alpha) - n(-P, \alpha)}{n(+P, \alpha) + n(-P, \alpha)} \\ &= \textcolor{green}{A} P \beta(\alpha) \mathcal{F}(\alpha) + P S(\alpha) [\textcolor{blue}{N} G(\alpha) + \textcolor{red}{R} \beta(\alpha) \mathcal{H}(\alpha)]\end{aligned}$$

$$\begin{aligned}S(|\alpha|) &\equiv \frac{\sqrt{n(+P, +\alpha)n(-P, -\alpha)} - \sqrt{n(+P, -\alpha)n(-P, +\alpha)}}{\sqrt{n(+P, +\alpha)n(-P, -\alpha)} + \sqrt{n(+P, -\alpha)n(-P, +\alpha)}} \\ &= \textcolor{blue}{N} \frac{PSG(|\alpha|)}{\beta(|\alpha|)(1 - A^2 P^2 \beta^2(|\alpha|) \mathcal{F}^2(|\alpha|))}\end{aligned}$$

$$\begin{aligned}\mathcal{U}(|\alpha|) &\equiv \frac{\sqrt{n(+P, +\alpha)n(+P, -\alpha)} - \sqrt{n(-P, +\alpha)n(-P, -\alpha)}}{\sqrt{n(+P, +\alpha)n(+P, -\alpha)} + \sqrt{n(-P, +\alpha)n(-P, -\alpha)}} \\ &= AP\beta(|\alpha|) \mathcal{F}(|\alpha|) + \textcolor{red}{R} PS(|\alpha|) \mathcal{H}(|\alpha|)\end{aligned}$$

nTRV@PSI - final results

A. Kozela et al., Phys. Rev. C 85, 045501 (2012)

Run	Sign.	$\Sigma (n^+ + n^-)$	$P \times 10^2$
2003	VV	19000	$80.3 \pm 1.3 \pm 1.6$
2004	VV	74000	$44.2 \pm 0.4 \pm 1.5$
2006	VV	312000	$80.0 \pm 1.0 \pm 1.5$
2006	V	111000	$80.0 \pm 1.0 \pm 1.5$
2007	VV	1747000	$77.4 \pm 0.2 \pm 0.7$
2007	V	711000	$77.4 \pm 0.2 \pm 0.7$
Total		2974000	

Run	Sign.	$N \times 10^3$ (Eq. 2)	$N \times 10^3$ (Eq. 3)	$R \times 10^3$ (Eq. 2)	$R \times 10^3$ (Eq. 4)
2003	VV	$89 \pm 92 \pm 31$	$139 \pm 124 \pm 27$	$-90 \pm 137 \pm 42$	$-55 \pm 152 \pm 42$
2004	VV	$74 \pm 80 \pm 17$	$171 \pm 103 \pm 15$	$-14 \pm 131 \pm 30$	$-58 \pm 146 \pm 30$
2006	VV	$94 \pm 35 \pm 10$	$97 \pm 35 \pm 10$	$-13 \pm 48 \pm 10$	$-36 \pm 48 \pm 12$
2006	V			$-50 \pm 55 \pm 21$	
2007	VV	$59 \pm 13 \pm 5$	$63 \pm 14 \pm 5$	$13 \pm 18 \pm 6$	$-5 \pm 18 \pm 6$
2007	V			$9 \pm 20 \pm 13$	
Total		$64 \pm 12 \pm 4$	$69 \pm 13 \pm 4$	$5 \pm 13 \pm 5$	$-10 \pm 17 \pm 5$

$$N_{SM} \times 10^3 = 68 \pm 1$$

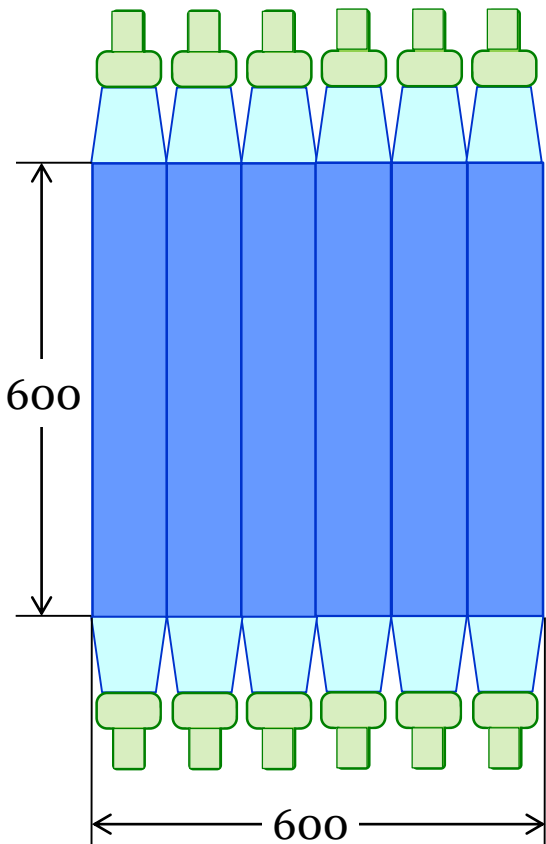
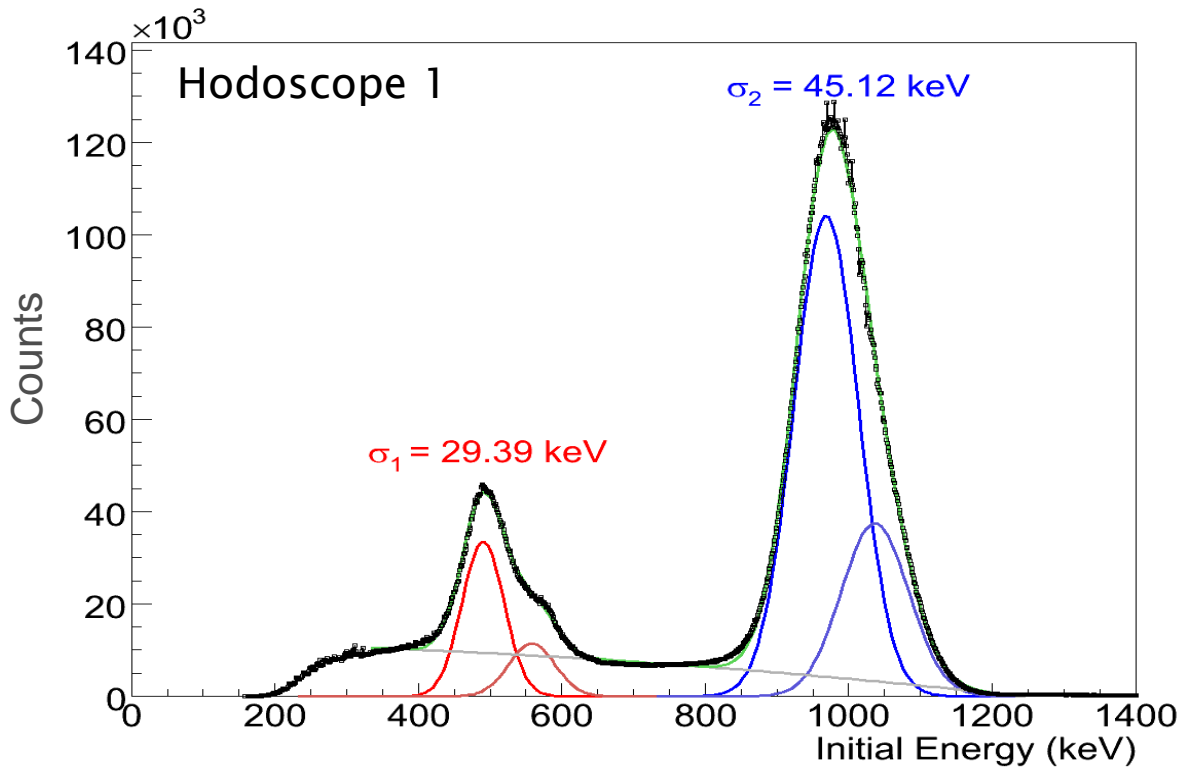
$$R_{SM} \times 10^3 = 0.5$$

Electron tracking, vertex reconstruction

- ❑ Unavoidable for electron spin analysis in Mott scattering
- ❑ Allows for direct measurement of geometry factors
- ❑ Reduces background in electron energy detector induced by gammas
- ❑ Allows for implementation of corrections based on parameter maps (e.g. effective Sherman function corrected for target thickness variation and for angle of incidence)
- ❑ Allows for accurate gain balance of large plastic scintillators
- ❑ Improves diagnostics of beam in fiducial volume

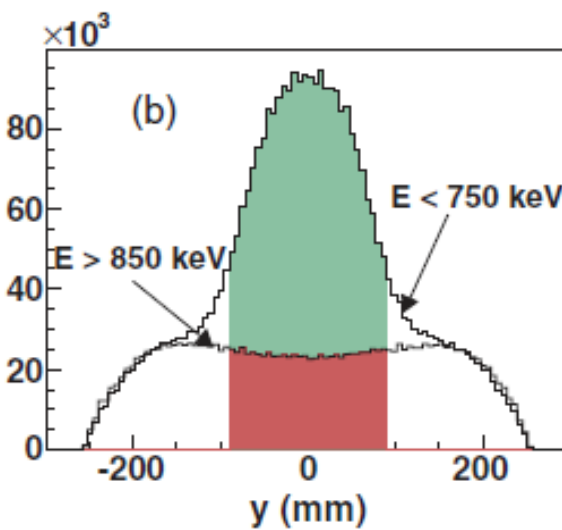
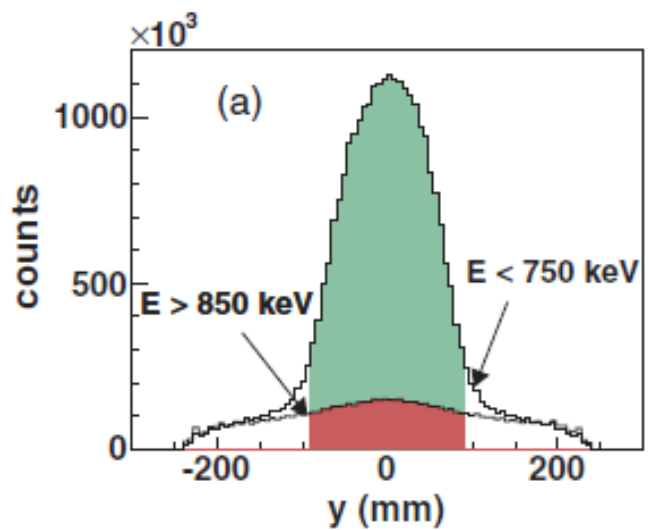
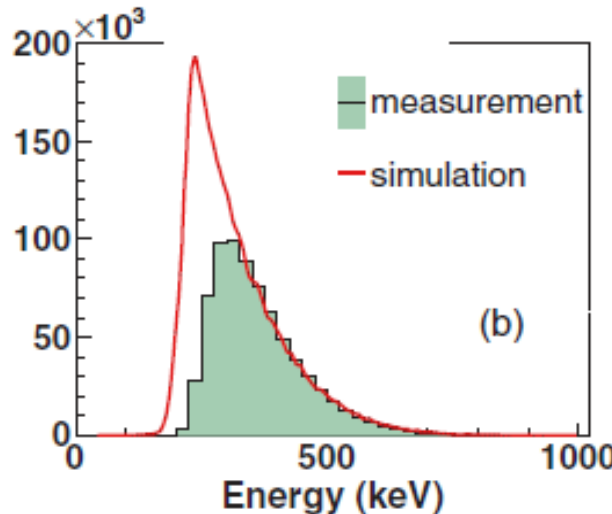
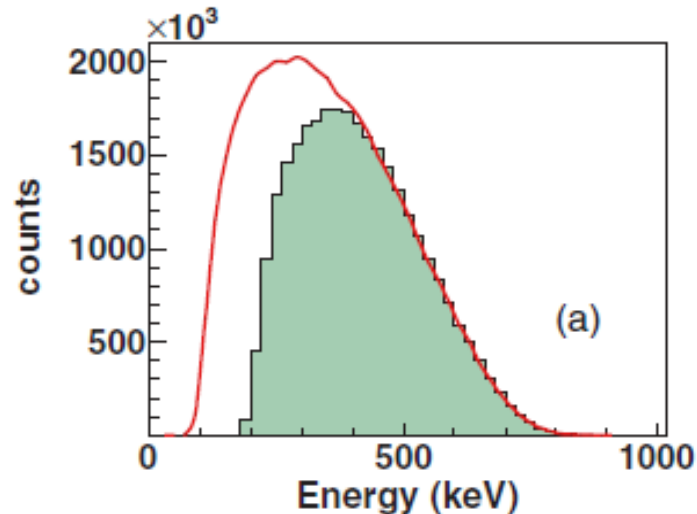
nTRV@PSI: Energy resolution

□ Conversion electrons from ^{207}Bi

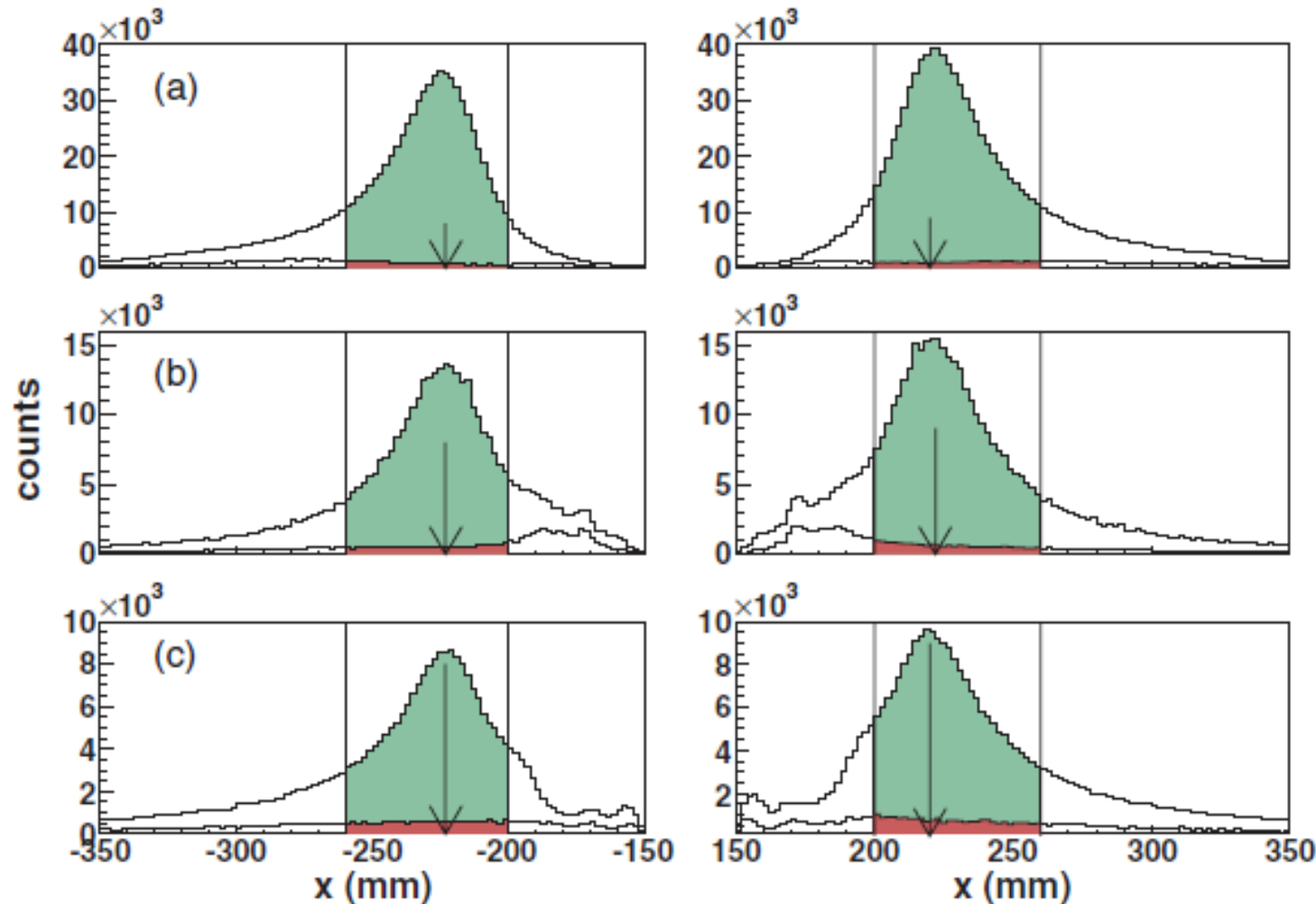


Gaussian fit with fixed relative line positions E_i and intensities I_i
 $\sigma_i(E) = c_1 + c_2 \cdot \sqrt{E_i}$
Background $b(E) = b_0 + b_1 \cdot E + b_2 \cdot E^2$

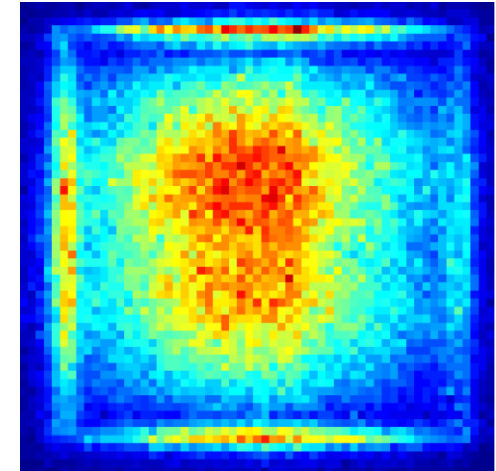
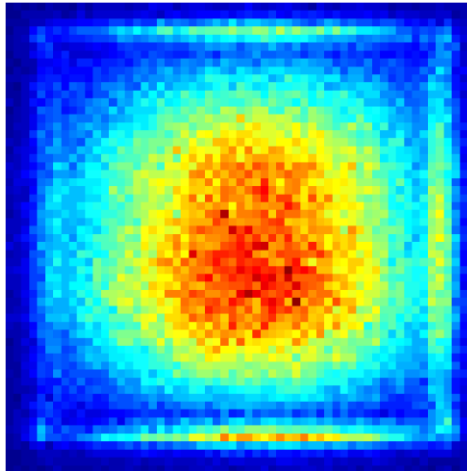
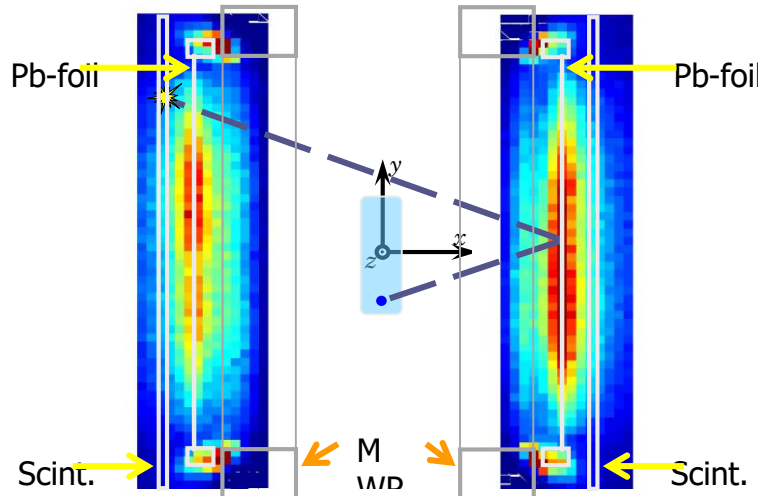
nTRV@PSI: beam profile



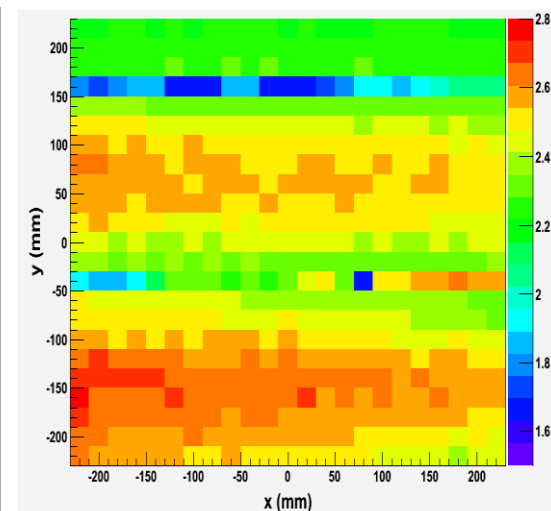
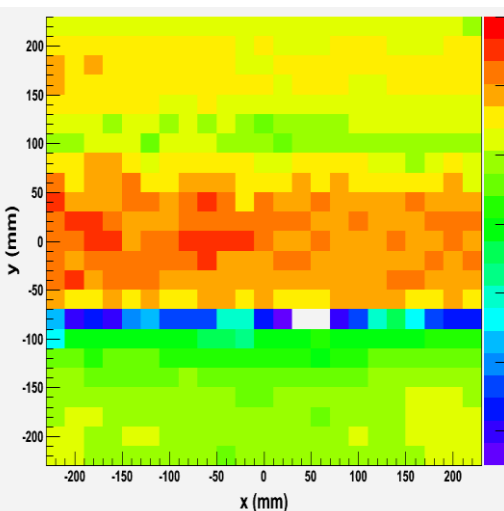
nTRV@PSI: Mott vertex



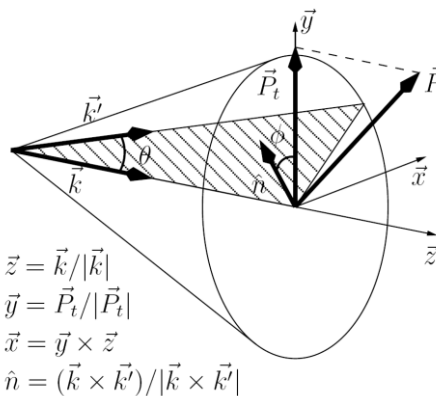
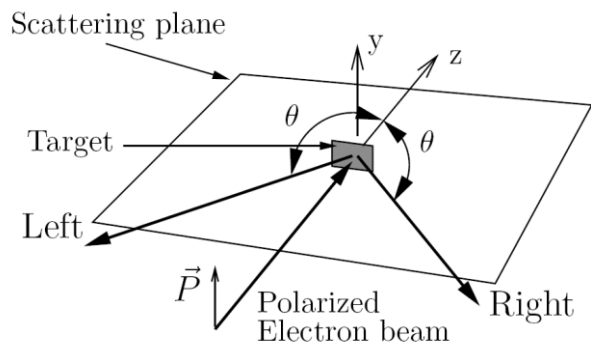
nTRV@PSI: Projection of vertices onto XY-plane



- Mott target thickness scan with X-rays
 - Spatial resolution: ~1 cm
 - Relative thickness accuracy: ~1%
 - Absolute calibration: ~2%



Transport of polarized electrons in matter (multiple Coulomb scattering)



$$\frac{d\sigma(\theta, \phi, E)}{d\omega} = I(\theta, E)[1 - S(\theta, E) \vec{P} \cdot \hat{n}]$$

$$I(\theta) = |f(\theta)|^2 + |g(\theta)|^2$$

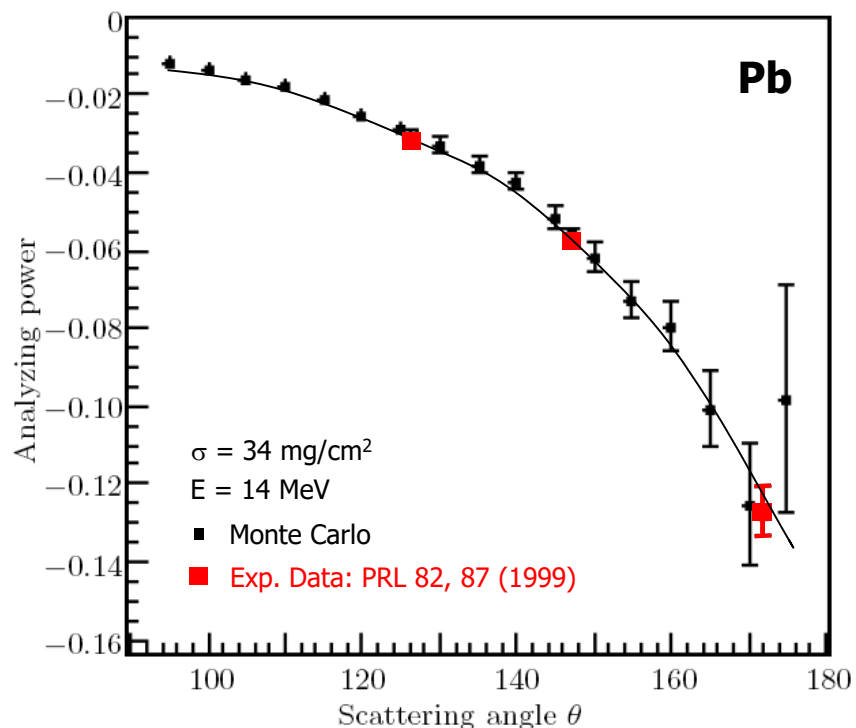
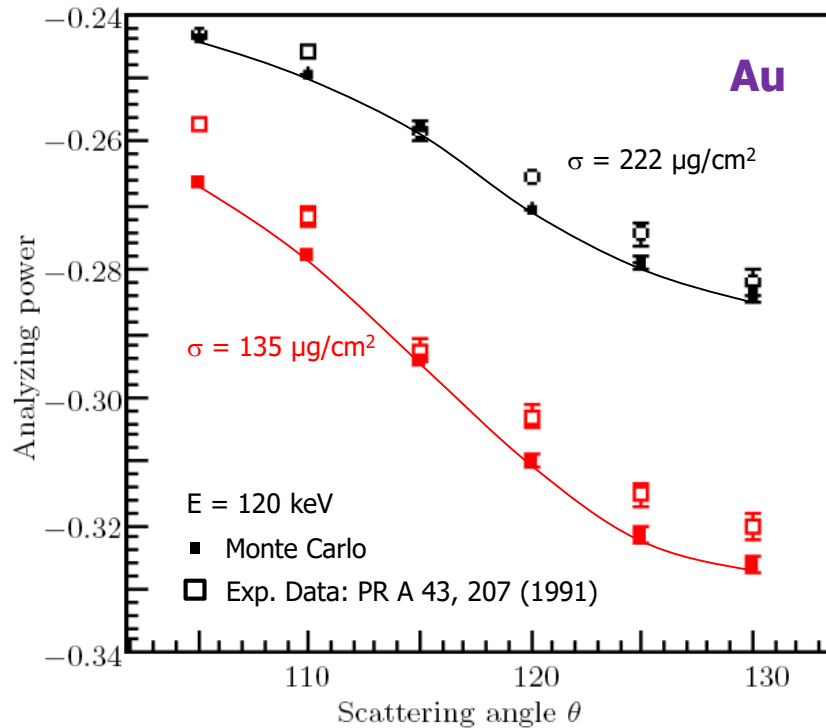
$$S(\theta) = i \frac{f(\theta)g^*(\theta) - f^*(\theta)g(\theta)}{|f(\theta)|^2 + |g(\theta)|^2}$$

$$\vec{P}' = \frac{[\vec{P} \cdot \hat{n} + S]\hat{n} + T\hat{n} \times [\vec{P} \times \hat{n}] + U[\hat{n} \times \vec{P}]}{1 + S \vec{P} \cdot \hat{n}}$$

$$T(\theta) = \frac{|f(\theta)|^2 - |g(\theta)|^2}{|f(\theta)|^2 + |g(\theta)|^2}$$

$$U(\theta) = \frac{f(\theta)g^*(\theta) + f^*(\theta)g(\theta)}{|f(\theta)|^2 + |g(\theta)|^2}$$

Effective Sherman function



At 120 keV (worst case): MC/Exp. :

$$1.0119 \pm 7.10^{-4} \text{ for } 222 \mu\text{g}/\text{cm}^2$$

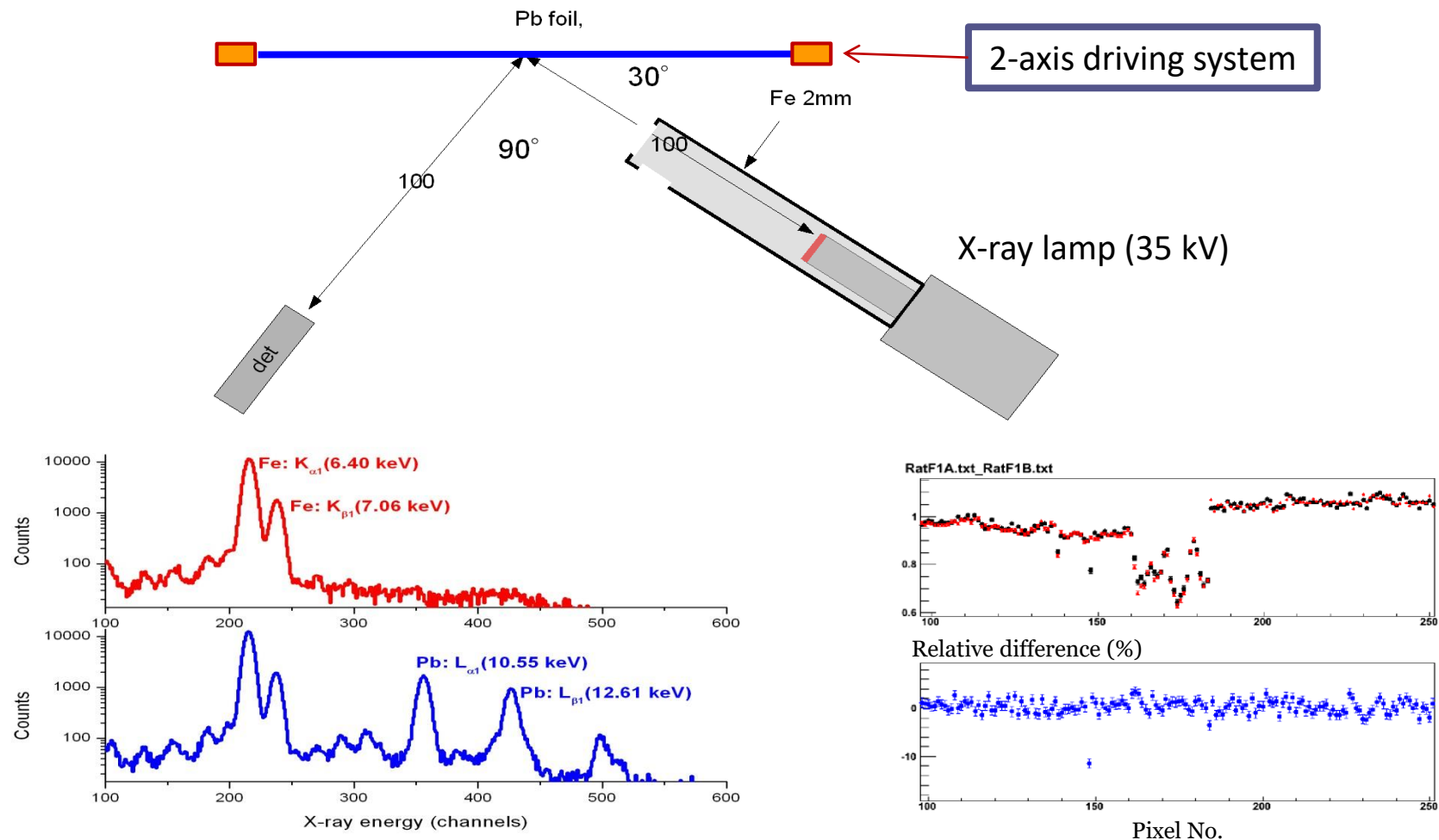
$$1.0222 \pm 8.10^{-4} \text{ for } 135 \mu\text{g}/\text{cm}^2$$

MC based on Geant4 + ELSEPA

ELSEPA

F. Salvat, A. Jablonski, C. Powell, Comput. Phys. Comm. 165 (2005) 157.

nTRV@PSI: Mott target thickness scan





ELSEVIER

Nuclear Instruments and Methods in Physics Research A 440 (2000) 609–617

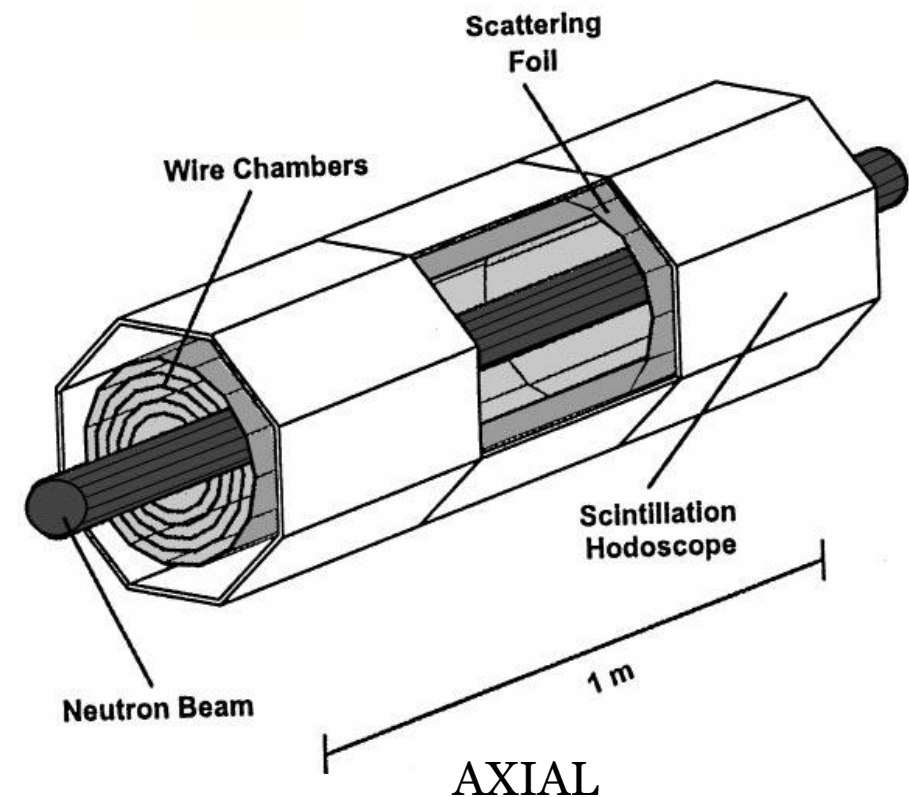
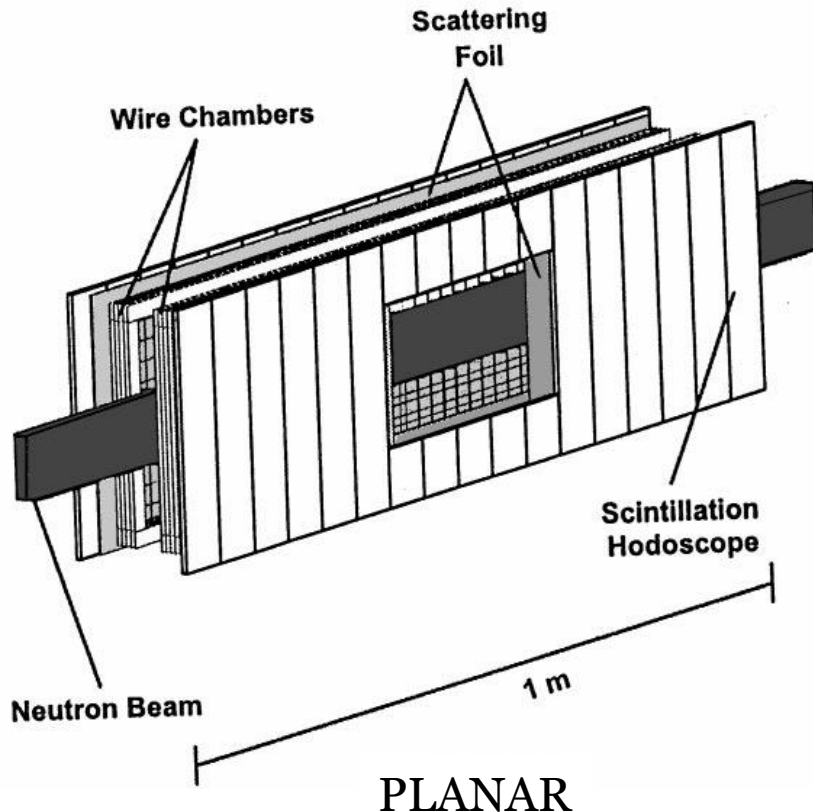
**NUCLEAR
INSTRUMENTS
& METHODS
IN PHYSICS
RESEARCH**

Section A

www.elsevier.nl/locate/nima

T Violation in the weak scalar and tensor interaction: neutron and nuclei

J. Sromicki

Institut für Teilchenphysik, Eidgenössische Technische Hochschule Zürich, CH-8093 Zürich, Switzerland

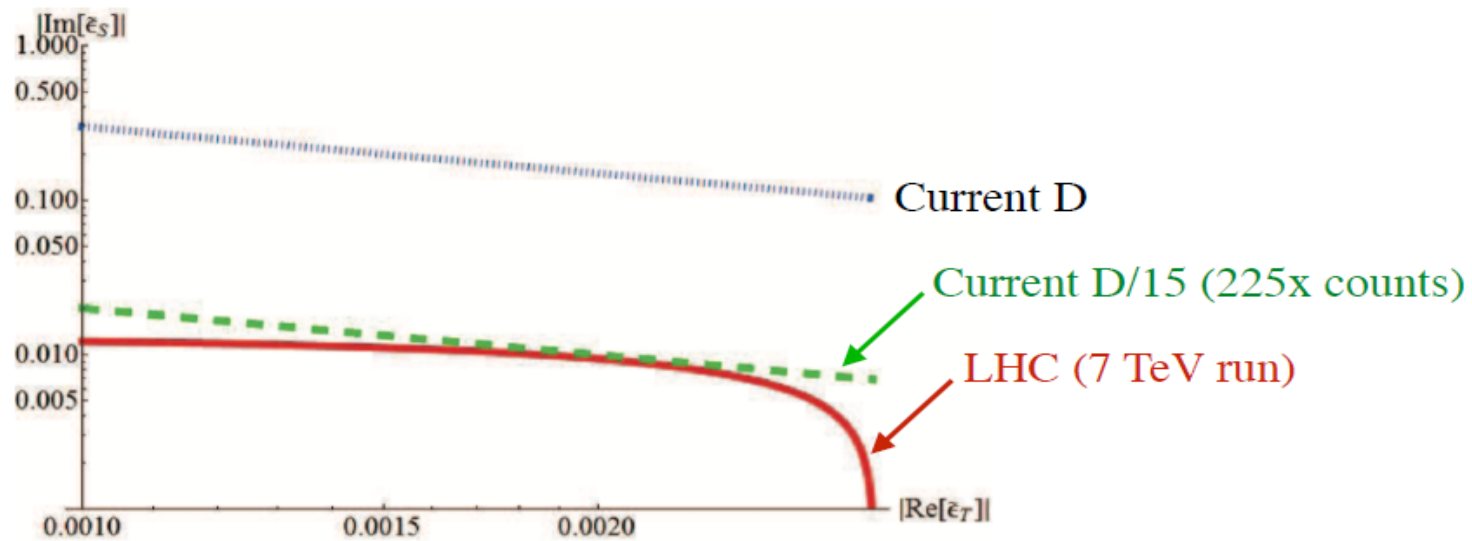
Why the Current Discussion?

Right-Handed Neutrinos and T-Violating, P-Conserving Interactions

Basem Kamal El-Menoufi,¹ Michael J. Ramsey-Musolf,^{1,2} and Chien-Yeah Seng¹

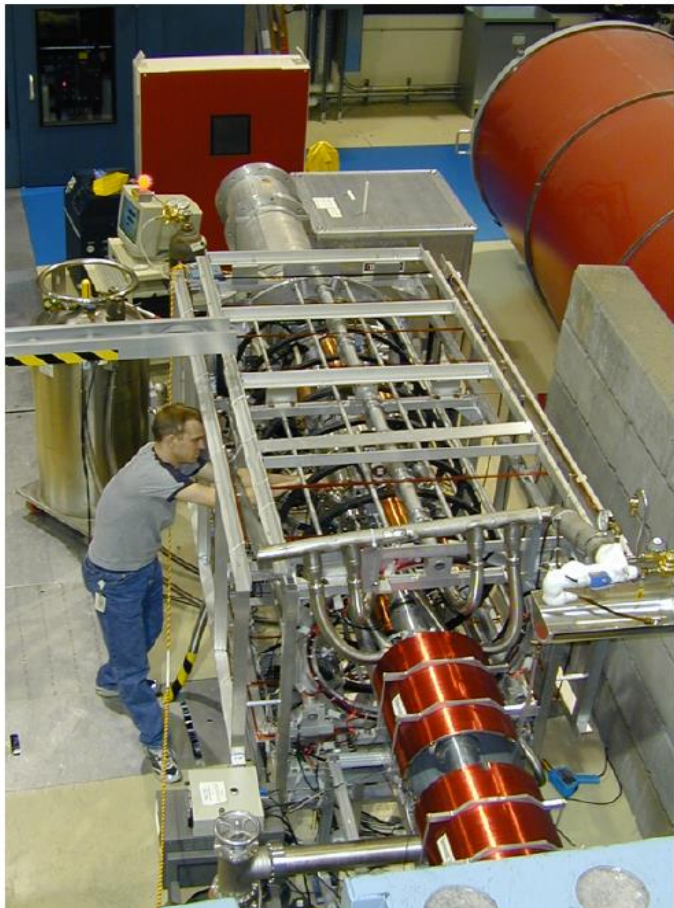
¹Amherst Center for Fundamental Interactions, Department of Physics, University of Massachusetts Amherst, MA 01003, USA

²Kellogg Radiation Laboratory, California Institute of Technology, Pasadena, CA 91125 USA



Limits of scalar and tensor RH neutrino couplings from D and LHC

Time Reversal Violation in Beta-decay



H.P. Mumm, J.S. Nico, and A.K. Thompson
National Institute of Standards and Technology

S.J. Freedman and B.K. Fujikawa
*University of California - Berkeley/
Lawrence Berkeley National Laboratory*

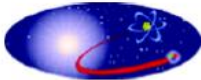
G.L. Jones
Hamilton College

C. Trull and F.E. Wietfeldt
Tulane University

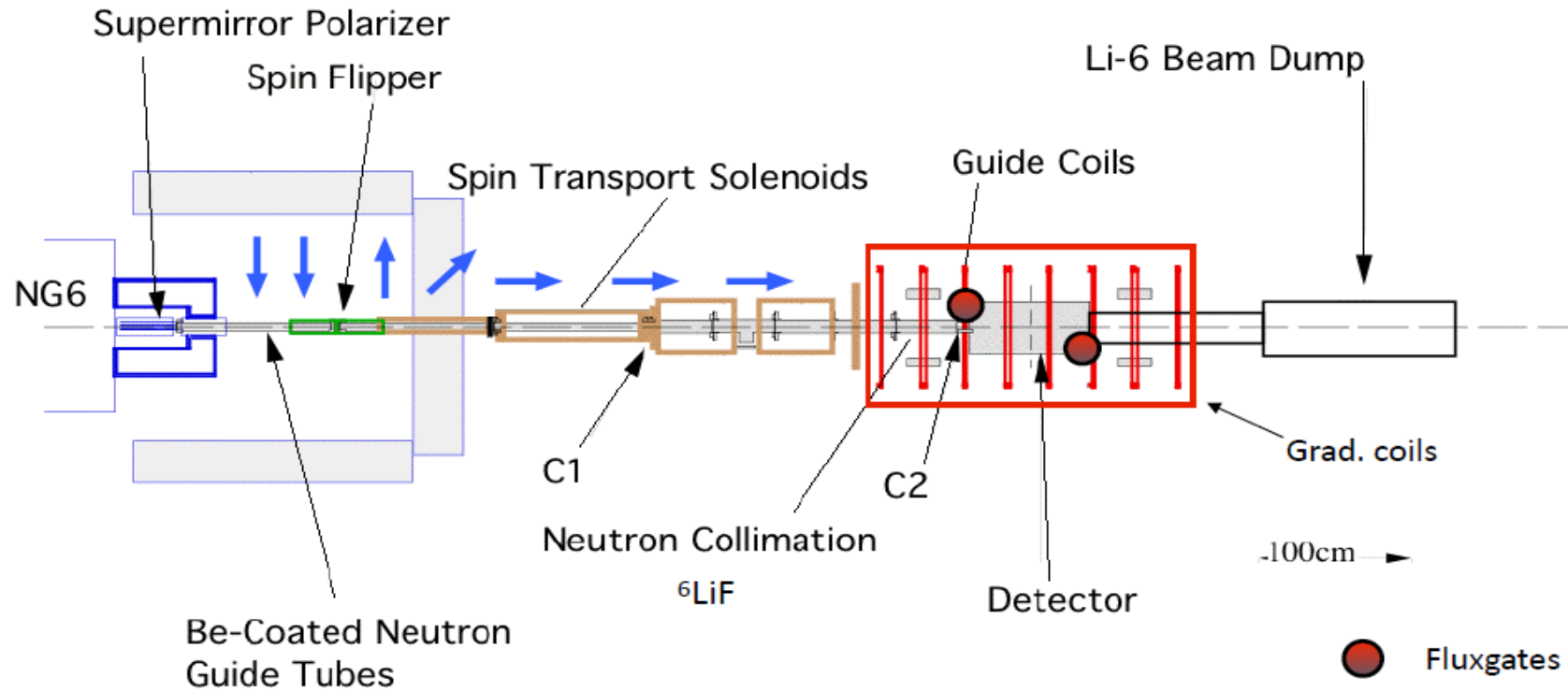
T.E. Chupp and R.L. Cooper, K.P. Coulter
University of Michigan

J.F. Wilkerson
*University of North Carolina & Oak Ridge National
Laboratory*

A. Garcia
University of Washington



emiT neutron transport

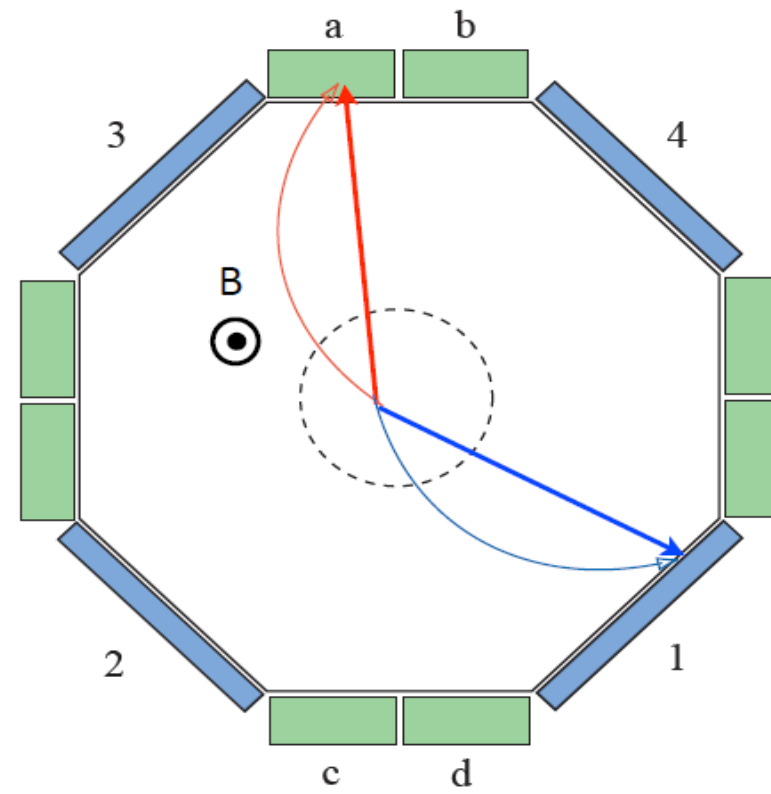
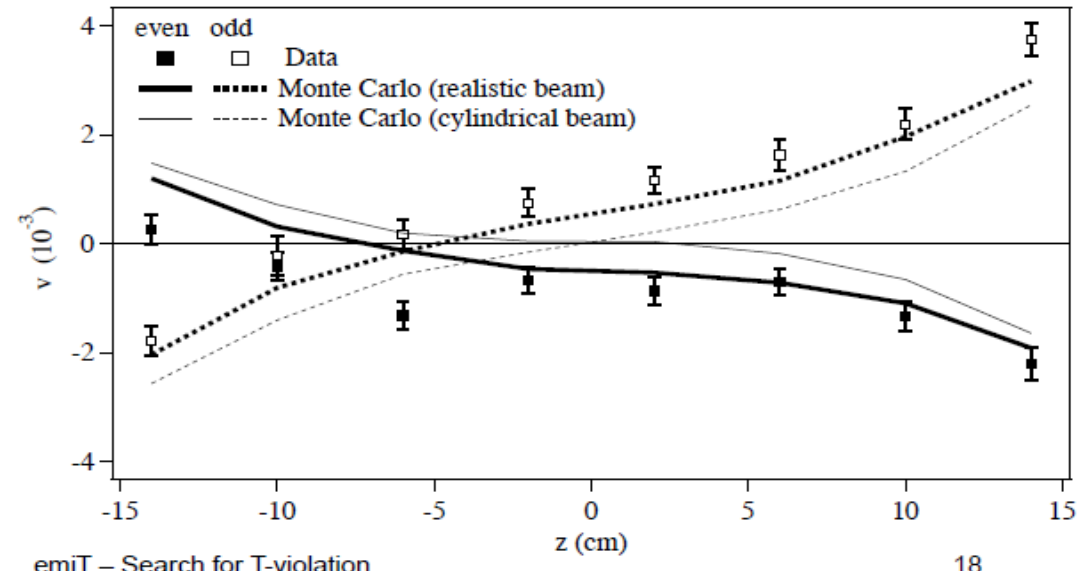


- High continuous neutron flux ($1.7 \times 10^8 \text{ cm}^{-2} \text{ s}^{-1}$ at “C2”), measured with fission chamber.
- $560 \mu\text{T}$ guide field, mapped with 3-axis fluxgate magnetometer, monitored during run.
- Beam profile at entrance, mid-point, and exit via Dysprosium foil activated by the beam.
- Polarization checked with second supermirror analyzer.

Systematics: effect of guide field & beam expansion

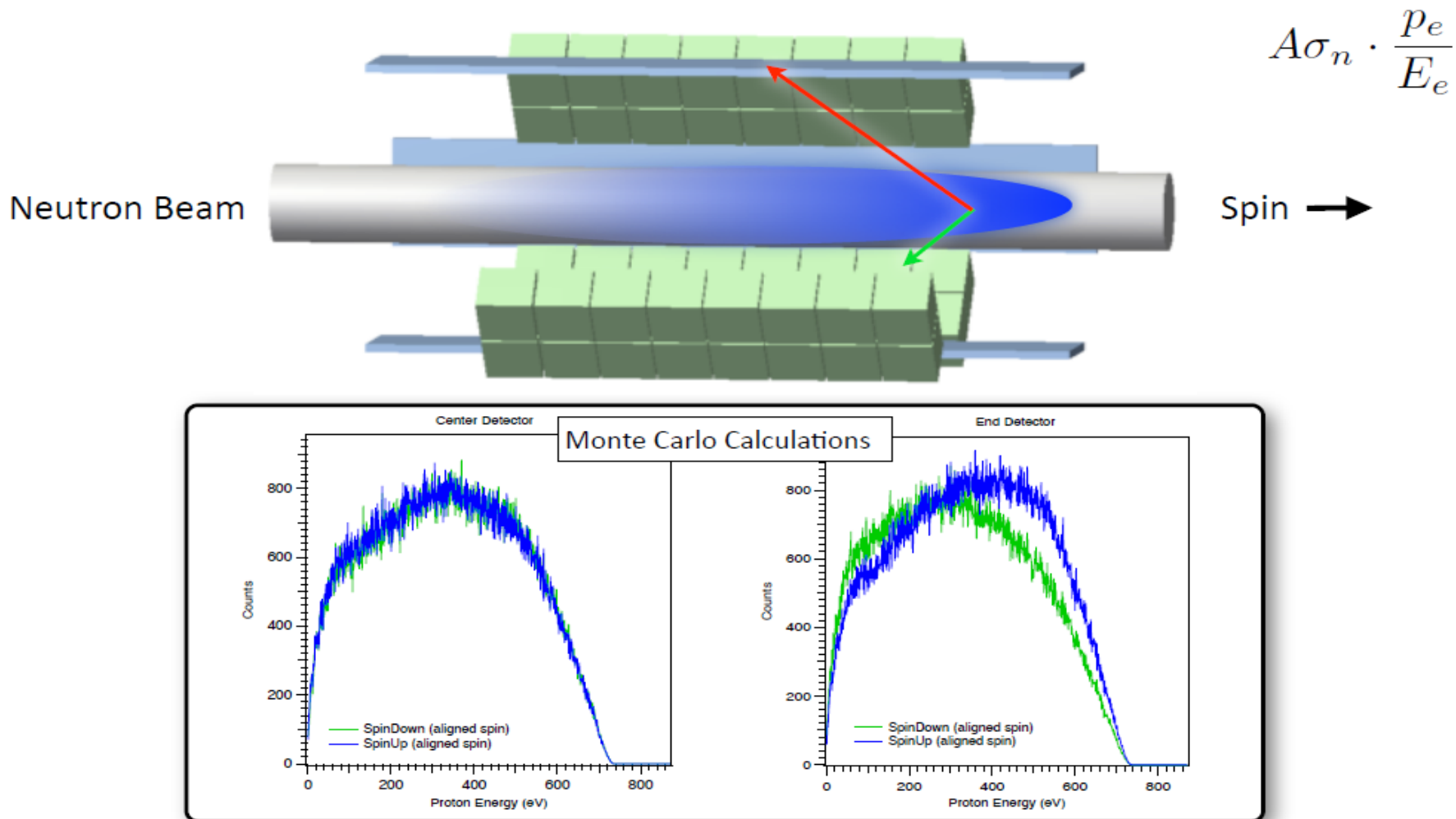
In addition to the spin dependent proton acceptance, there is also a dependence on magnetic fields.

Solution: Detailed Monte Carlo.

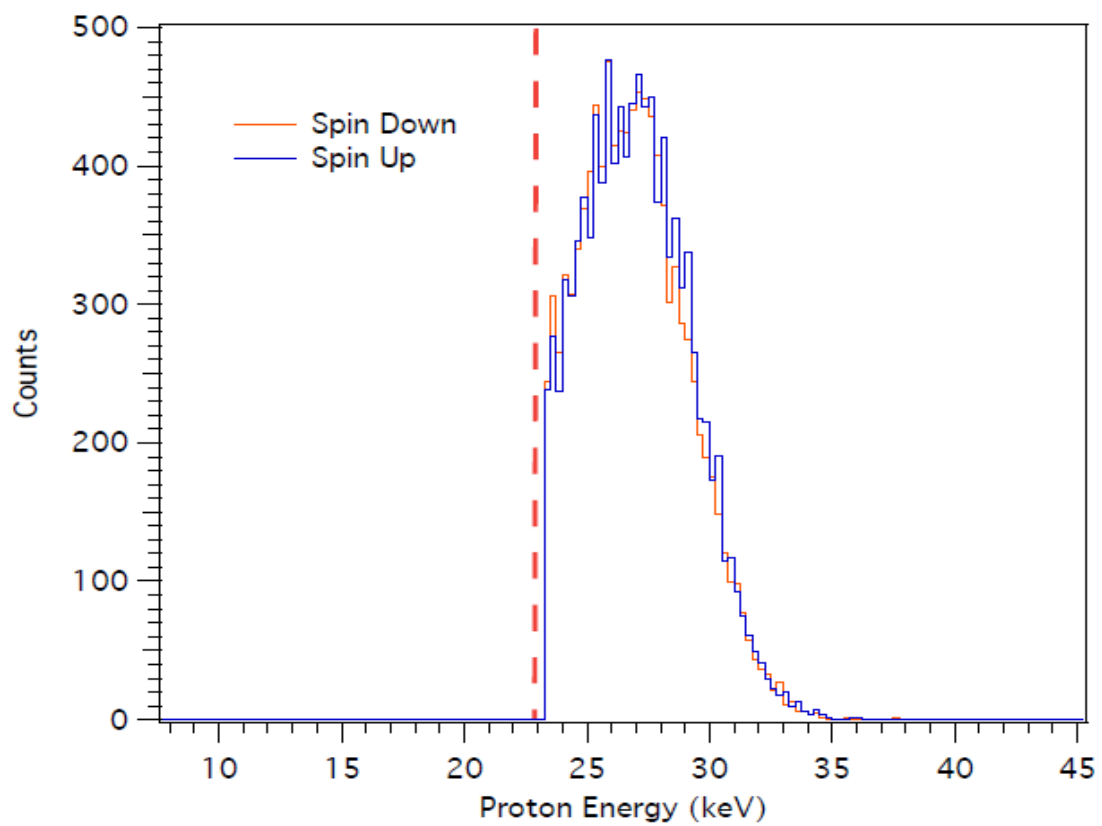


Systematics: spin dependent proton energy

Parity violating asymmetries and the kinematics of the decay result in **LARGE** correlations.



Systematics: spin dependent energy spectrum



Shift of 159 eV

With a threshold of 23 keV
 $w_{\text{false}} = 0.0079$

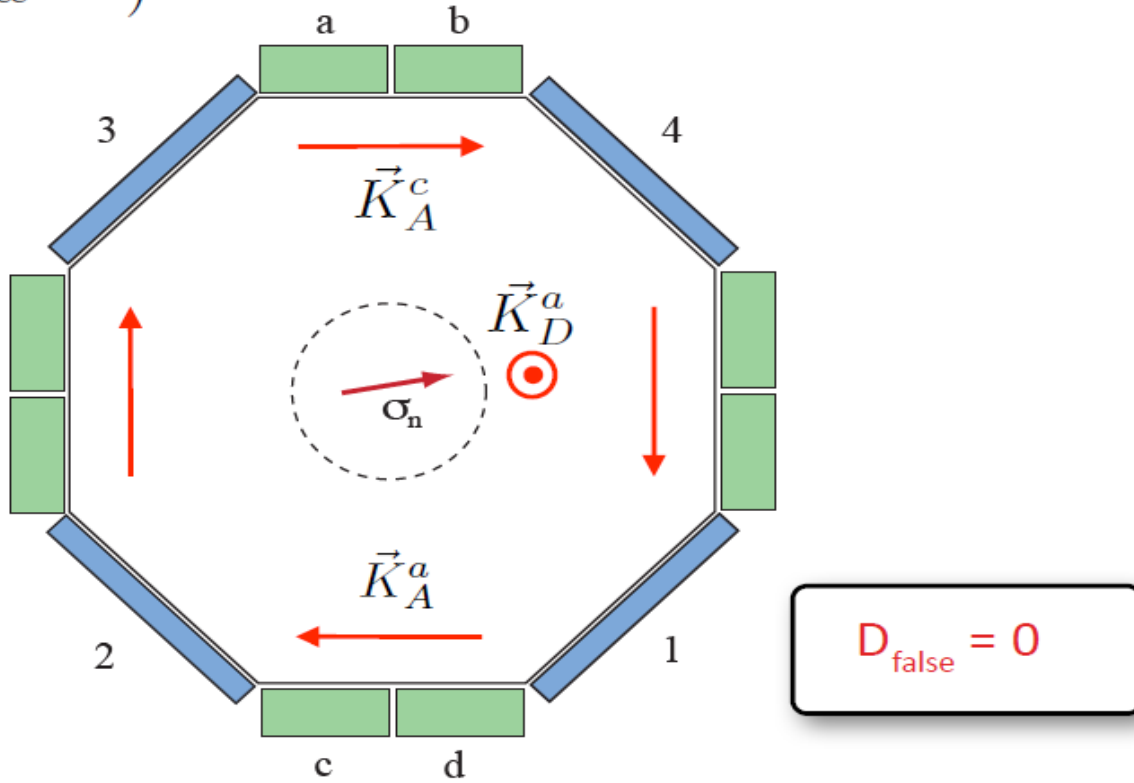
$$v^{p_i} = \frac{1}{2}(w^{p_i R} - w^{p_i L})$$

$$v^{p_i} = PD\hat{z} \cdot \left(\tilde{\mathbf{K}}_D^{p_i e_R} - \tilde{\mathbf{K}}_D^{p_i e_L} \right)$$

Systematics: Measured Intensity Distribution (Tilt ATP)

$$w^{p_i e_j} \approx \mathbf{P} \cdot \left(A \tilde{\mathbf{K}}_A^{p_i e_j} + B \tilde{\mathbf{K}}_B^{p_i e_j} + D \tilde{\mathbf{K}}_D^{p_i e_j} \right)$$

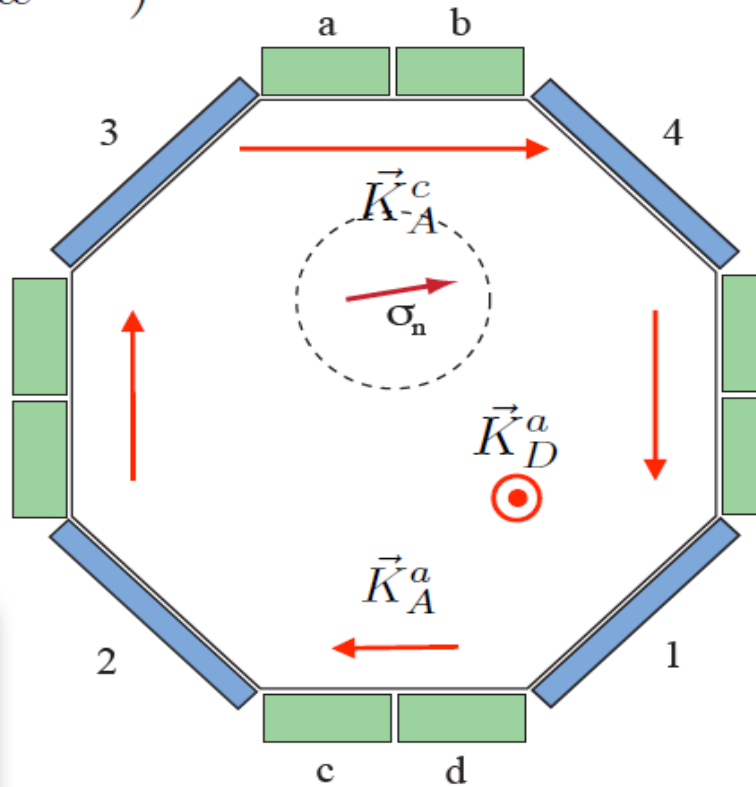
$$v^{p_i} = \frac{1}{2} (w^{p_i R} - w^{p_i L})$$



Systematics: Measured Intensity Distribution (Tilt ATP)

$$w^{p_i e_j} \approx \mathbf{P} \cdot \left(A \tilde{\mathbf{K}}_A^{p_i e_j} + B \tilde{\mathbf{K}}_B^{p_i e_j} + D \tilde{\mathbf{K}}_D^{p_i e_j} \right)$$

$$v^{p_i} = \frac{1}{2}(w^{p_i R} - w^{p_i L})$$



Monte Carlo
15 mrad polarization tilt,
beam displacement 5mm:
 $D_{\text{false}} \sim 1 \times 10^{-4}$

$D_{\text{false}} \neq 0$
Two perpendicular
asymmetries do *not*
cancel

Systematics: Measured Intensity Distribution (Tilt ATP)

